Surface-No. 15-MOC-CMA

Report on the Quality of Land Surface Observations in Region II (Asia)

January - June 2025

No. 15

Regional WIGOS Centre, Beijing

China Meteorological Administration

No. 46 Zhongguancun Nandajie

Beijing, CHINA

Contents

Report on the Quality of Land Surface Observations in Region II
(No. 15)
January - June 2025

Introduction

In its role as Regional WMO Integrated Global Observing System (WIGOS) Centre, Beijing (RWC-Beijing) in Regional Association (RA) II, China Meteorological Administration (CMA) has issued the 15th report on the land surface observation quality monitoring for the period from January to June 2025. The report includes a consolidated list of stations suspected of producing low-quality observational data.

RWC-Beijing was designated as RWC in 2021, in support to the Members of the Region as an operational RWC with a certification. It is responsible for monitoring the availability and quality of meteorological observations and maintaining consolidated lists of stations suspected of reporting low-quality observational data together with adequate evidence. The lists are to be passed on to the WMO Secretariat as well as to Members of RA II for their reference.

1. Monitored Data

Monitored surface observational data are obtained at 00, 06, 12 and 18 UTC and collected at CMA before the data cut-off time, defined as the end of the period in which observational data are gathered for operational analysis. The cut-off times for CMA global analysis are shown in Table 1.

Table 1 Data cut-off times for CMA global analysis

Analysis time	Data cut-off time
00 UTC	11:50 UTC
06 UTC	17:50 UTC
12 UTC	23:50 UTC
18 UTC	05:50 UTC

The observation elements monitored are (1) station level pressure, (2) mean sea level pressure, and (3) geopotential height, hereafter referred to as SLP, MSLP, and GZ respectively. In accordance with the Manual on Codes (WMO No. 306) Volume II, GZ data on an agreed standard pressure level are reported at the stations whose elevation is higher than 800 m. Standard pressure levels defined in line with station elevation are shown in Table 2.

Table 2 Elevation of stations reporting GZ data and corresponding standard pressure Levels

Station elevation (m)	Pressure level (hPa)
800 – 2,300	850
2,300 – 3,700	700
Higher than 3,700	500

The numbers of stations reporting SLP, MSLP and/or GZ data in Region II are shown in Table 3, and the data availability of these land surface stations are shown in Figure 1.

Table 3 Numbers of stations reporting SLP, MSLP and/or GZ data in Region II

Element	Number of stations	Number of GBON staions
SLP	2391	1605
MSLP	2437	1571
GZ	188	109

2. Monitoring Methods

The three items described below are examined for each element.

(i) Monthly statistics on observation deviations from the most recent forecast of CMA's global model (referred to as first-guess values) (observation minus guess, hereafter referred to as O-G) and on related trends over the monitoring period

(ii) Reference information from other monitoring centres

Information on the latitude, longitude and altitude of each station is necessary for calculation of first-guess values. Such data for land surface station locations are retrieved from the surface-based observing system component of the Observing Systems Capability Analysis and Review Tool (OSCAR/Surface) *.

* https://oscar.wmo.int/surface/index.html#/

The monitoring procedure has two steps as outlined below.

(1) Exclusion of data with gross errors from the statistical calculation sample

The following thresholds are applied for the gross error check in the first step:

|O-G| >= 15 hPa for SLP and MSLP

|O-G| >= 100 gpm for GZ

Gross error data are excluded from the calculation of BIAS (the mean of O-G) and SD (the standard deviation of O-G).

(2) Identification of suspect stations

When the total number of observations (NOBS) is 181 or more, the next criteria are applied:

- BIAS |BIAS| >= 3 hPa for SLP and MSLP
  |BIAS| >= 30 gpm for GZ

- SD SD >= 5 hPa for SLP and MSLP
  SD >= 40 gpm for GZ

- Percentage of gross errors (PGE) PGE >= 25%

Stations with even one statistic exceeding the threshold are considered suspect.

Note:
(i) The quality of observational data from stations are not checked when the NOBS value is less than 181 or the difference between H and HM is greater than 1,000 m. MSLP reports are also not checked for stations located at altitudes higher than 1,000 m above sea level.
(ii) In case of low quality of the first-guess field, those statistics can exceed the threshold and the stations are listed in the consolidated list. To avoid such situations, statistics of surrounding stations and information from other monitoring centres are also used to judge whether the quality of the station's first-guess field value is appropriate.

3. Monitoring Results

3.1 Consolidated list of suspect stations throughout the period

Table 4 List of suspect land surface stations throughout the period

WMO IDENT	LAT (N)	LON (E)	H (m)	HM (m)	ELEM	NUM OBS	PGE %	SD	BIAS	RMS
36914*	42.73	75.02	1775	1692.6	P	675	100	-	-	-
					GZ850	676	0	13.26	1.72	13.37
36934*	42.64	77.07	1613	2536.7	P	679	0	1.5	-10.46	10.57
					GZ850	680	75	9.03	-88.14	88.6
38262*	42.95	59.8	94.5	58.5	P	715	0	0.87	3.63	3.74
					MSLP	715	0	0.98	0.13	0.99
38349*	42.16	72.89	2000	2874.9	P	675	1	1.42	4.89	5.09
					GZ850	675	1	16.97	49.74	52.55
38359*	42.32	73.8	3500	3104.3	P	678	99	-	-	-
					GZ700	675	1	8.75	-37.23	38.25

38471*	41.95	71.38	2027	2939	P	676	93	0.98	-13.88	13.92
					GZ850	671	100	-	-	-
38476*	41.29	72.83	1748	2017.9	P	679	0	0.89	9.32	9.36
					GZ850	676	18	8.02	87.58	87.95
38567	40.13	65.35	341.4	444.5	P	710	0	1.43	-6.81	6.95
					MSLP	710	0	1.75	-7.71	7.9
38829	38.27	67.9	520.7	653.8	P	687	0	1.15	-3.47	3.65
					MSLP	686	0	1.74	-4.66	4.97
38875	39.02	73.55	3930	4307.8	P	341	100	-	-	-
					-	-	-	-	-	-
38880*	37.99	58.36	312	484.6	P	717	1	1.32	12.27	12.34
					MSLP	717	0	1.27	-0.17	1.28
38944*	37.48	69.38	447	563.3	P	714	0	1.33	-5.82	5.98
					MSLP	715	0	2.08	-6.87	7.18
41315*	17.25	54.09	881	512.9	P	491	99	0.05	14.63	14.63
					GZ850	491	98	50.9	-50.47	71.68
41565	33.82	71.88	1371	533.7	P	690	0	2.03	4.76	5.18
					GZ850	689	95	19.74	28.04	34.29
41757	25.13	62.33	96	23.8	P	713	0	1.14	10.53	10.59
					MSLP	713	0	0.9	0.72	1.15
42045	33.5	75.17	1624	2401.2	P	538	0	1.11	-4.8	4.92
					GZ850	538	0	12.49	-60.16	61.44
42083	31.1	77.17	2270	1502.2	P	349	99	-	-	-
					GZ850	18	100	-	-	-
42114	30.38	78.43	1931	1547.3	P	358	0	0.96	3.56	3.69
					-	-	-	-	-	-
42147	29.47	79.65	2311	1609.7	P	358	0	0.8	5.73	5.78
					GZ700	2	100	-	-	-
42515	25.25	91.73	1313	494	P	521	0	0.8	4.77	4.84
					-	-	-	-	-	-

47037*	39.98	125.25	101	198.6	P	718	0	1.35	-3.82	4.05
					MSLP	718	0	1.39	-4.15	4.37
48921	21.63	101.88	1360	1068.8	P	513	0	1.01	-3.58	3.72
					GZ850	510	99	10.07	-86.47	87.05
48925	20.68	102	636	960.9	P	484	0	1.38	-3.65	3.9
					MSLP	483	0	1.75	-4.56	4.88
48926	20.25	100.43	531.8	506.6	P	479	12	1.84	13.5	13.62
					MSLP	479	0	1.31	-0.76	1.51
48944	18.28	102.63	185	309.5	P	288	100	-	-	-
					MSLP	288	0	3.01	-7.24	7.84
48952	15.68	106.43	180	302.8	P	523	0	1.41	3.49	3.77
					MSLP	523	0	1.34	1.41	1.95

WMO IDENT:	WMO station identification number (“*” represents GBON station)
LAT:	station latitude
LON:	station longitude
H:	station elevation
HM:	model elevation
ELEM:	observed element
NOBS:	total number of observations during the period
PGE:	percentage gross error
SD:	standard deviation of (observation - guess)
BIAS:	bias of (observation - guess)
RMS:	root mean square of (observation - guess)

Kyrgyzstan

36914* – Positive bias of O-G at the station level(Figure 2)

36934* – Negative bias of O-G at the station level(Figures 3 and 4)

38349* – Positive bias of O-G at the station level(Figures 7 and 8)

38359* – Positive bias of O-G at the station level(Figure 9)

38471* – Negative bias of O-G at the station level(Figure 10)

38476* – Positive bias of O-G at the station level(Figures 11 and 12)

Uzbekistan

38262* – Positive bias of O-G at the station level(Figures 5 and 6)

38567 – Negative bias of O-G at the station level(Figures 13 and 14)

38829 – Negative bias of O-G at the station level(Figures 15 and 16)

Tajikistan

38875 – Positive bias of O-G at the station level(Figure 17)

38944* – Negative bias of O-G at the station level(Figures 20 and 21)

Turkmenistan

38880* – Positive bias of O-G at the station level(Figures 18 and 19)

Oman

41315* – Positive bias of O-G at the station level(Figure 22)

Pakistan

41565 – Positive bias of O-G at the station level(Figures 23 and 24)

41757 – Positive bias of O-G at the station level(Figures 25 and 26)

India

42045 – Negative bias of O-G at the station level(Figures 27 and 28)

42083 – Positive bias of O-G at the station level(Figure 29)

42114 – Positive bias of O-G at the station level(Figures 30 and 31)

42147 – Positive bias of O-G at the station level(Figures 32 and 33)

42515 – Positive bias of O-G at the station level(Figures 34 and 35)

Democratic People's Republic of Korea

47037* – Negative bias of O-G at the station level(Figures 36 and 37)

Lao People's Democratic Republic

48921 – Negative bias of O-G at the station level(Figures 38 and 39)

48925 – Negative bias of O-G at the station level(Figures 40 and 41)

48926 – Positive bias of O-G at the station level(Figures 42 and 43)

48944 – Negative bias of O-G at the station level(Figure 44)

48952 – Positive bias of O-G at the station level(Figures 45 and 46)

3.2 Stations where quality deteriorated during the period

Table 5 List of suspect stations where quality deteriorated during the period

WMO IDENT	LAT (N)	LON (E)	H (m)	HM (m)	ELEM	NUM OBS	PGE %	SD	BIAS	RMS
28764	54.51	65.75	159	169.1	P	582	62	3.8	1.4	4.05
					MSLP	582	60	3.88	1.34	4.1
35497	48.85	72.87	655.2	712.1	P	691	40	0.75	0	0.75
					MSLP	692	40	1.37	-0.89	1.63

36859	44.16	80.05	641	659	P	701	10	4.38	3.67	5.71
					MSLP	701	10	5.06	3.24	6.01
36874	43.5	76.28	641	601.8	P	715	0	5.35	1.94	5.69
					MSLP	715	8	5.63	0.43	5.65
36877	43.23	76.3	813	1179.3	P	615	29	1.11	1.11	1.57
					MSLP	616	29	2.56	-0.31	2.58
36974*	41.43	76	2039	2458.8	P	712	1	1.23	3.21	3.43
					GZ850	711	0	20.08	13.93	24.44
38577*	40.04	67.58	600.7	666.1	P	704	0	0.85	3.48	3.58
					MSLP	704	0	2.02	-0.52	2.09
38708	39.12	67.53	2034	2723.5	P	698	0	1.04	-10.9	10.95
					MSLP	699	0	-	-	-
38719*	39.08	68.87	3373	3118.5	P	354	3	3.42	4.31	5.5
					GZ700	710	9	32.41	37.31	49.42
38749	39.95	71.13	1201	1931.1	P	669	100	-	-	-
					MSLP	668	0	-	-	-
38827	38.2	67.2	1241.3	1373.9	P	696	0	5.33	2.5	5.89
					GZ850	691	3	44.24	26.98	51.82
38947*	37.23	69.08	327	507.6	P	354	0	1.7	-3.54	3.92
					MSLP	710	0	2.38	-0.53	2.44
41175	25	51.03	47	36.2	P	322	0	0.49	5.88	5.9
					MSLP	322	0	0.51	6.09	6.11
41177	24.72	51.22	45	21	P	322	0	0.53	5.36	5.39
					MSLP	321	0	0.54	5.64	5.67
41508*	35.2	71.85	1369	2183.3	P	705	0	1.57	3.27	3.62
					GZ850	699	95	18.23	27.17	32.72

Kazakhstan

28764 – Positive bias of O-G at the station level (Figure 47). In addition, since RWC-Beijing worked with NFP (Kazakhstan) using the Incident Management System and another device was installed, the bias of O-G at the station level has improved since the end of May 2025. We will remove this station in the next report.

35497 – The positive bias of O-G at the station level has improved since March 2025. We will remove this station in the next report (Figure 48).
36859 – Positive bias of O-G at the station level (Figures 49 and 50). In addition, since RWC-Beijing worked with NFP (Kazakhstan) using the Incident Management System and the instrument was replaced, the bias of O-G at the station level has improved since May 2025. We will remove this station in the next report.
36874 – The positive bias of O-G at the station level has improved since February 2025. We will remove this station in the next report (Figures 51 and 52).
36877 – Positive bias of O-G at the station level (Figure 53). In addition, RWC-Beijing worked with NFP (Kazakhstan) using the Incident Management System, the bias of O-G at the station level has improved since March 2025. We will remove this station in the next report.

Kyrgyzstan
36974* – Positive bias of O-G at the station level(Figures 54 and 55)

Uzbekistan
38577* – Positive bias of O-G at the station level(Figures 56 and 57)
38708 – Negative bias of O-G at the station level(Figures 58 and 59)
38749 – Positive bias of O-G at the station level(Figure 62)
38827 – Positive bias of O-G at the station level(Figures 63 and 64)

Tajikistan
38719* – Positive bias of O-G at the station level(Figures 60 and 61)
38947* – Negative bias of O-G at the station level(Figures 65 and 66)

Qatar
41175 – Positive bias of O-G at the station level(Figures 67 and 68)
41177 – Positive bias of O-G at the station level(Figures 69 and 70)

Pakistan
41508* – Positive bias of O-G at the station level(Figures 71 and 72)

3.3 Stations improved and excluded from the previous consolidated list

Kazakhstan
36729 – The positive pressure bias of O-G at the station level has improved (Figure 73). In addition, since RWC-Beijing worked with NFP (Kazakhstan) using the Incident Management System and the instrument was replaced, the bias of O-G at the station level has improved.

3.4 Stations removed from the previous consolidated list

Myanmar

48018* – Although station 48018 still displays positive biases of O-G at the station level, it was removed from the consolidated list because the number of reports (2) was insufficient for quality checking (Figure 74).

Cambodia

48973 – It was removed from the consolidated list because the number of reports (2) was insufficient for quality checking (Figure 75).

48986 – It was removed from the consolidated list because the number of reports (2) was insufficient for quality checking (Figure 76).

4. Possible Causes of Remarkable and Sustained Biases

The following are possible causes of remarkable and sustained biases

a. The barometer used for observation is not correctly calibrated.

b. The latitude, longitude or altitude of the station in OSCAR/Surface has not been updated in a timely and appropriate manner. This could result in remarkable biases because it may cause incorrect calculated first-guess field values.

c. Biases are specific to the NWP model used in quality monitoring.

Note: Model biases are likely to appear in relatively large areas.

5. Technical Support

Any comments on the contents and the format of the report are welcome and could be sent to us.

Project Leader:

Shi Lijuan (Ms.), Yao Dan (Mr.)

Technical director:

Cui Xiai (Ms.)

Technical employee:

Dai Zhiying (Ms.), Ding Yuhao (Mr.)

Tel: 86-10-58991513

E-mail: rwc-bj@cma.gov.cn

Regional WIGOS Centre, Beijing

Meteorological Observation Centre of China Meteorological Administration

6. Figures

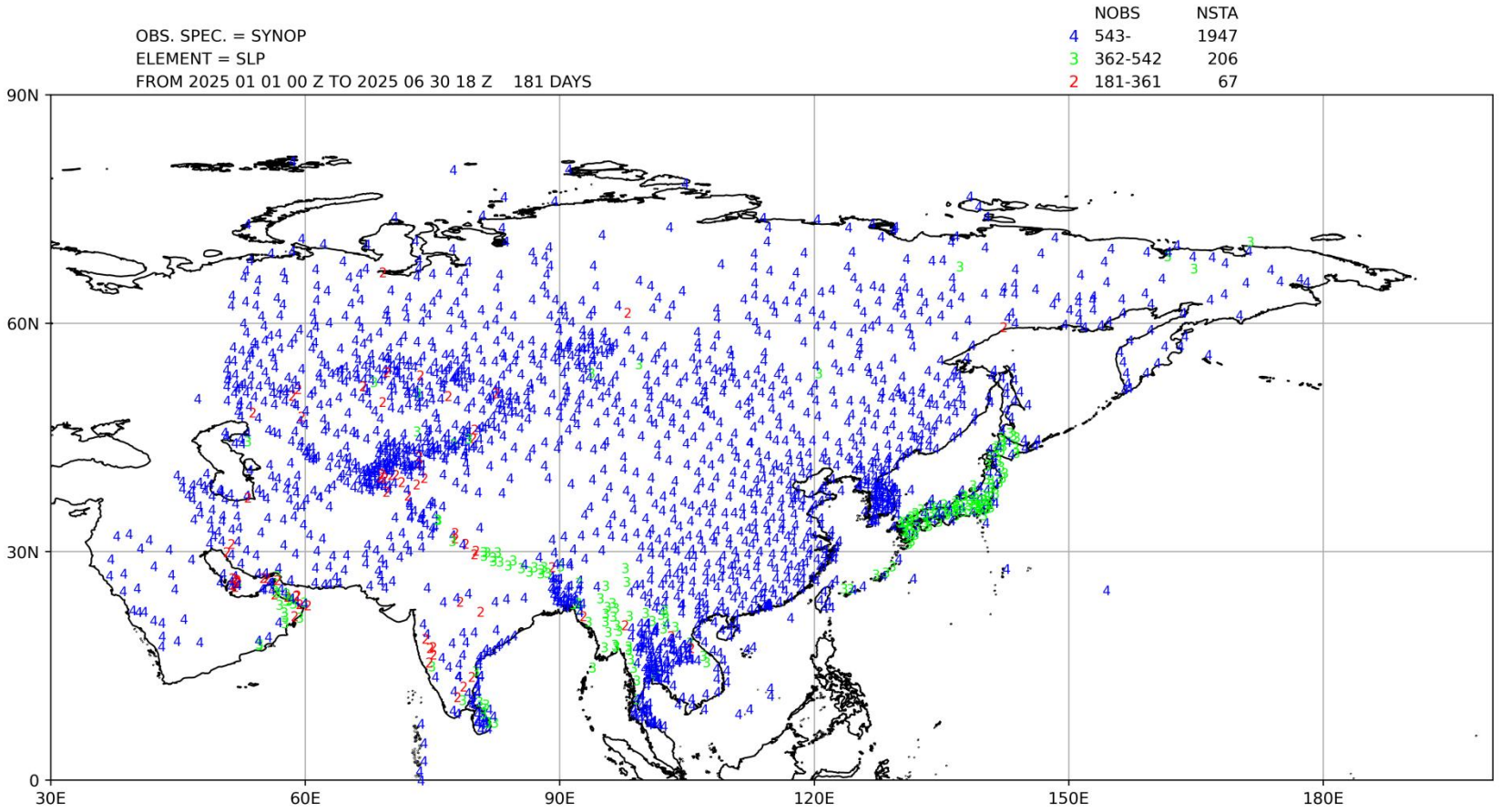

Figure 1(a) Location of all land surface stations reporting station level pressure (SLP) observations in Region II over the six-month period from January to June 2025. Numbers (2, 3, 4) show the total number of observations (NOBS) received at RWC-Beijing. The total numbers of stations (NSTA) reporting SLP are shown at the top of the figure. (Data availability)

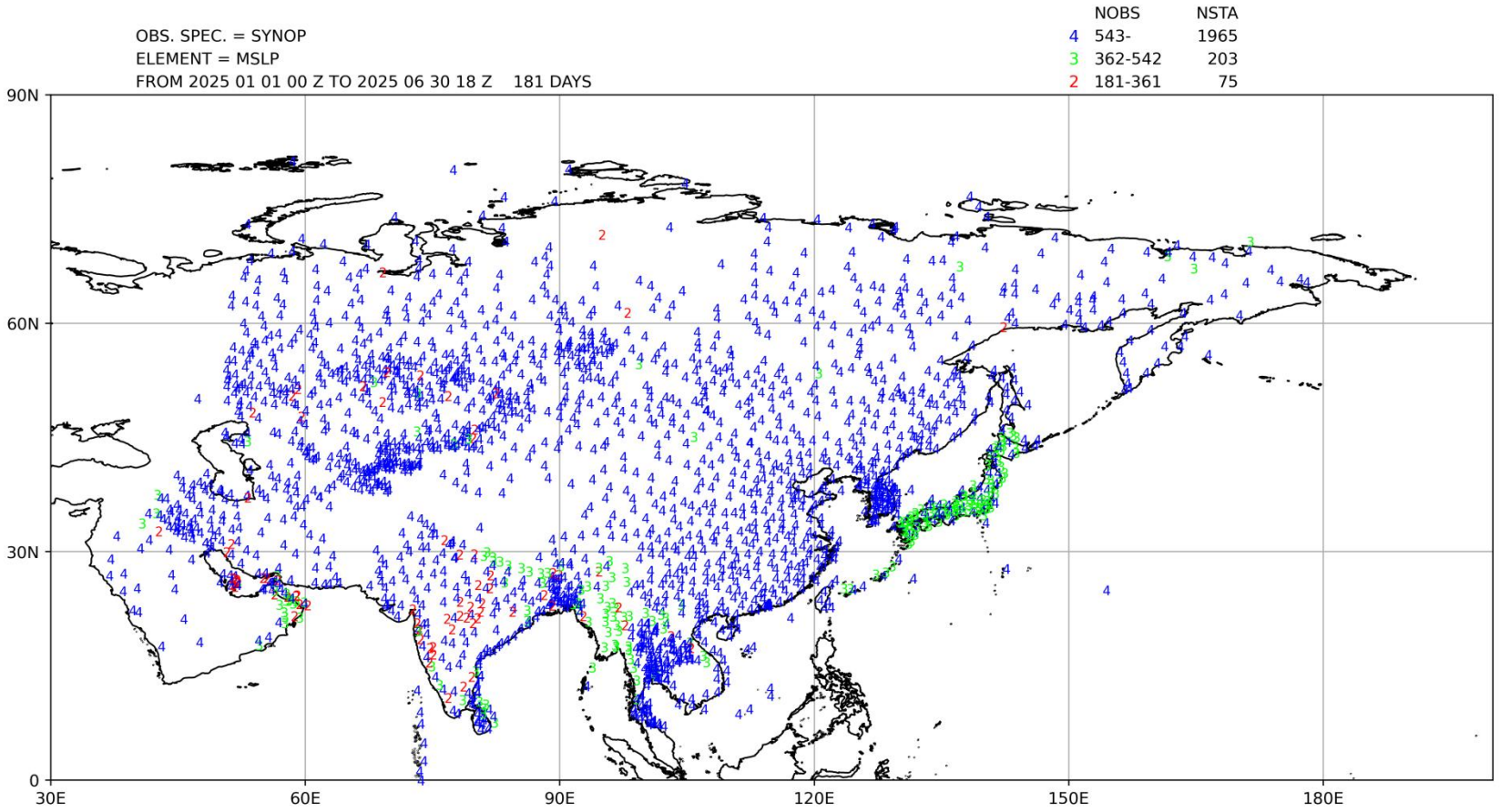

Figure 1(b) Location of all land surface stations reporting mean sea level pressure (MSLP) observations in Region II over the six-month period from January - June 2025. Numbers (2, 3, 4) show the total number of observations (NOBS) received at RWC-Beijing. The total numbers of stations (NSTA) reporting MSLP are shown at the top of the figure. (Data availability)

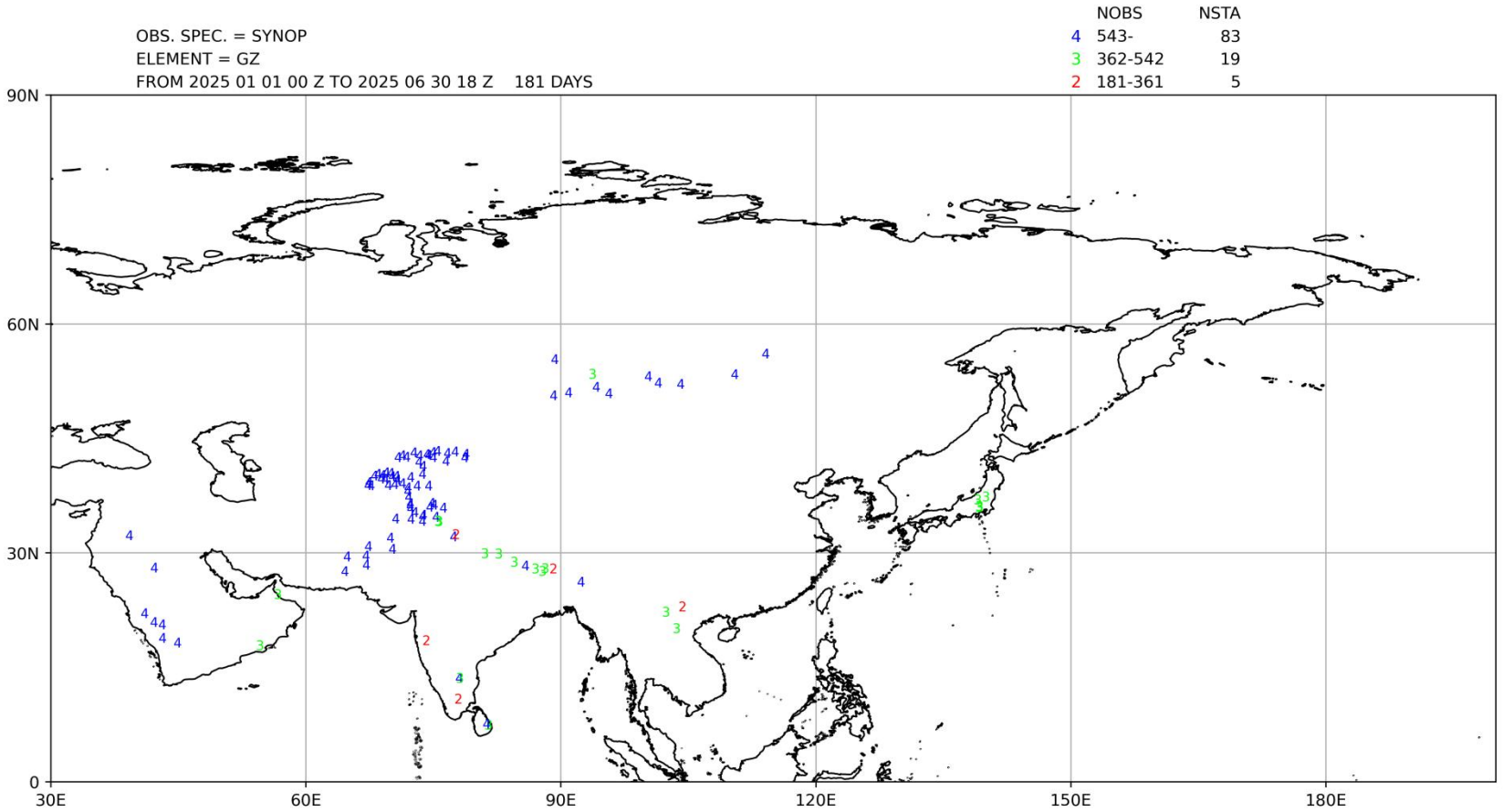

Figure 1(c) Location of all land surface stations reporting geopotential height (GZ) observations in Region II over the six-month period from January - June 2025. Numbers (2, 3, 4) show the total number of observations (NOBS) received at RWC-Beijing. The total numbers of stations (NSTA) reporting GZ are shown at the top of the figure. (Data availability)

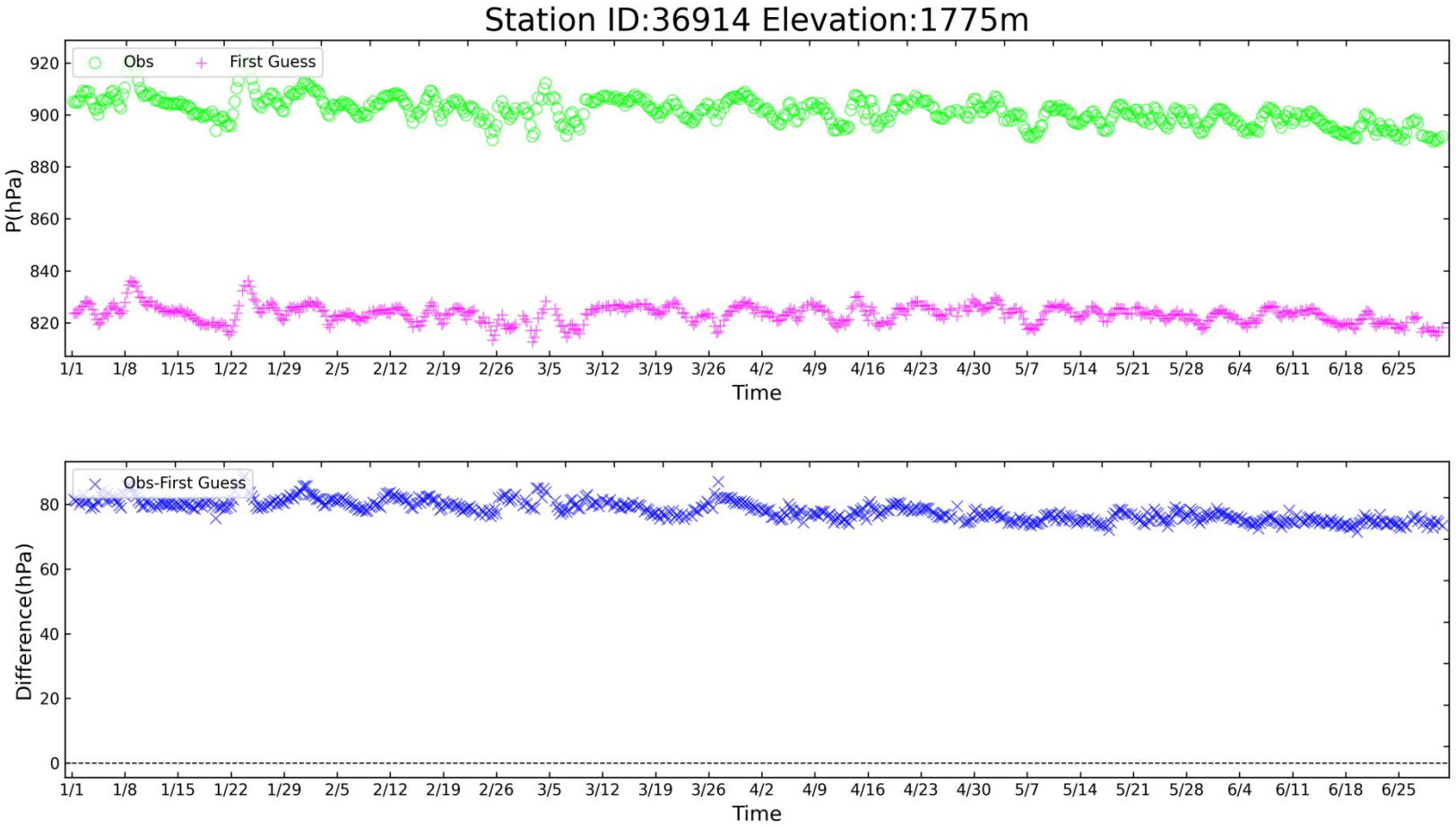

Figure 2 Time-series representation of SLP Obs minus FirstGuess for station 36914*

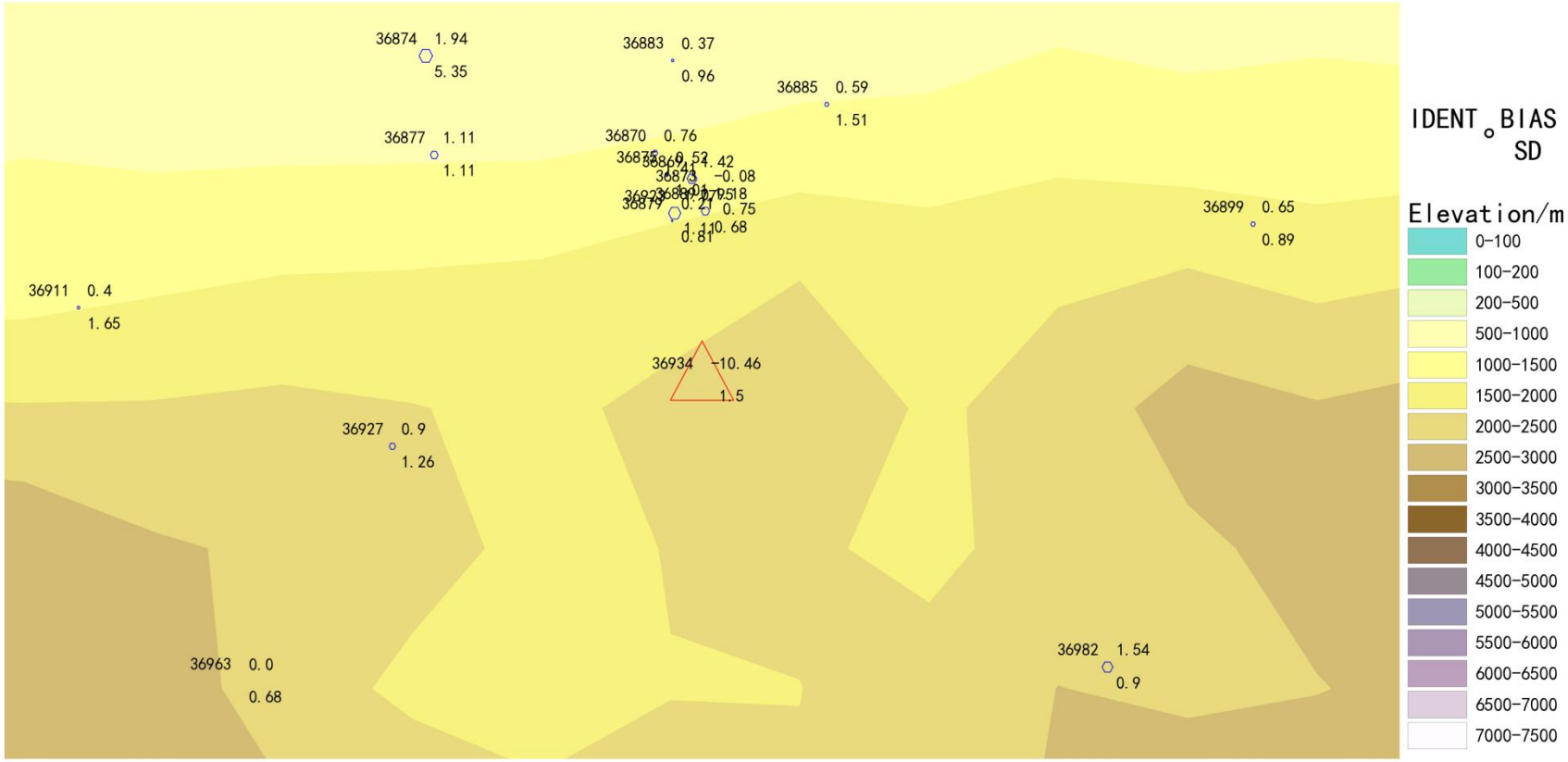

Figure 3 BIAS and SD of SLP for station 36934* (red) and surrounding stations (blue).

The number to the upper left of each symbol is the WMO IDENT, and those to the upper right are the values of BIAS and SD.

The size of each symbol is proportional to the value of BIAS, with hexagonal forms representing positive bias and triangular forms representing negative bias.

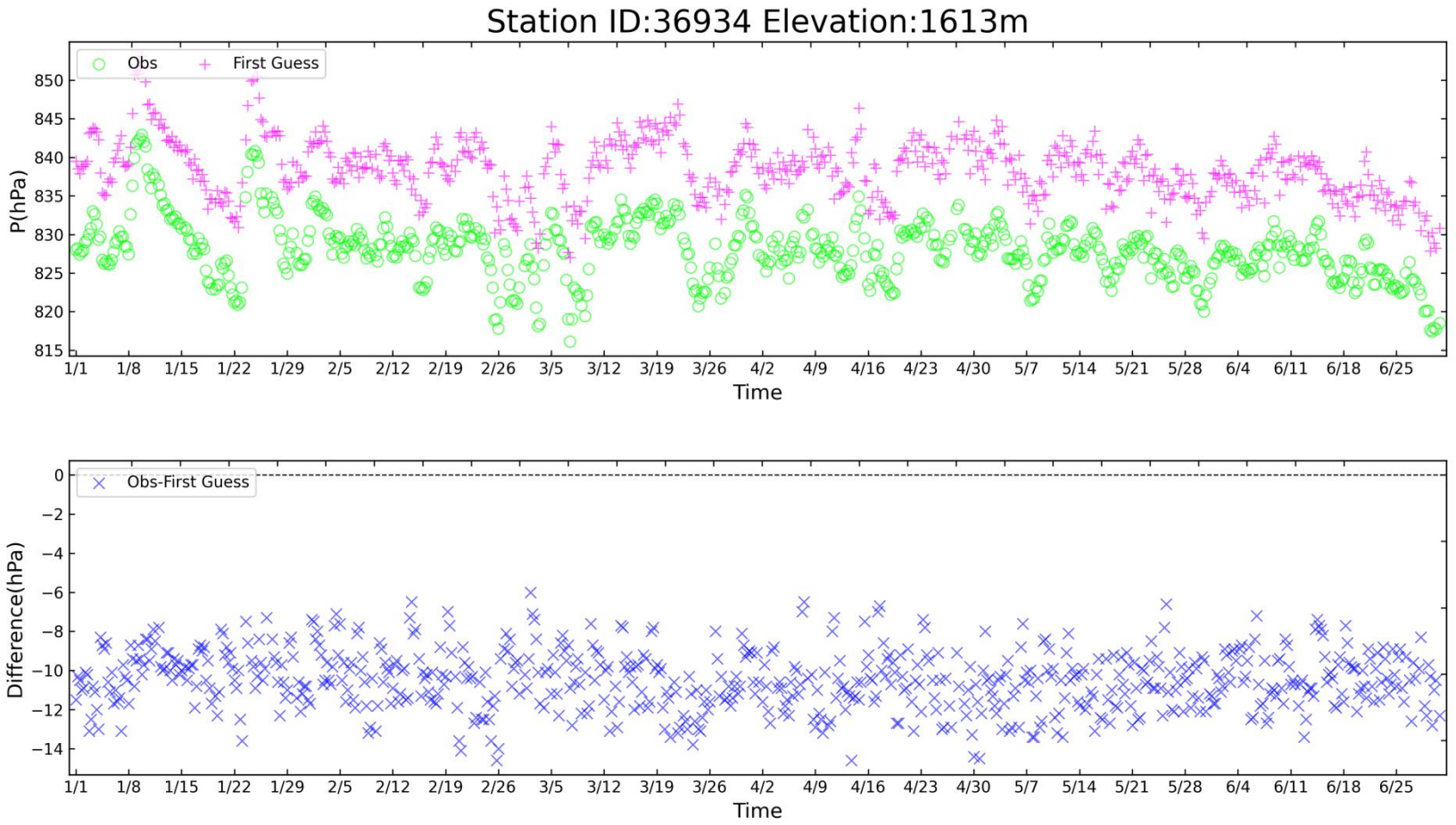

Figure 4 Time-series representation of SLP Obs minus FirstGuess for station 36934*

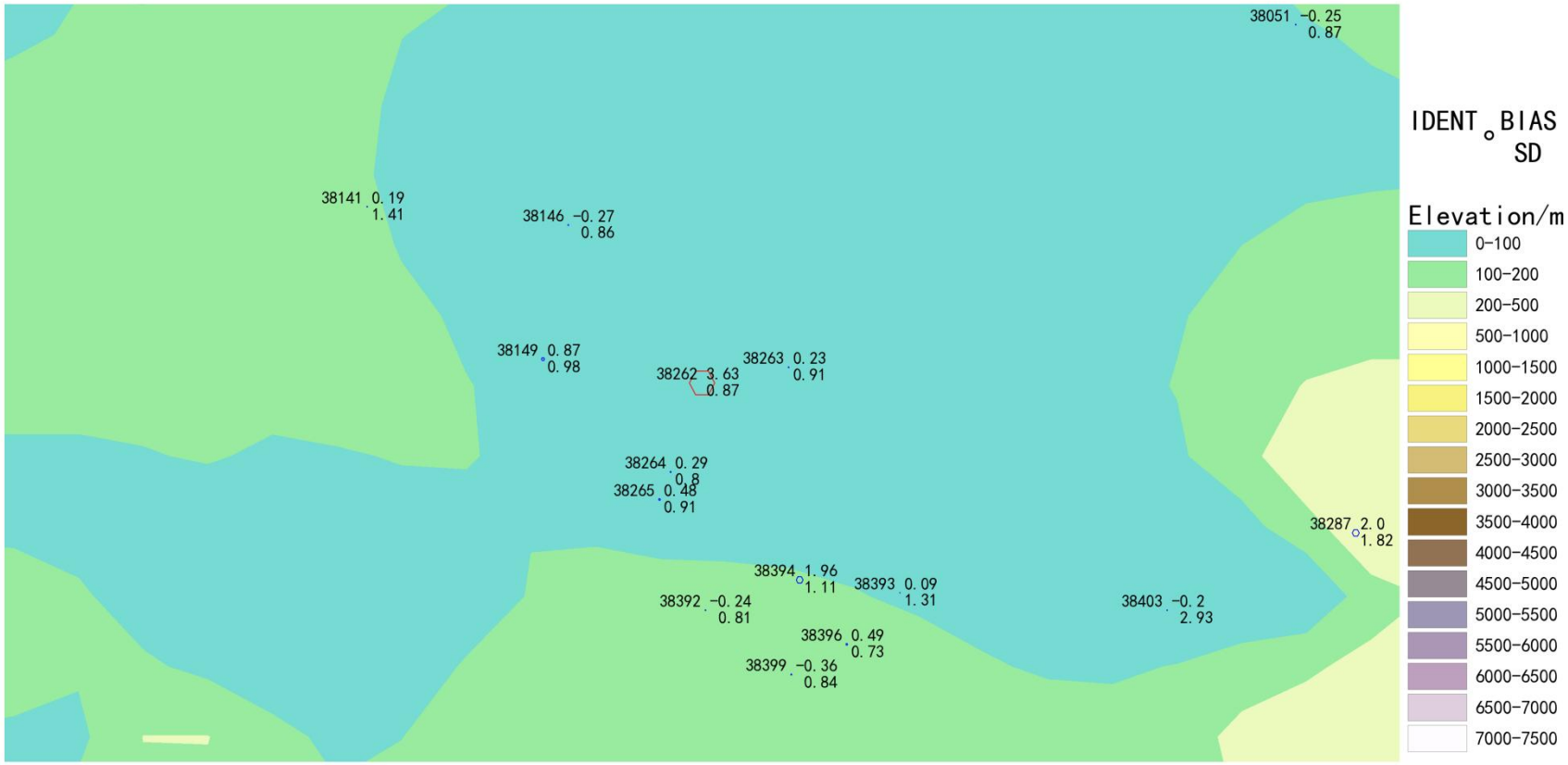

Figure 5 BIAS and SD of SLP for station 38262* (red) and surrounding stations (blue).

The number to the upper left of each symbol is the WMO IDENT, and those to the upper right are the values of BIAS and SD.

The size of each symbol is proportional to the value of BIAS, with hexagonal forms representing positive bias and triangular forms representing negative bias.

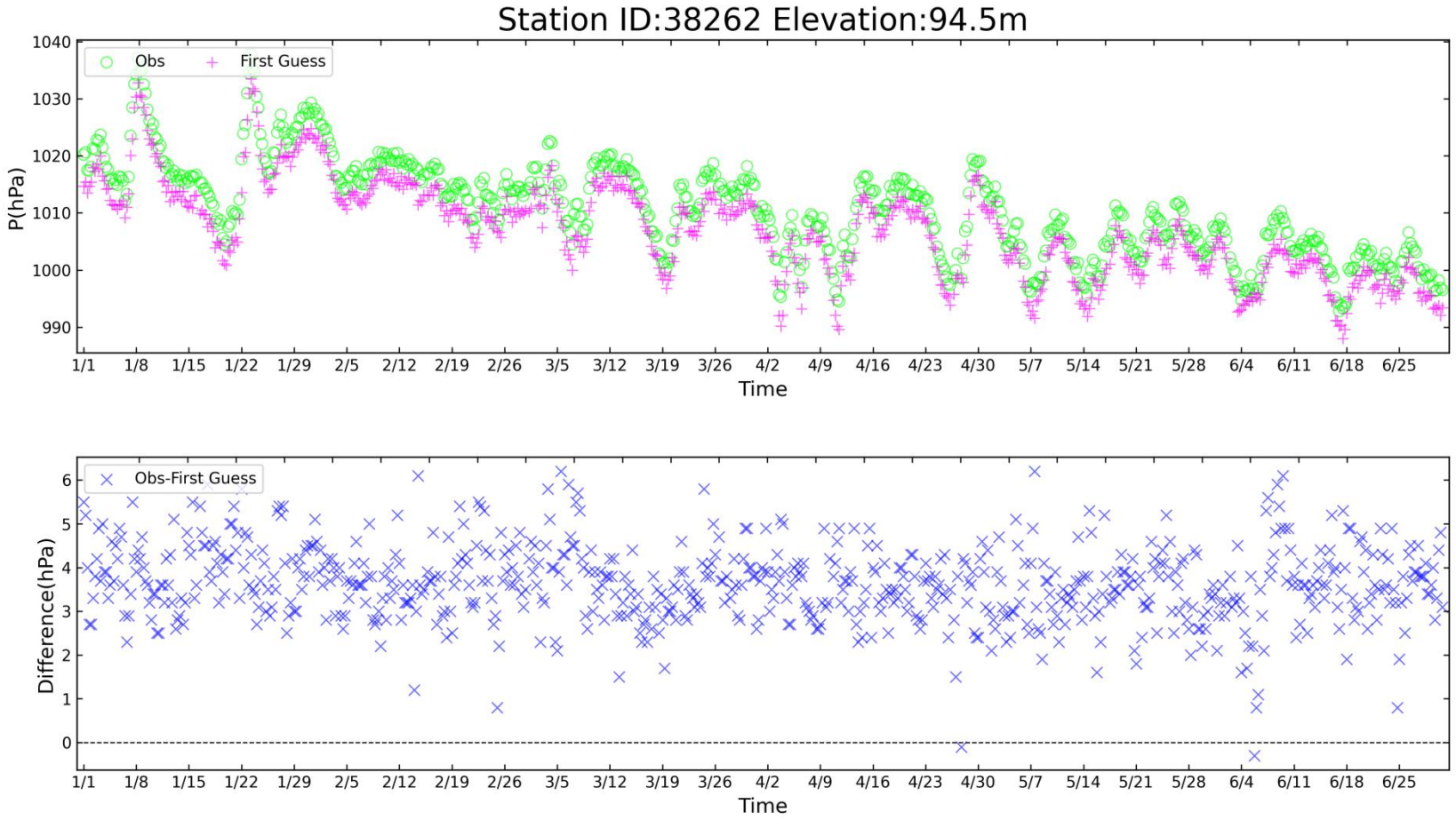

Figure 6 Time-series representation of SLP Obs minus FirstGuess for station 38262*

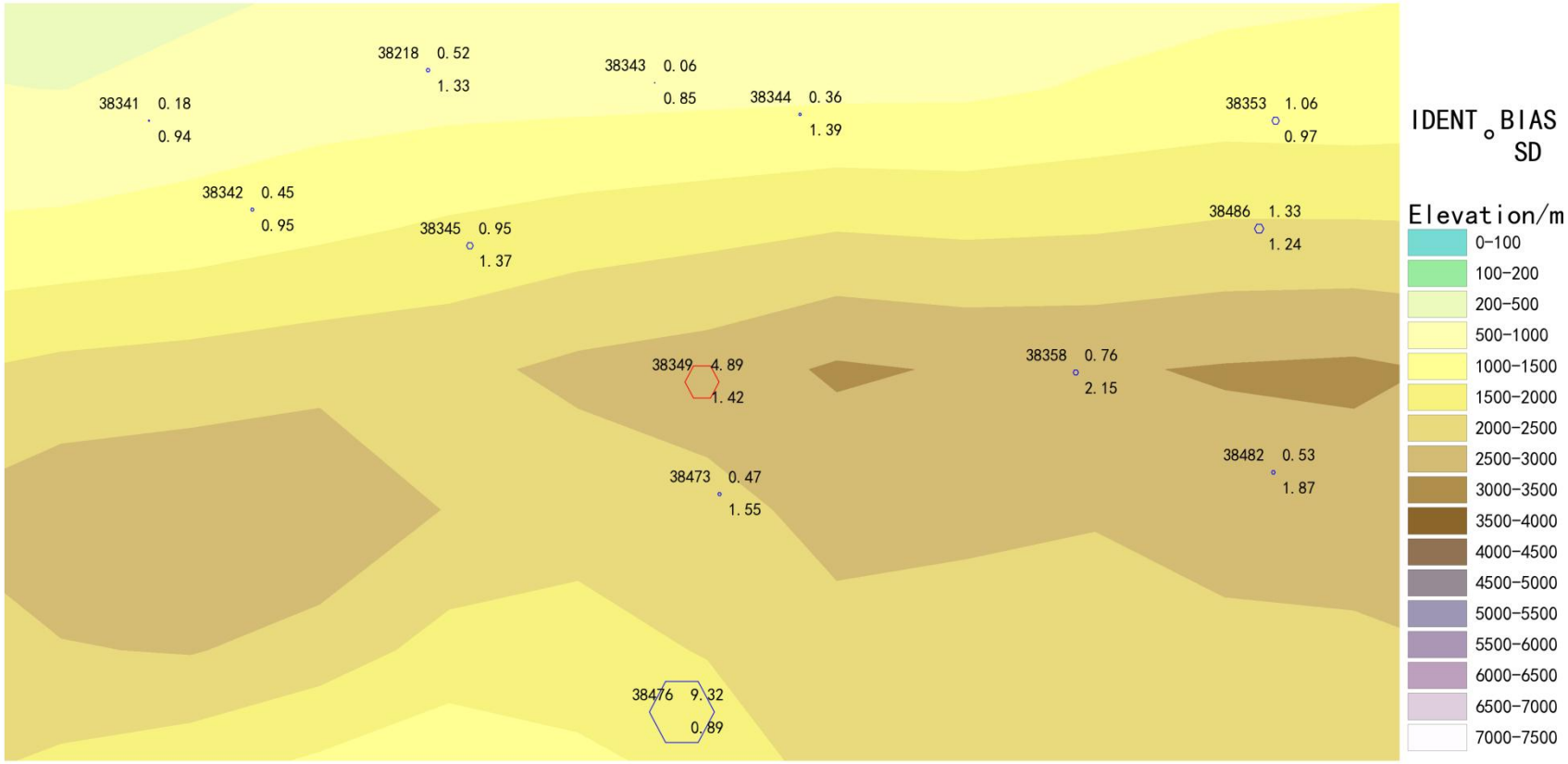

Figure 7 BIAS and SD of SLP for station 38349* (red) and surrounding stations (blue).
The number to the upper left of each symbol is the WMO IDENT, and those to the upper right are the values of BIAS and SD.
The size of each symbol is proportional to the value of BIAS, with hexagonal forms representing positive bias and triangular forms representing negative bias.

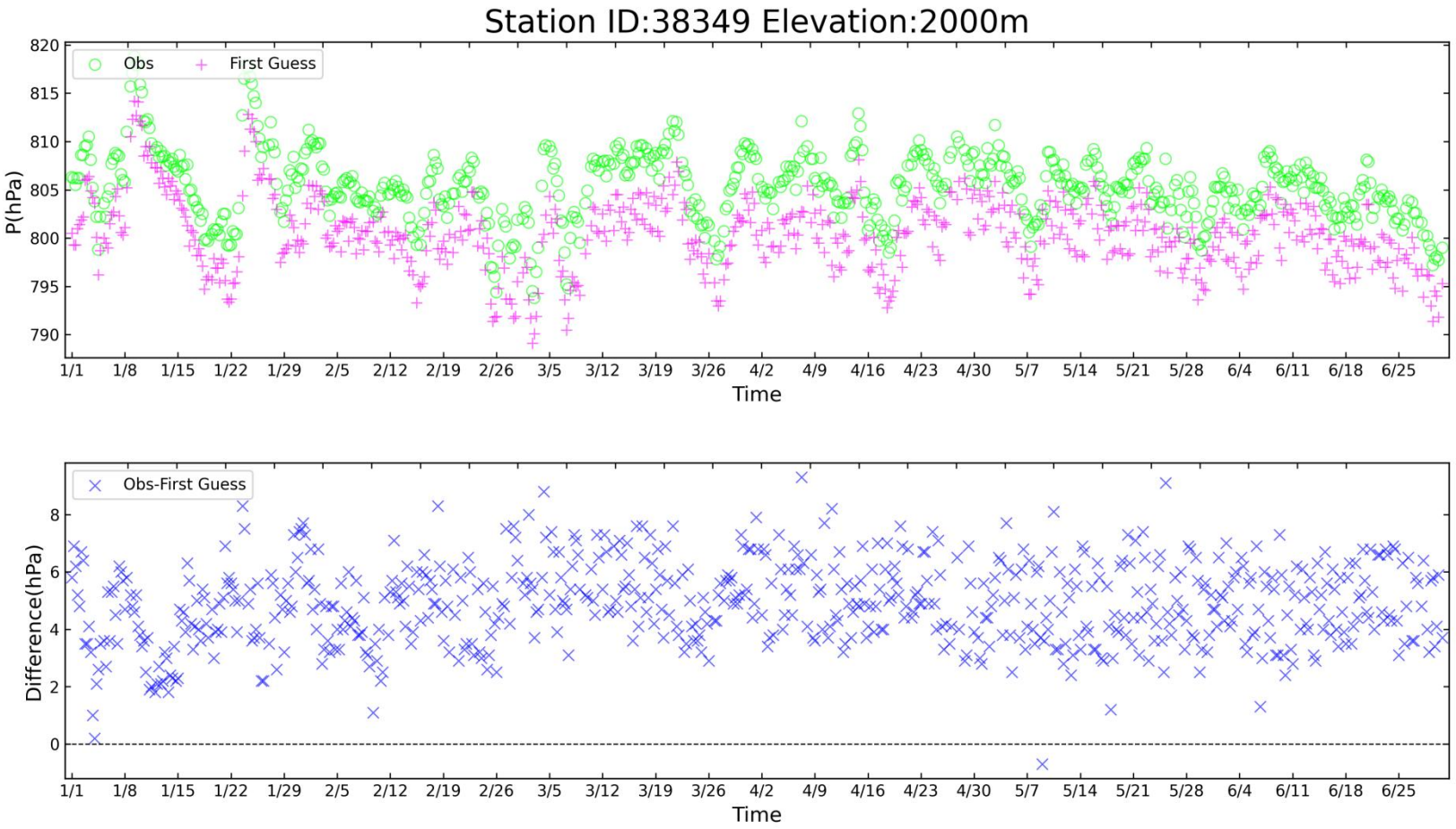

Figure 8 Time-series representation of SLP Obs minus FirstGuess for station 38349*

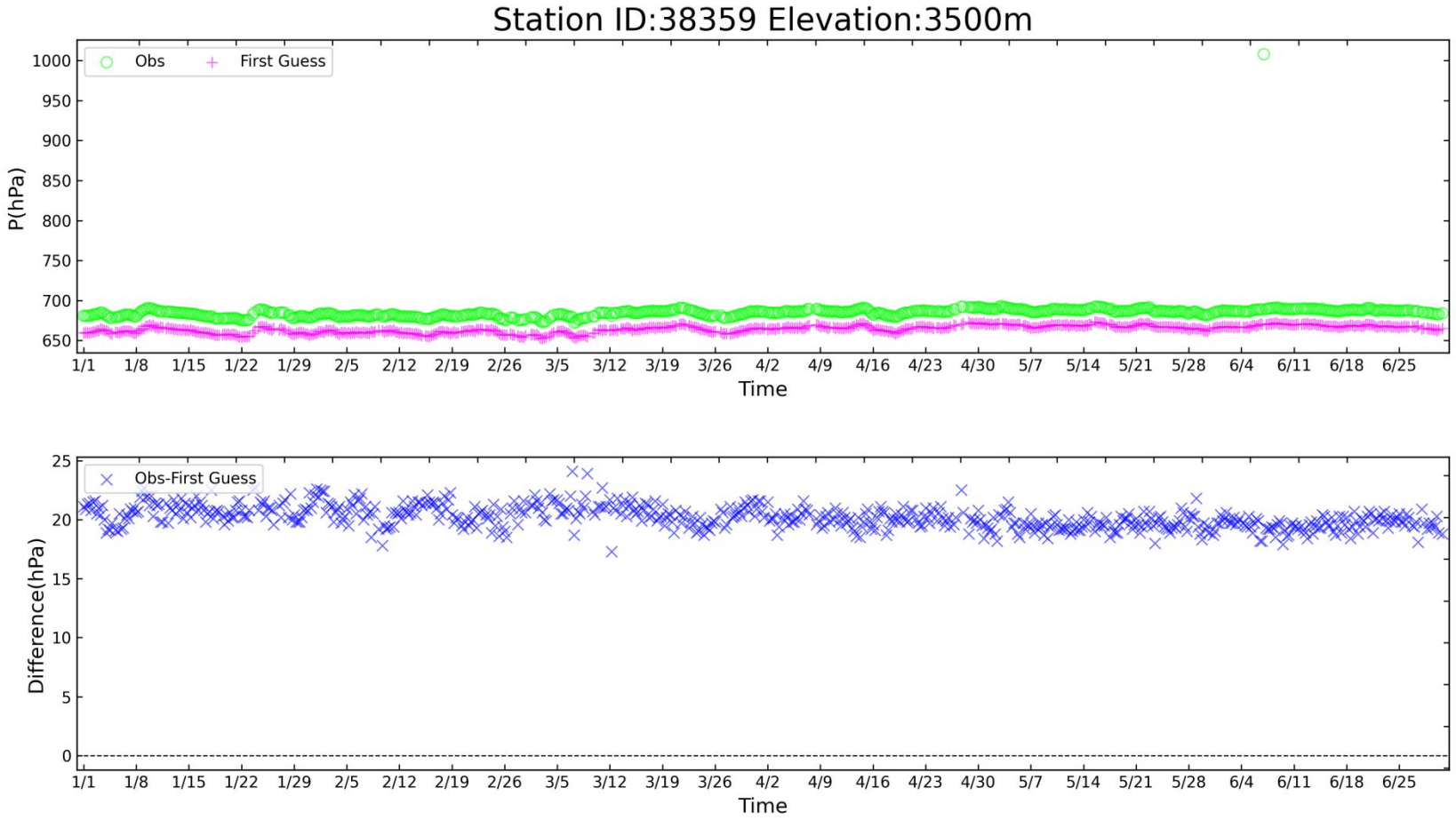

Figure 9 Time-series representation of SLP Obs minus FirstGuess for station 38359*

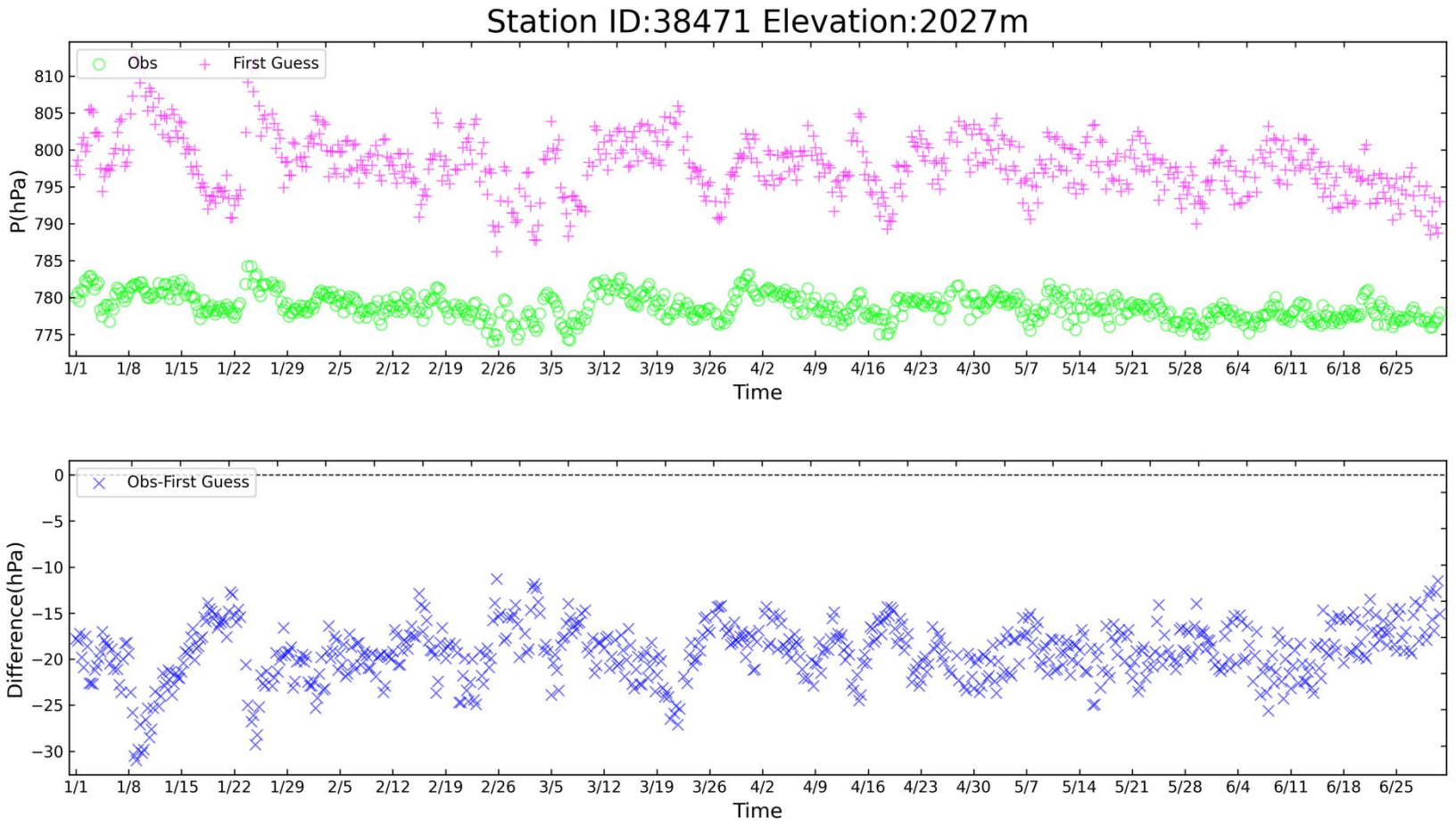

Figure 10 Time-series representation of SLP Obs minus FirstGuess for station 38471*

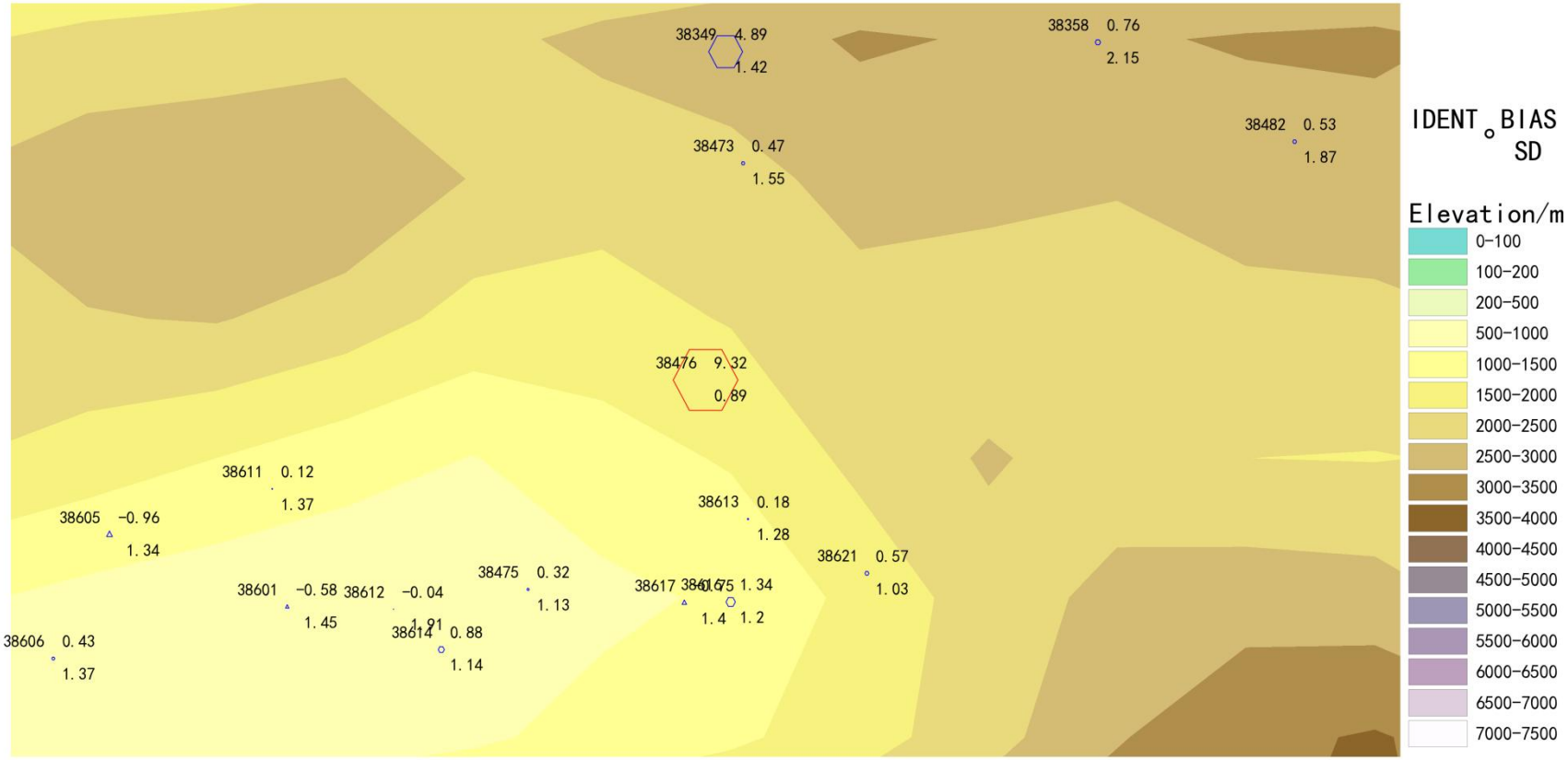

Figure 11 BIAS and SD of SLP for station 38476* (red) and surrounding stations (blue).
The number to the upper left of each symbol is the WMO IDENT, and those to the upper right are the values of BIAS and SD.
The size of each symbol is proportional to the value of BIAS, with hexagonal forms representing positive bias and triangular forms representing negative bias.

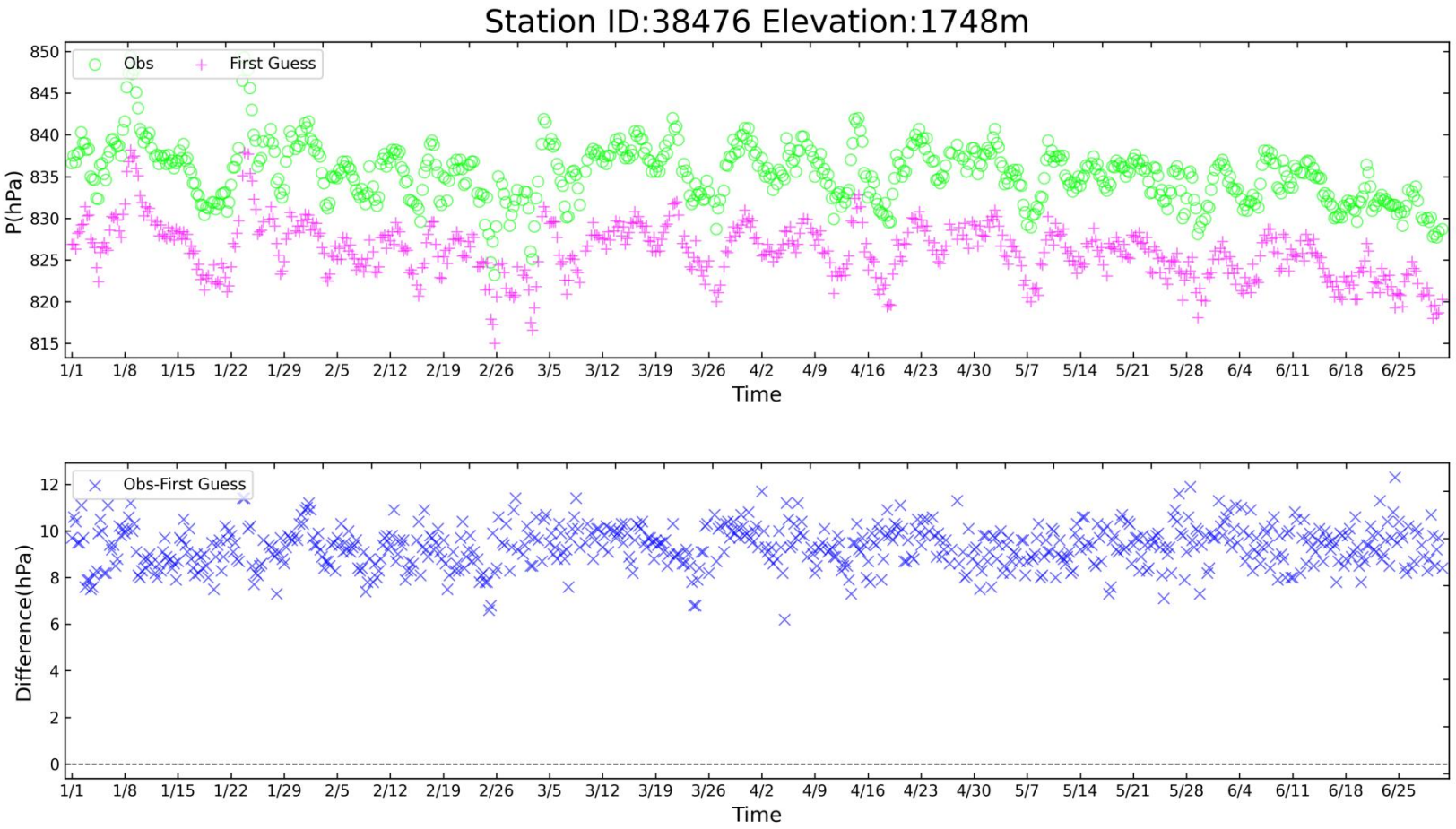

Figure 12 Time-series representation of SLP Obs minus FirstGuess for station 38476*

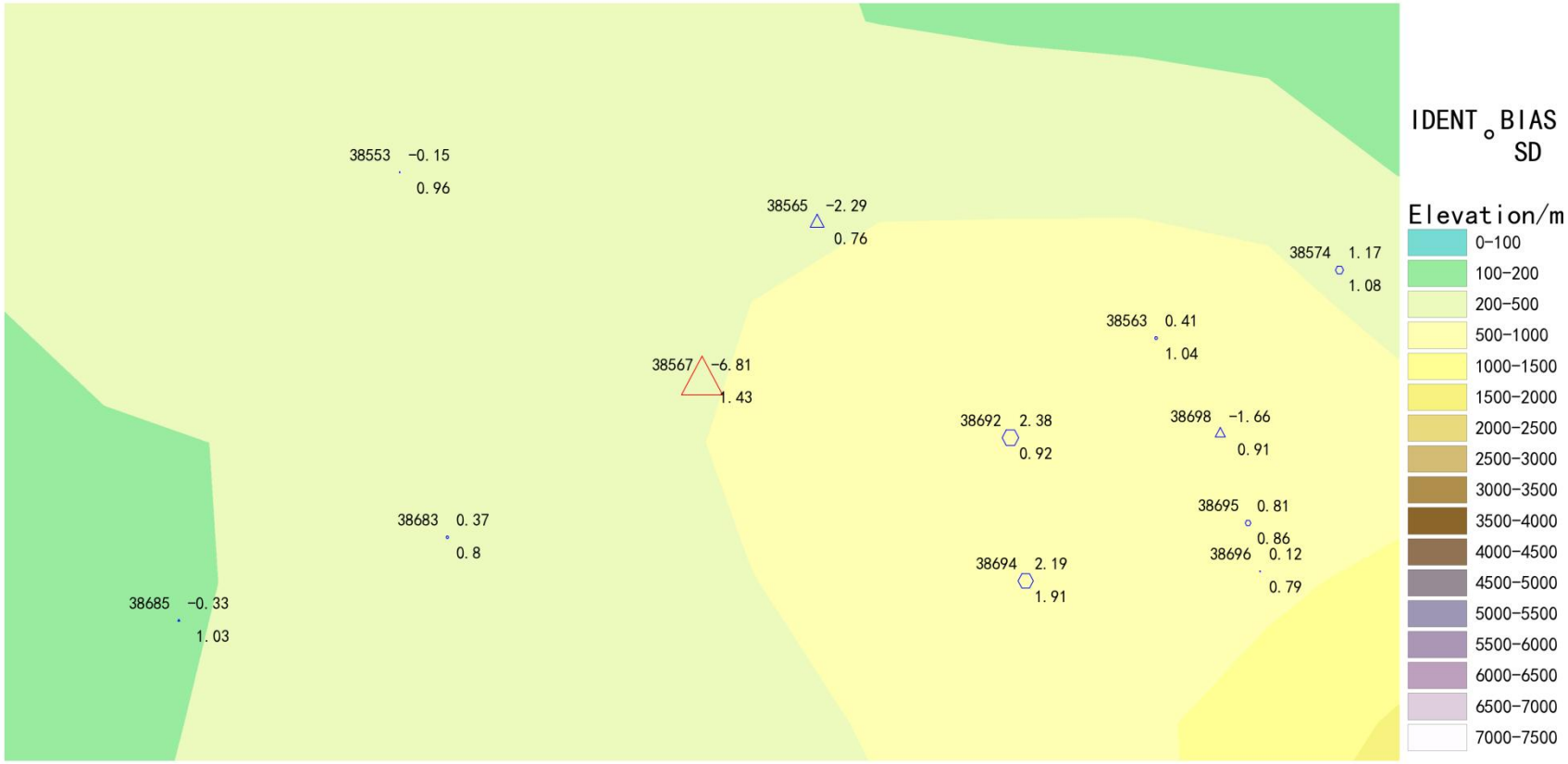

Figure 13 BIAS and SD of SLP for station 38567 (red) and surrounding stations (blue).
The number to the upper left of each symbol is the WMO IDENT, and those to the upper right are the values of BIAS and SD.
The size of each symbol is proportional to the value of BIAS, with hexagonal forms representing positive bias and triangular forms representing negative bias.

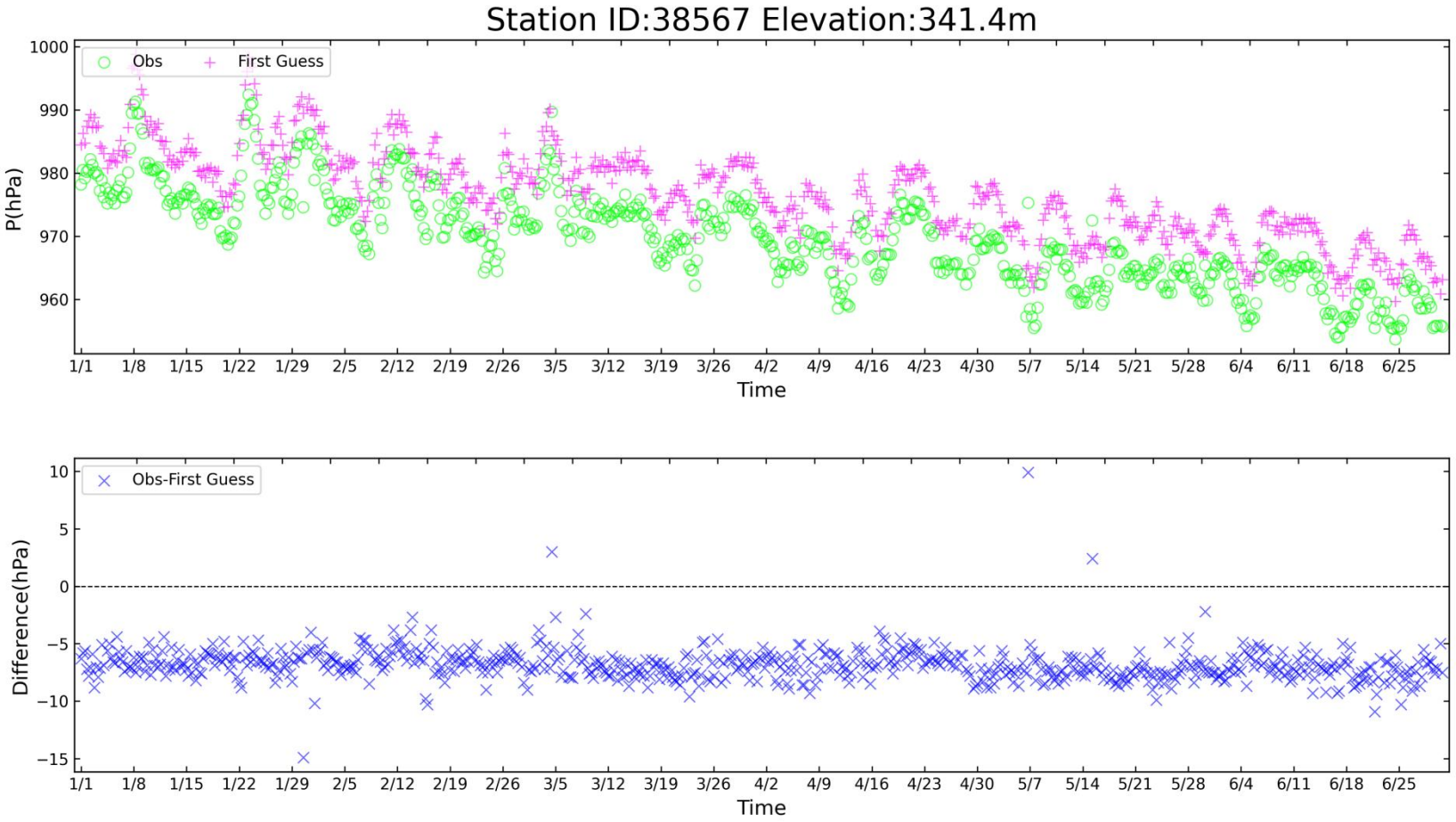

Figure 14 Time-series representation of SLP Obs minus FirstGuess for station 38567

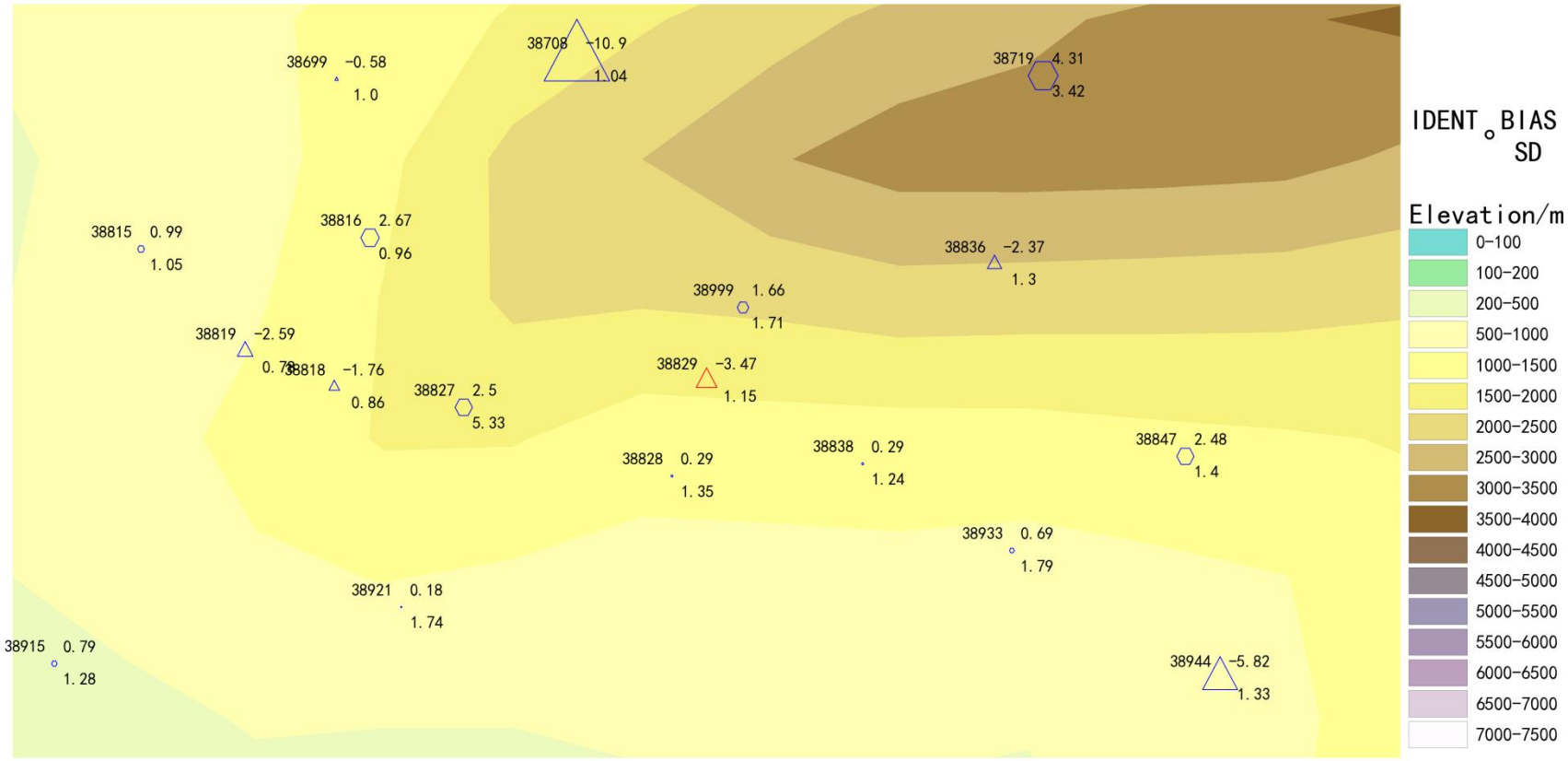

Figure 15 BIAS and SD of SLP for station 38829 (red) and surrounding stations (blue).

The number to the upper left of each symbol is the WMO IDENT, and those to the upper right are the values of BIAS and SD.

The size of each symbol is proportional to the value of BIAS, with hexagonal forms representing positive bias and triangular forms representing negative bias.

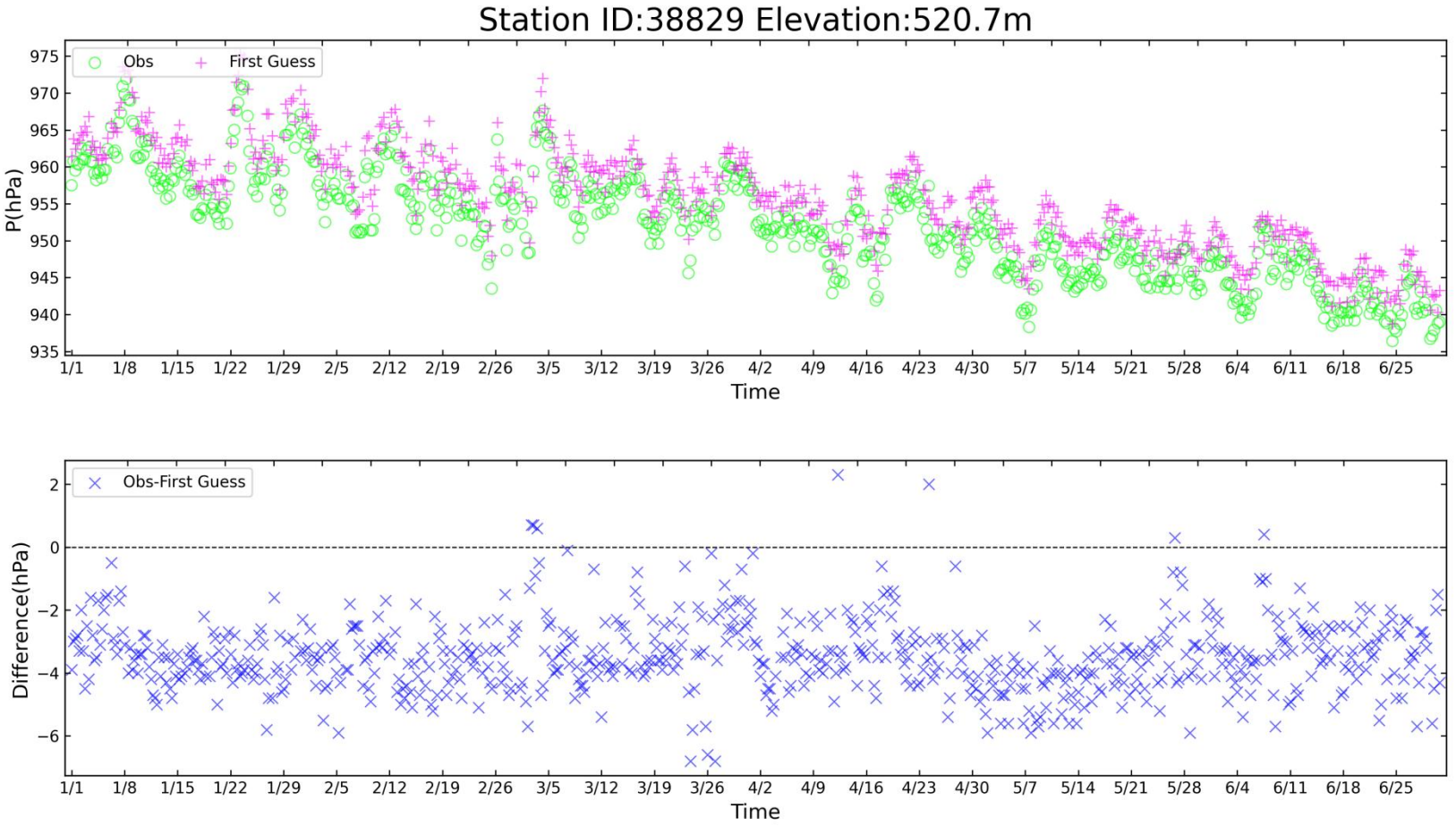

Figure 16 Time-series representation of SLP Obs minus FirstGuess for station 38829

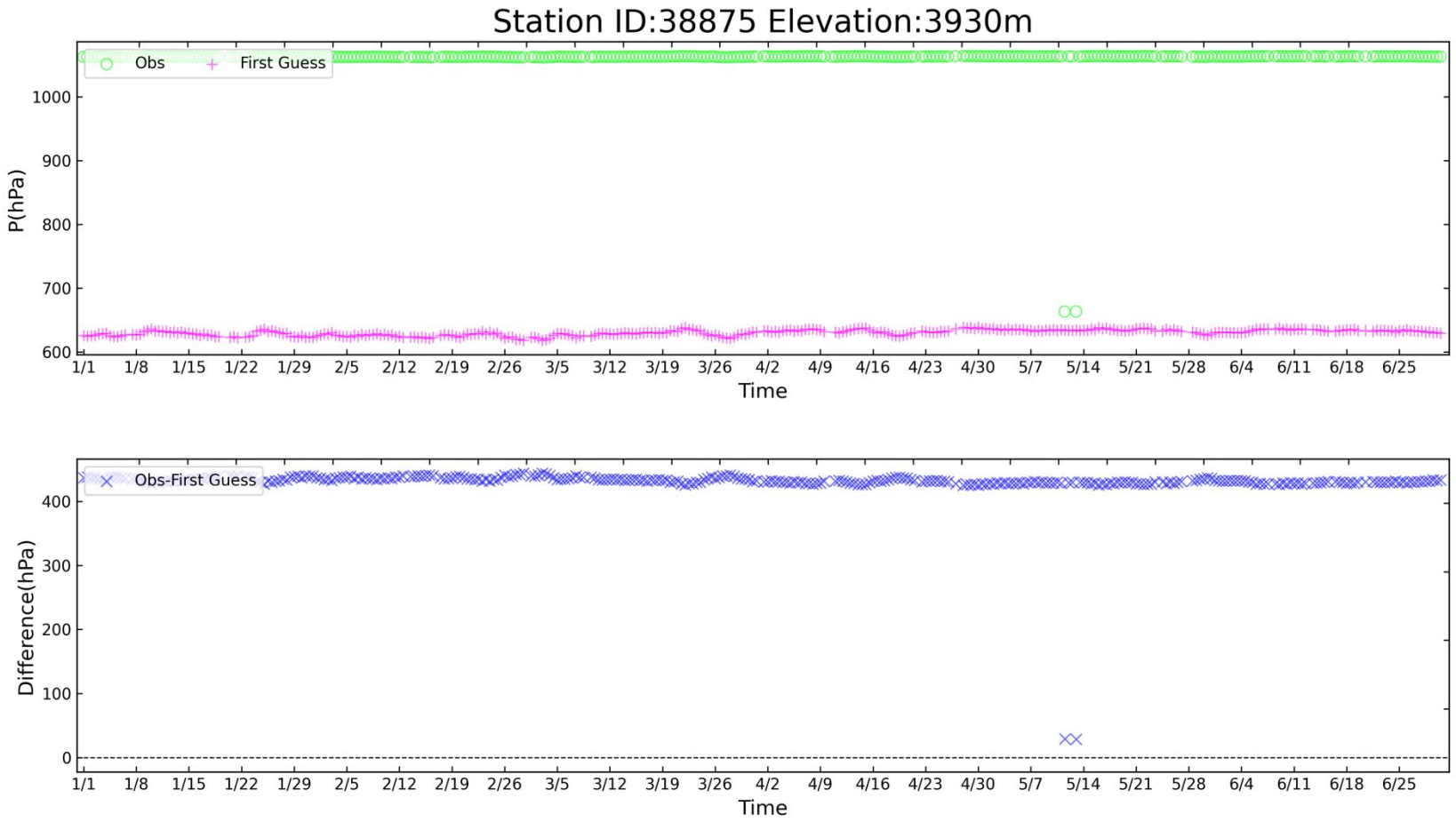

Figure 17 Time-series representation of SLP Obs minus FirstGuess for station 38875

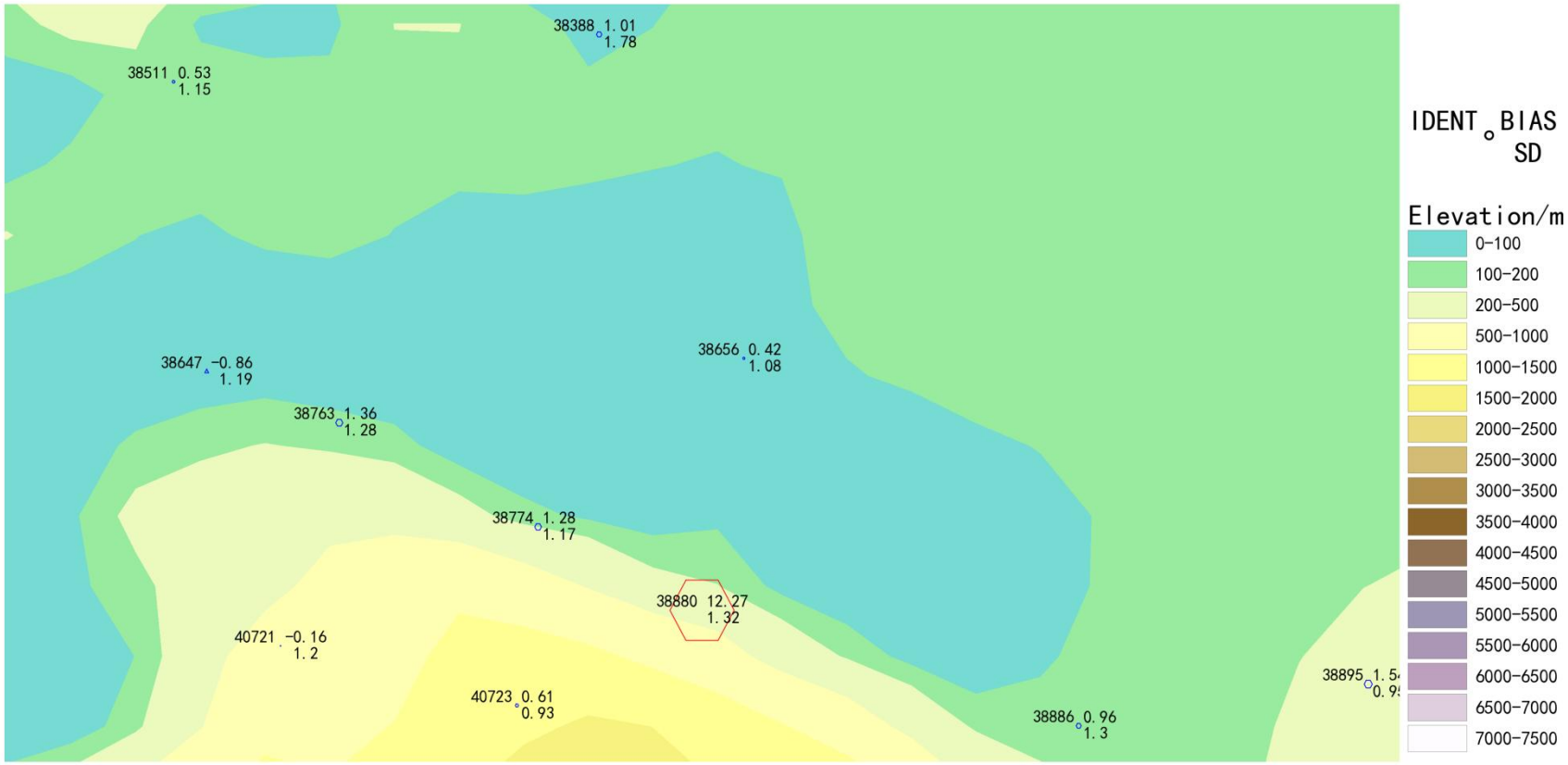

Figure 18 BIAS and SD of SLP for station 38880* (red) and surrounding stations (blue).
The number to the upper left of each symbol is the WMO IDENT, and those to the upper right are the values of BIAS and SD.
The size of each symbol is proportional to the value of BIAS, with hexagonal forms representing positive bias and triangular forms representing negative bias.

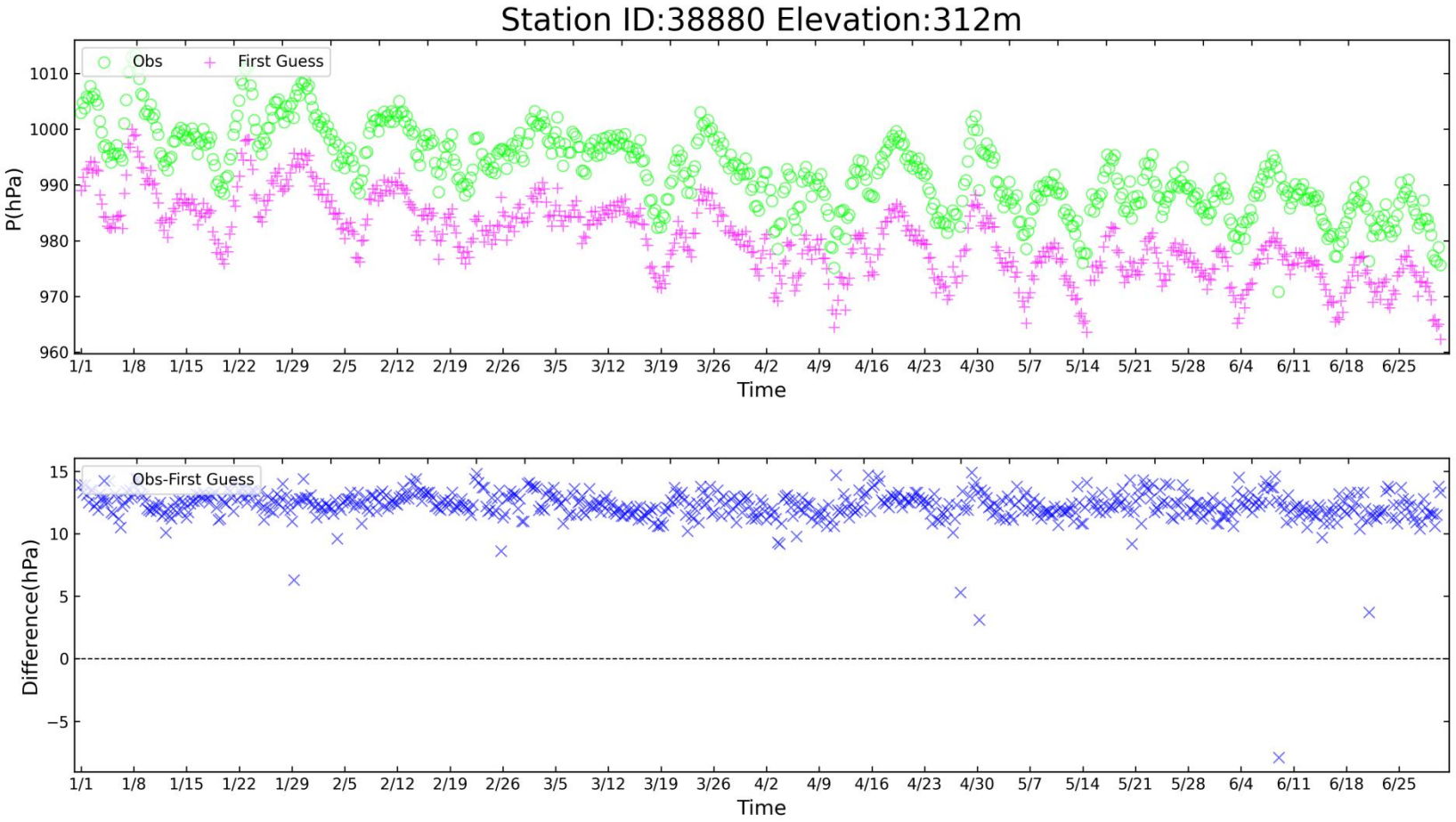

Figure 19 Time-series representation of SLP Obs minus FirstGuess for station 38880*

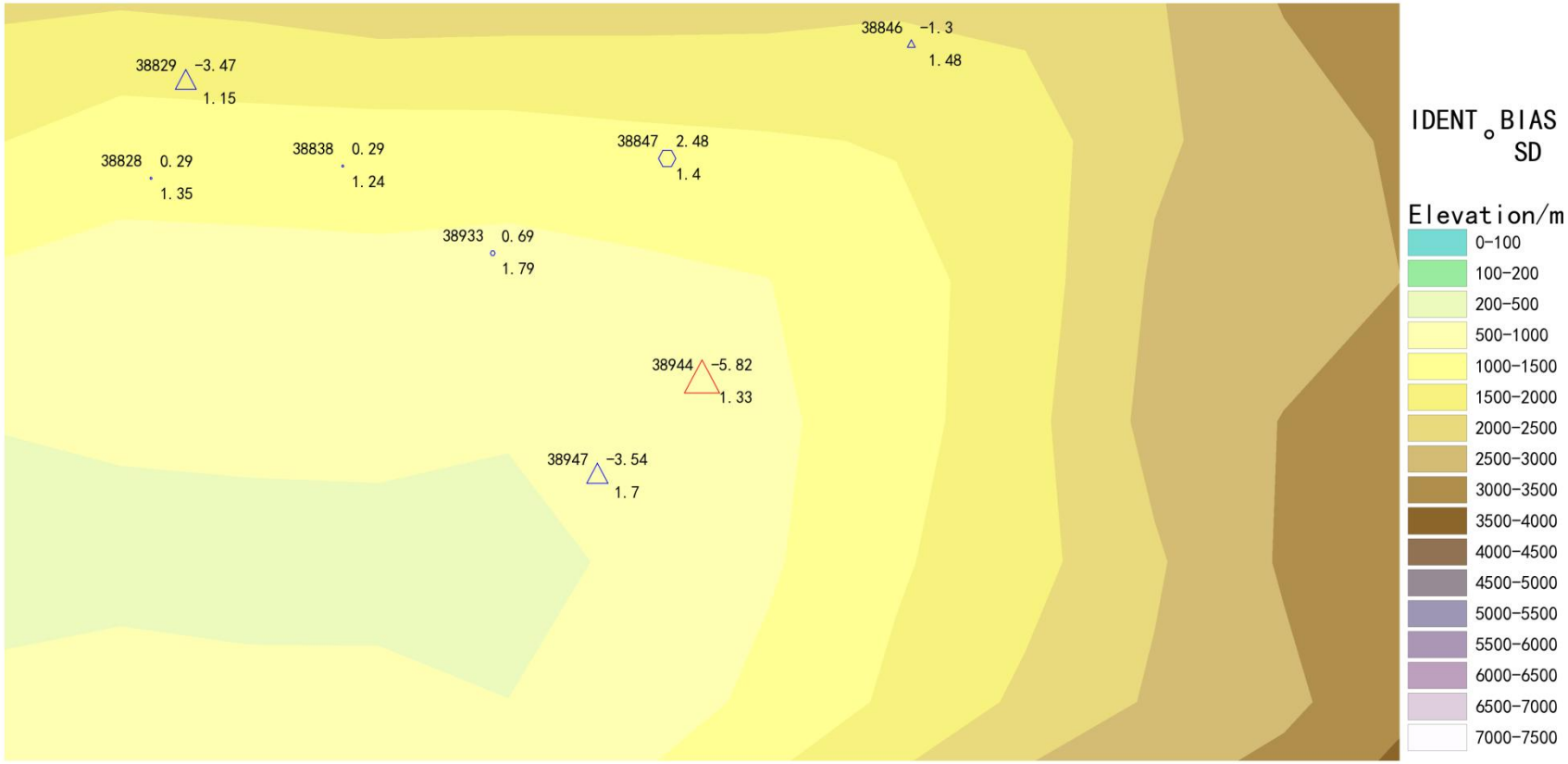

Figure 20 BIAS and SD of SLP for station 38944* (red) and surrounding stations (blue).
The number to the upper left of each symbol is the WMO IDENT, and those to the upper right are the values of BIAS and SD.
The size of each symbol is proportional to the value of BIAS, with hexagonal forms representing positive bias and triangular forms representing negative bias.

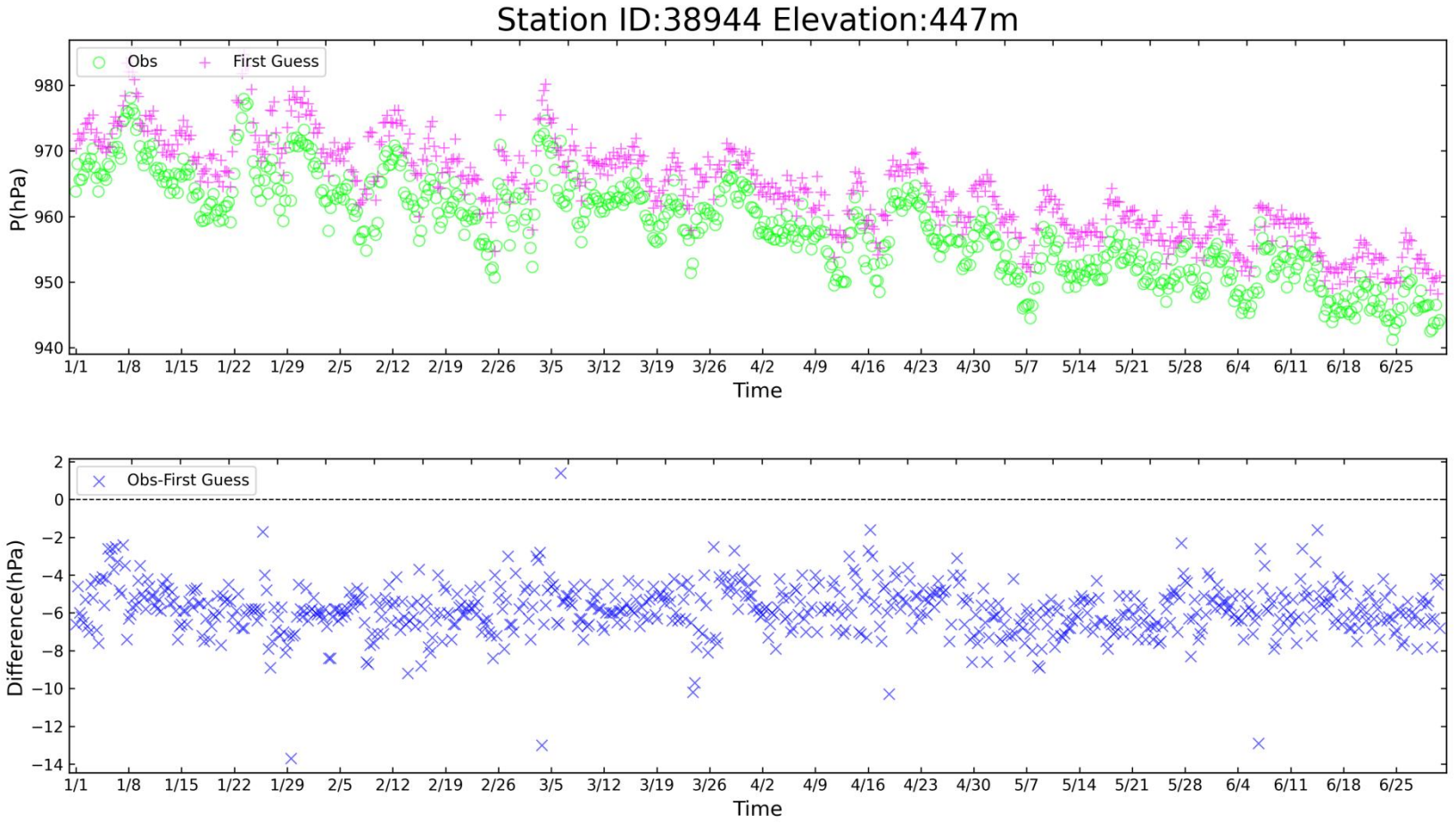

Figure 21 Time-series representation of SLP Obs minus FirstGuess for station 38944*

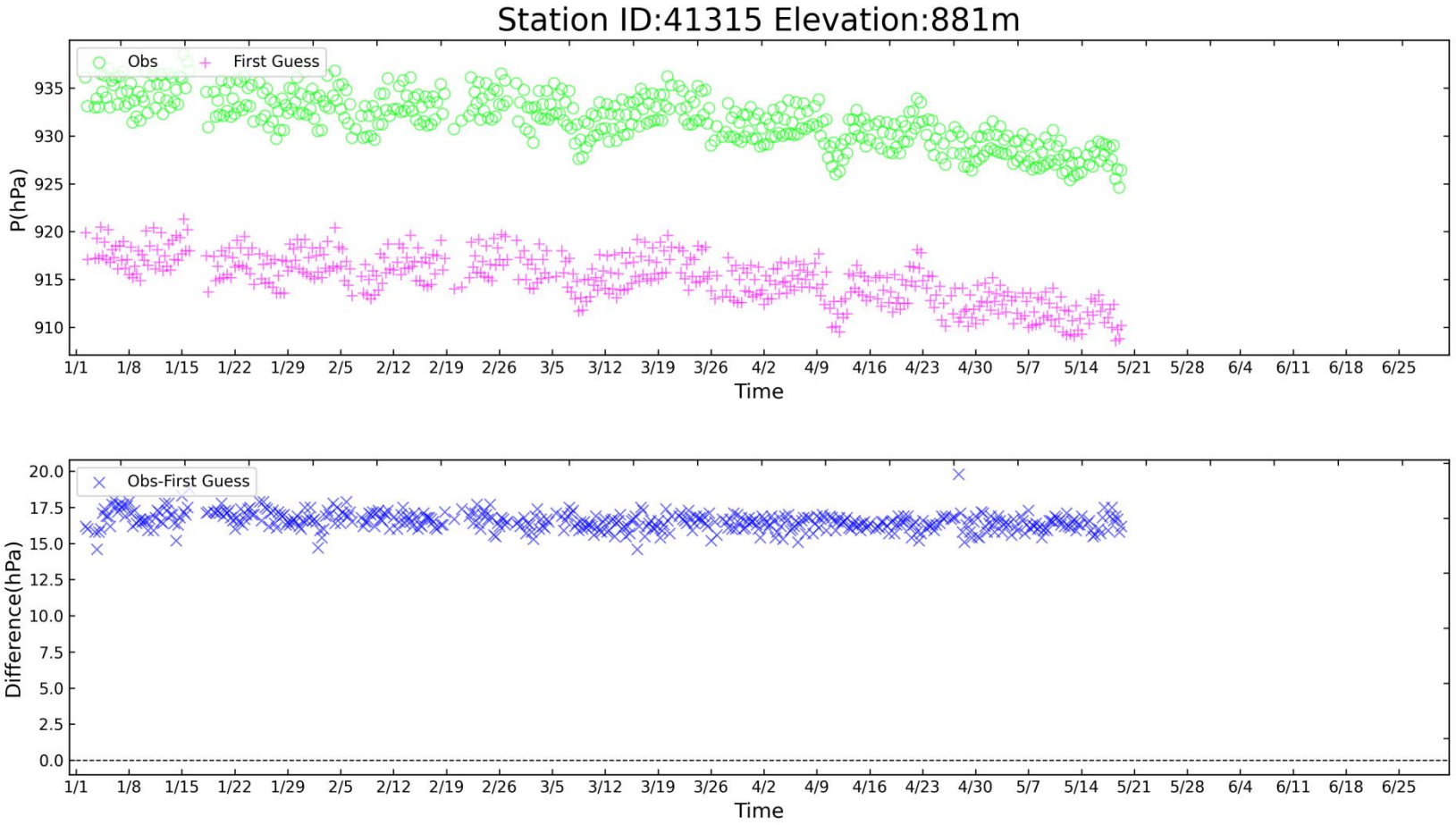

Figure 22 Time-series representation of SLP Obs minus FirstGuess for station 41315*

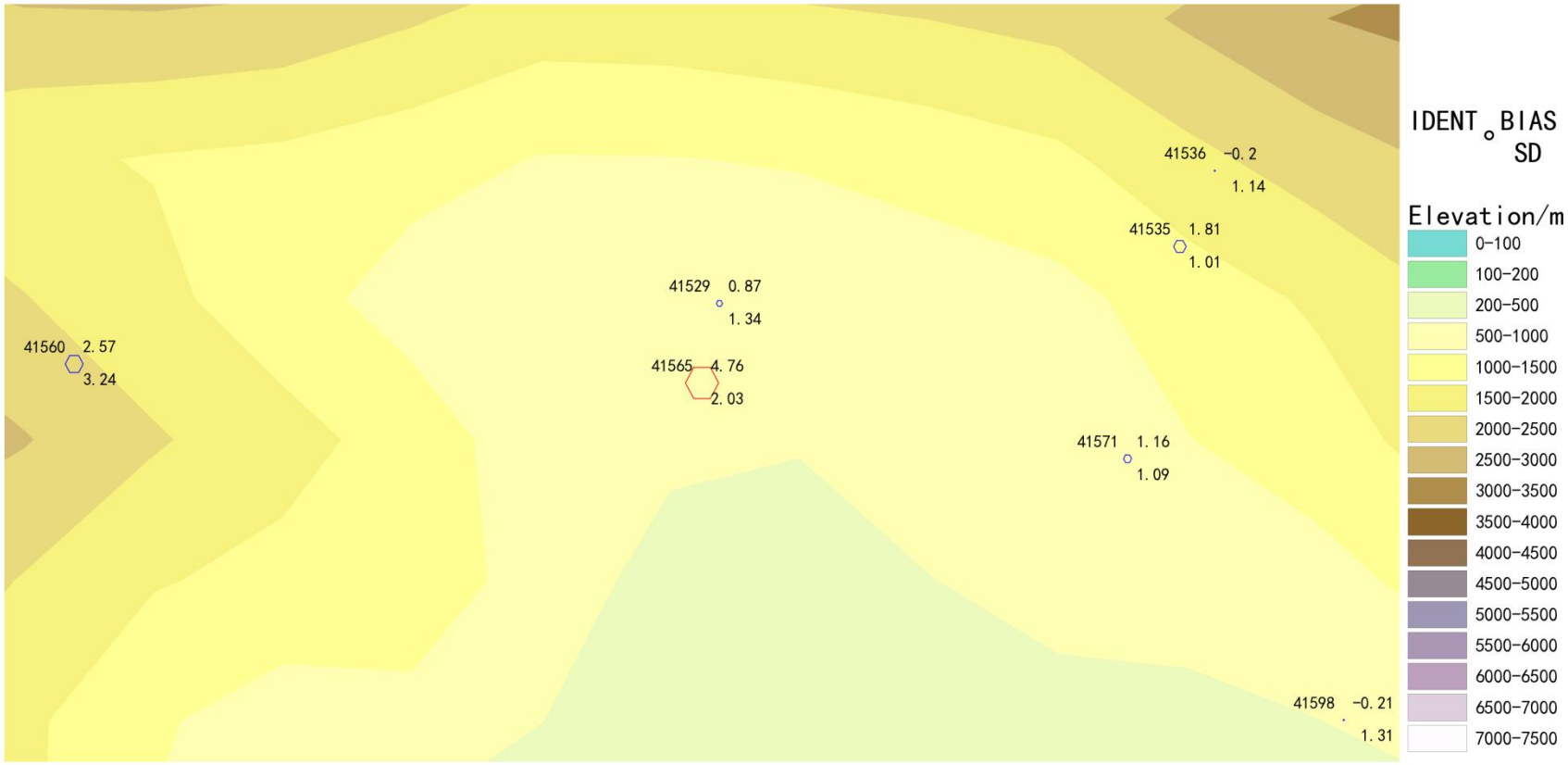

Figure 23 BIAS and SD of SLP for station 41565 (red) and surrounding stations (blue).
The number to the upper left of each symbol is the WMO IDENT, and those to the upper right are the values of BIAS and SD.
The size of each symbol is proportional to the value of BIAS, with hexagonal forms representing positive bias and triangular forms representing negative bias.

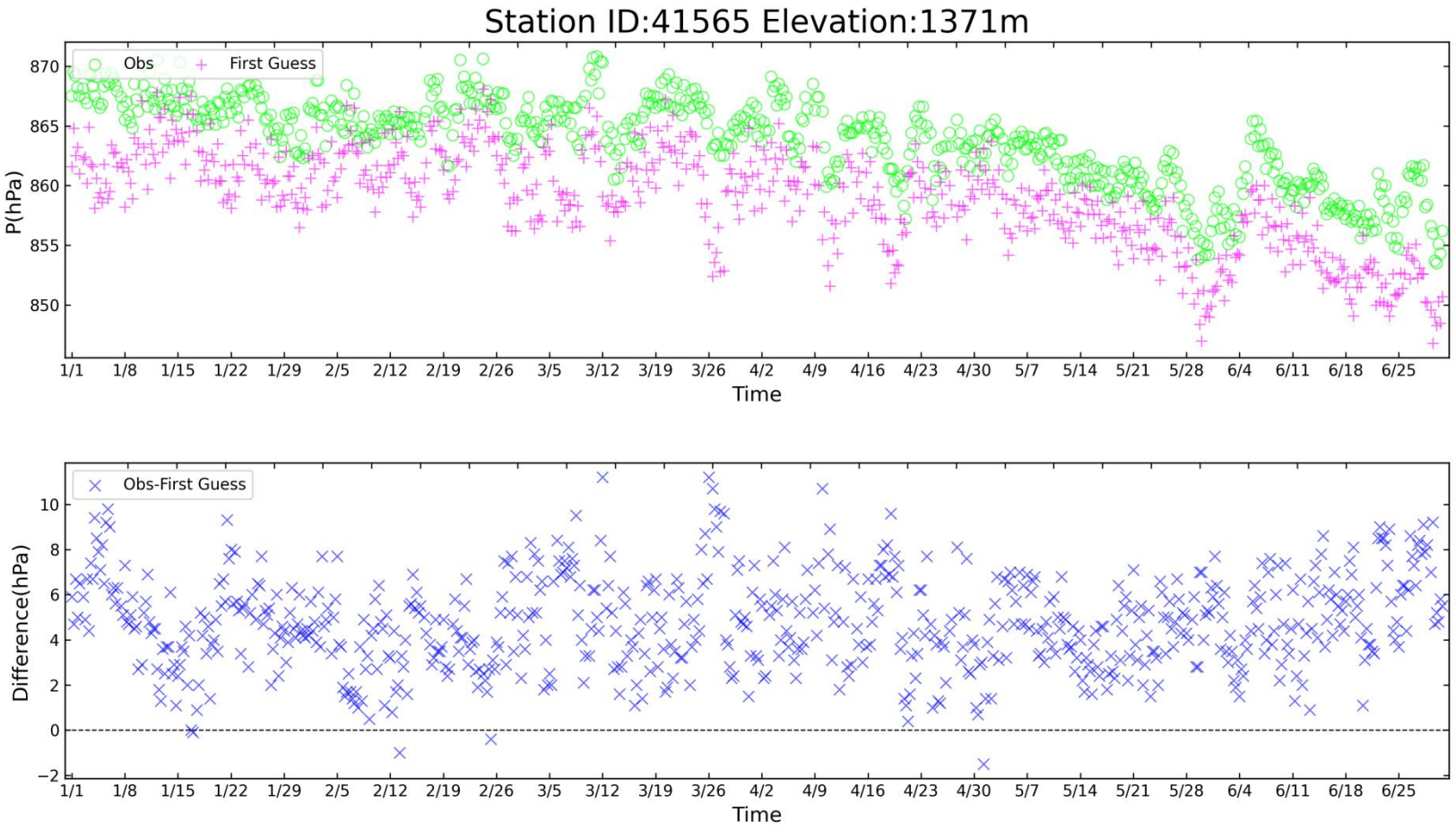

Figure 24 Time-series representation of SLP Obs minus FirstGuess for station 41565

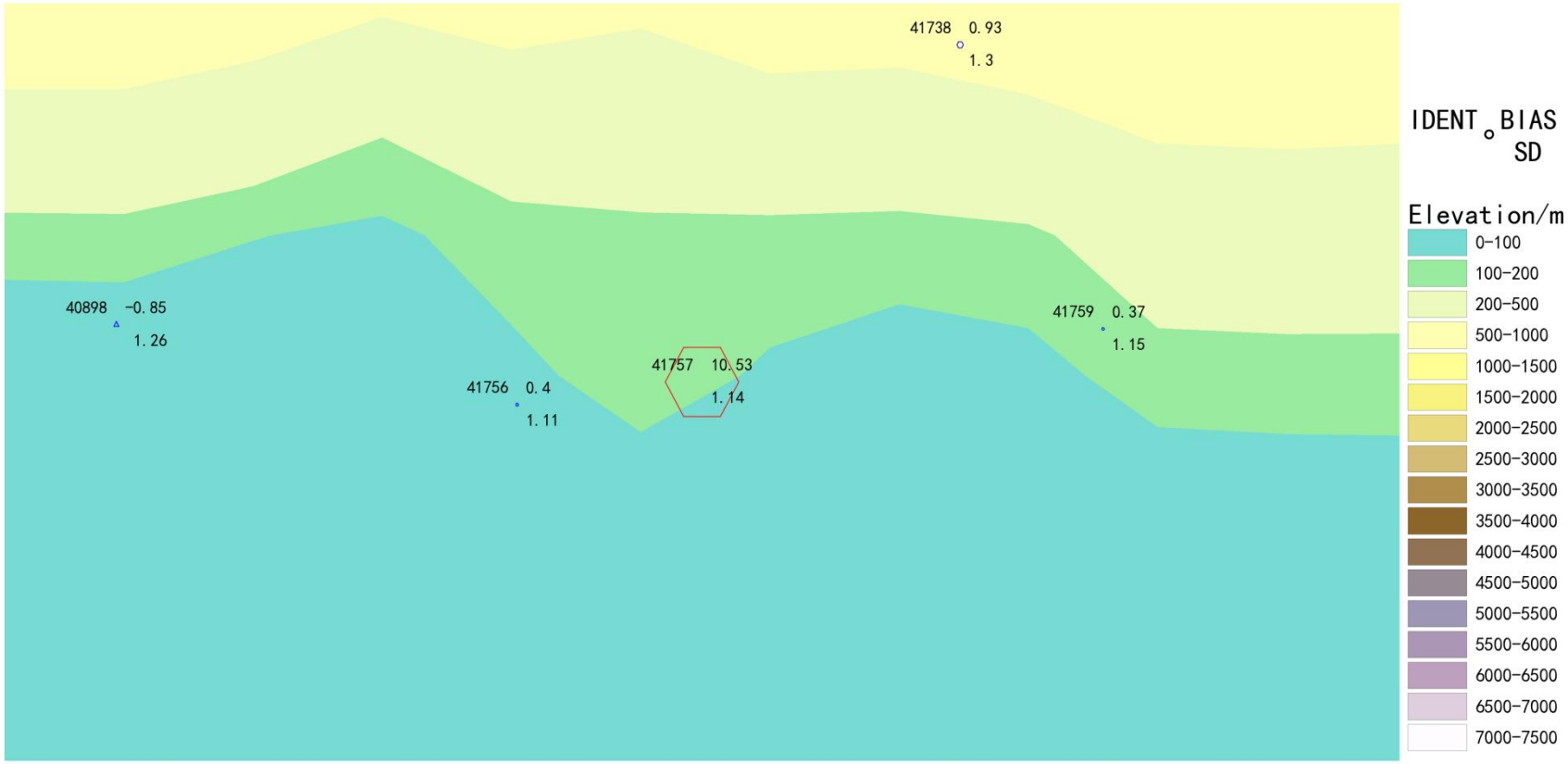

Figure 25 BIAS and SD of SLP for station 41757 (red) and surrounding stations (blue).
The number to the upper left of each symbol is the WMO IDENT, and those to the upper right are the values of BIAS and SD.
The size of each symbol is proportional to the value of BIAS, with hexagonal forms representing positive bias and triangular forms representing negative bias.

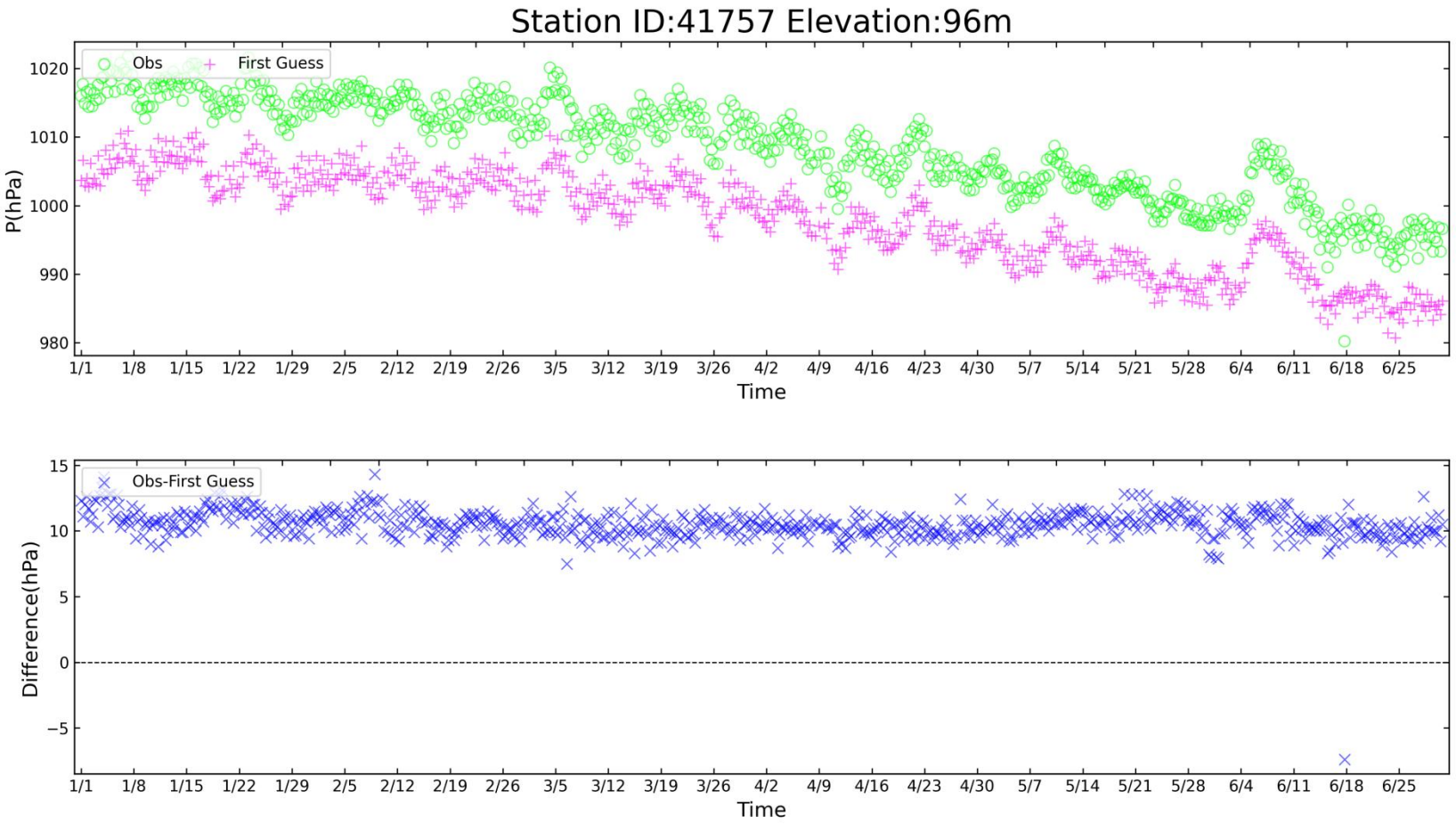

Figure 26 Time-series representation of SLP Obs minus FirstGuess for station 41757

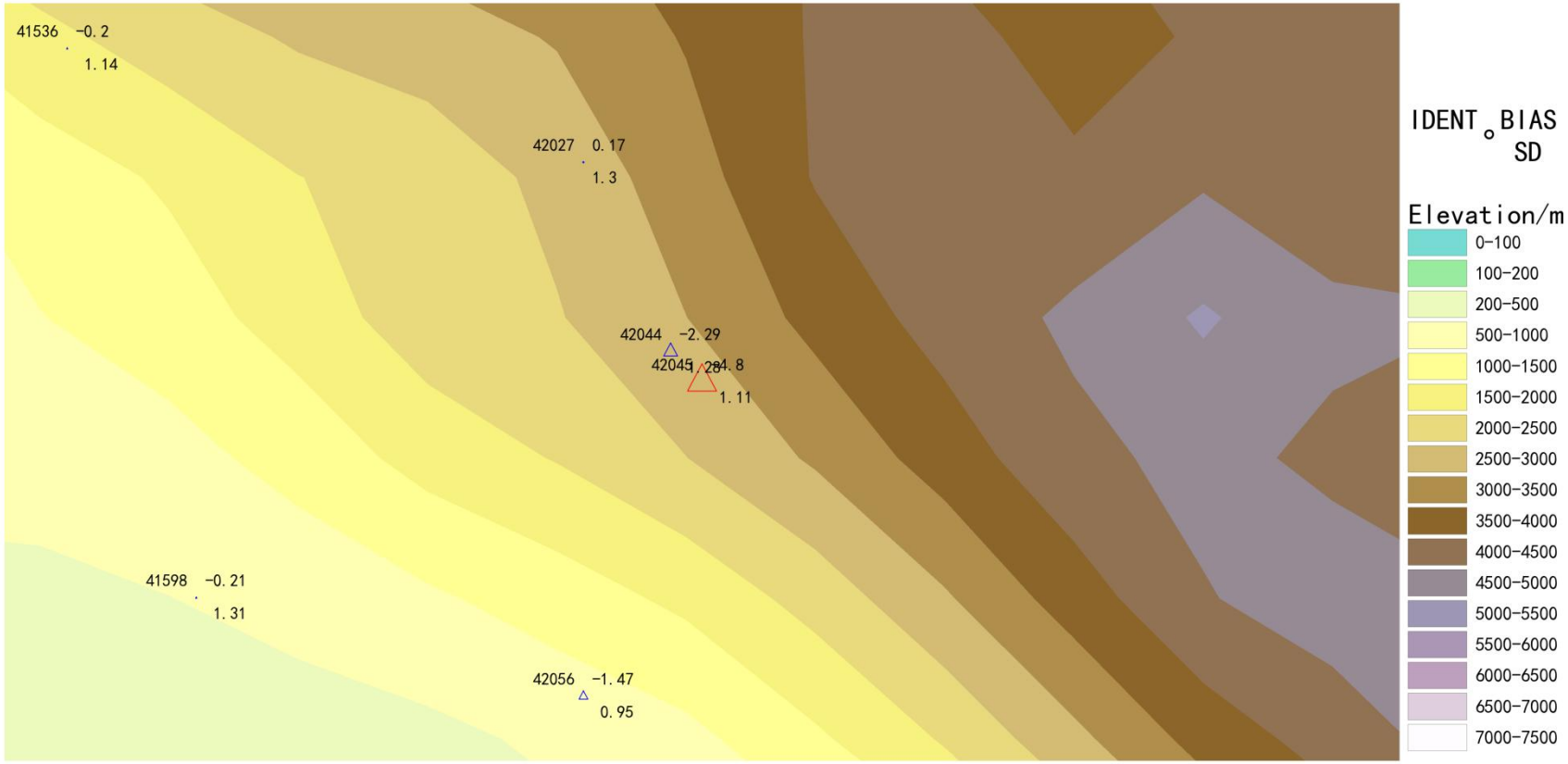

Figure 27 BIAS and SD of SLP for station 42045 (red) and surrounding stations (blue).

The number to the upper left of each symbol is the WMO IDENT, and those to the upper right are the values of BIAS and SD.

The size of each symbol is proportional to the value of BIAS, with hexagonal forms representing positive bias and triangular forms representing negative bias.

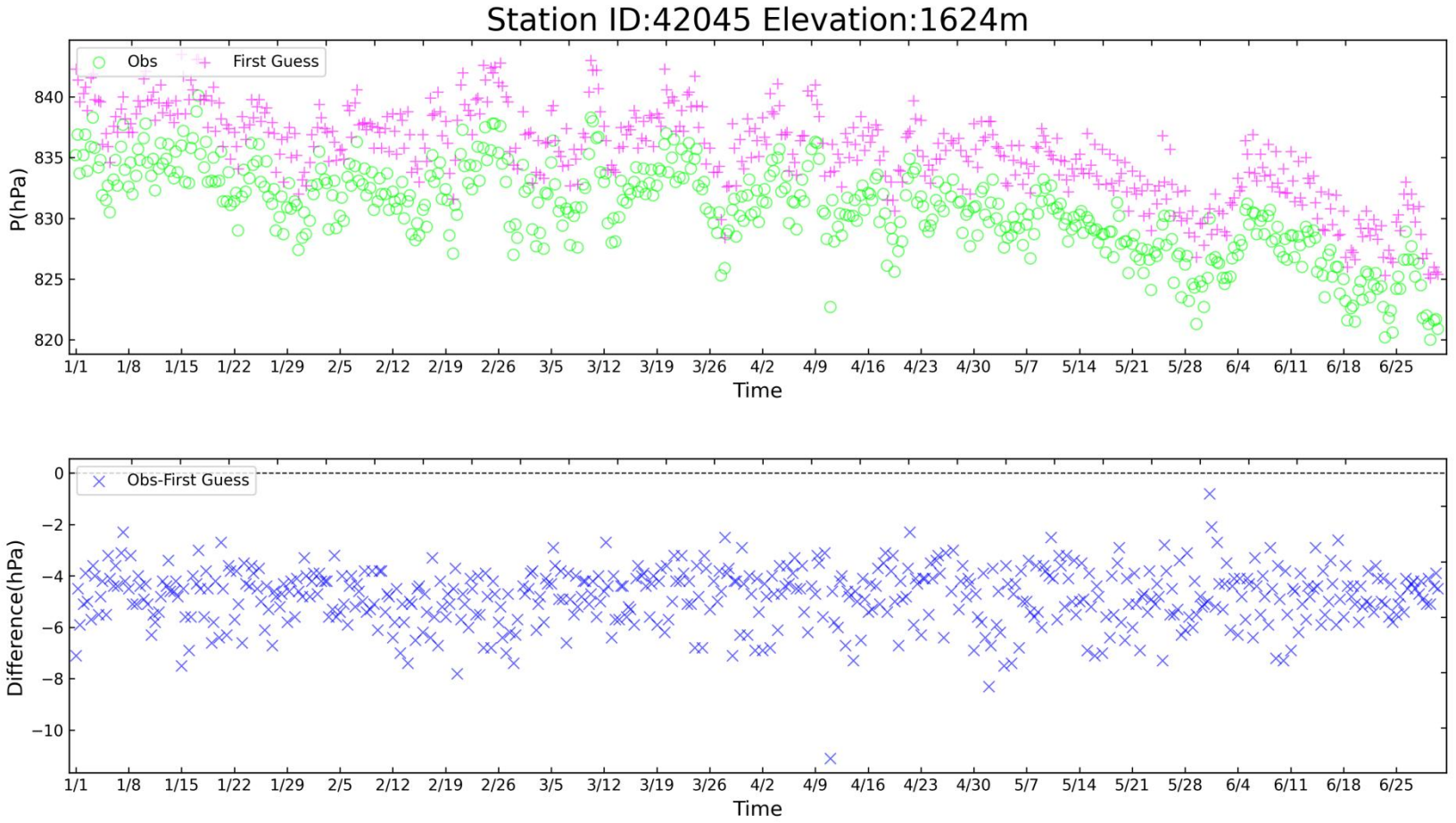

Figure 28 Time-series representation of SLP Obs minus FirstGuess for station 42045

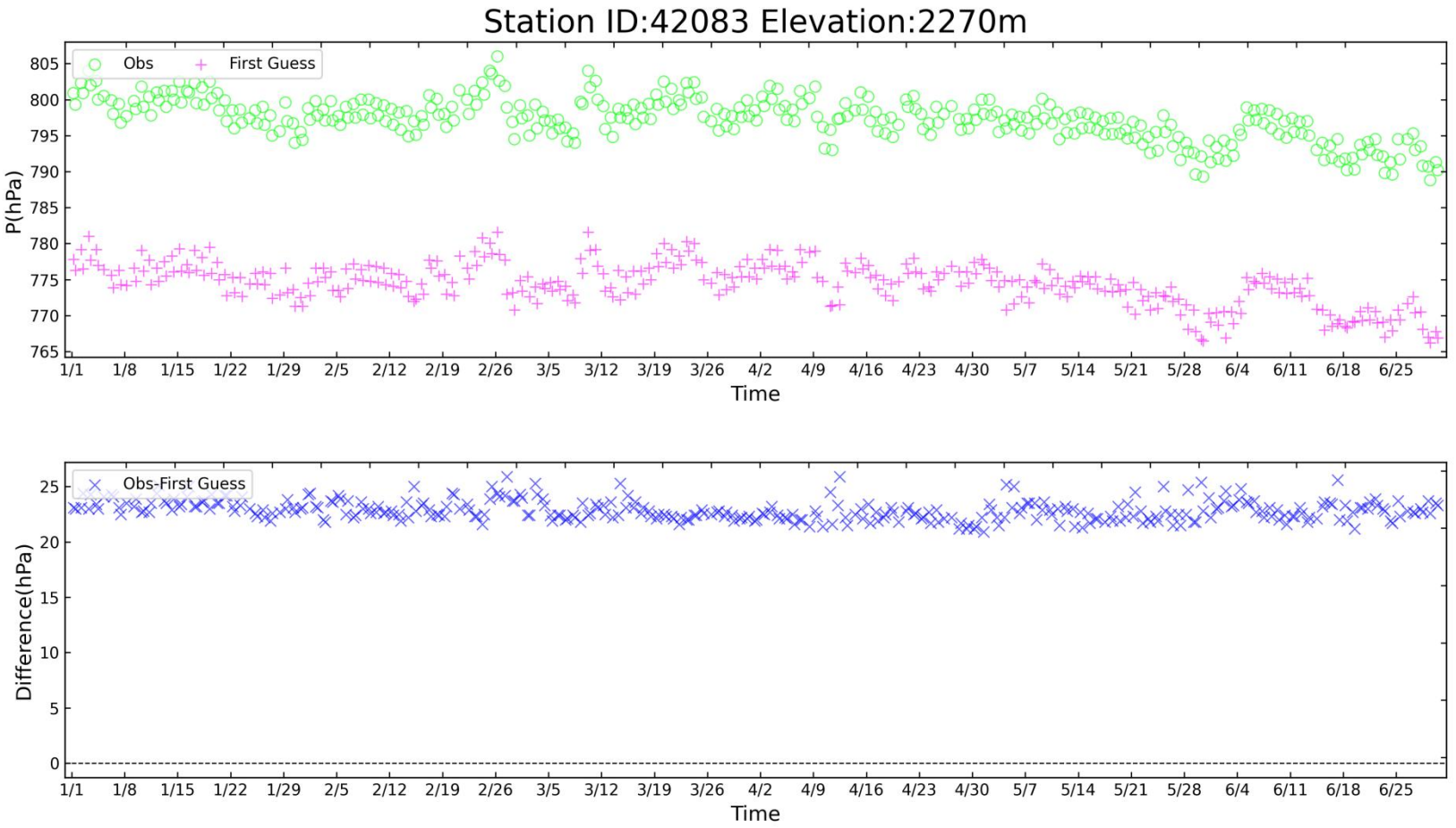

Figure 29 Time-series representation of SLP Obs minus FirstGuess for station 42083

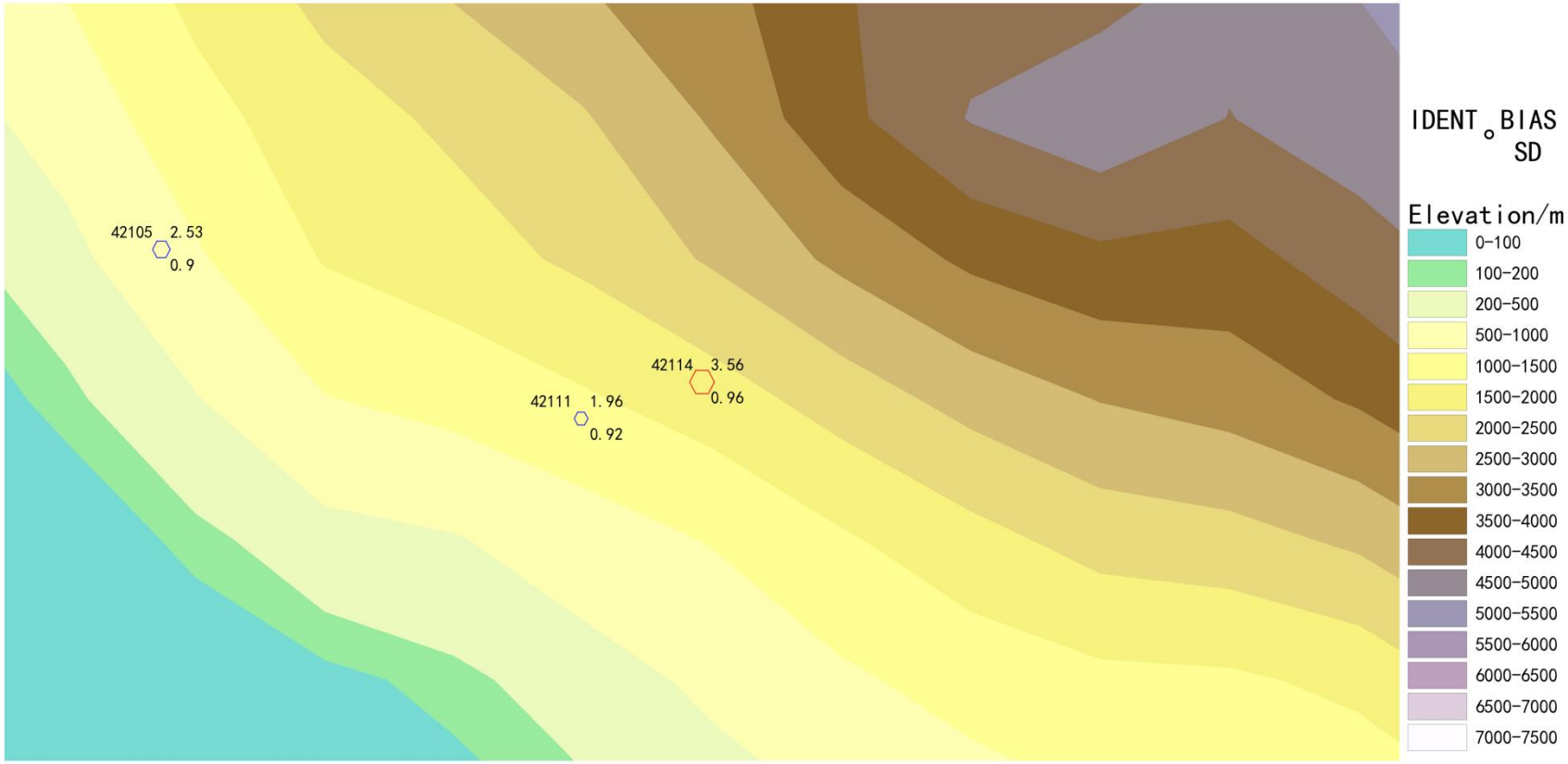

Figure 30 BIAS and SD of SLP for station 42114 (red) and surrounding stations (blue).

The number to the upper left of each symbol is the WMO IDENT, and those to the upper right are the values of BIAS and SD.

The size of each symbol is proportional to the value of BIAS, with hexagonal forms representing positive bias and triangular forms representing negative bias.

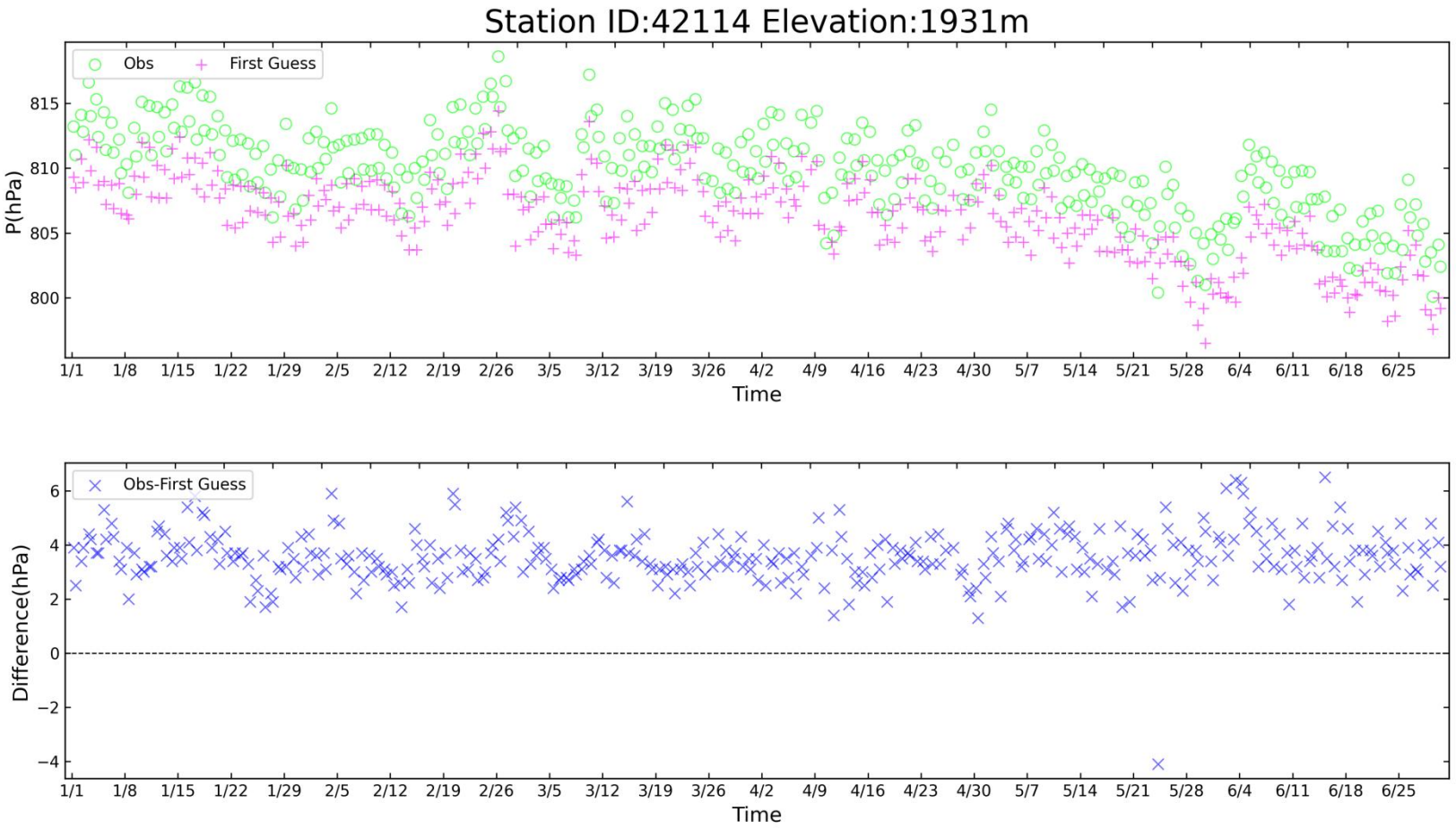

Figure 31 Time-series representation of SLP Obs minus FirstGuess for station 42114

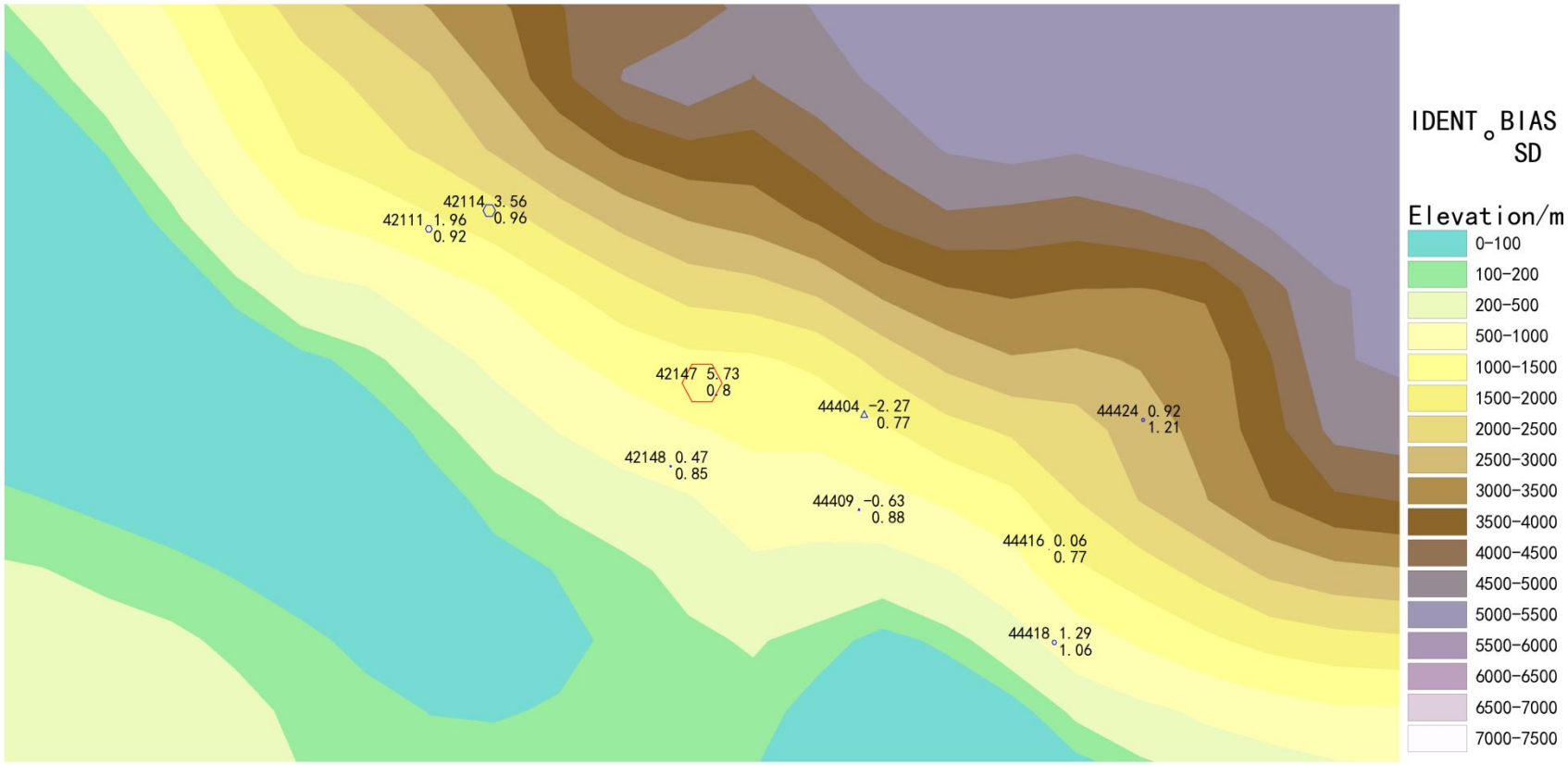

Figure 32 BIAS and SD of SLP for station 42147 (red) and surrounding stations (blue).

The number to the upper left of each symbol is the WMO IDENT, and those to the upper right are the values of BIAS and SD.

The size of each symbol is proportional to the value of BIAS, with hexagonal forms representing positive bias and triangular forms representing negative bias.

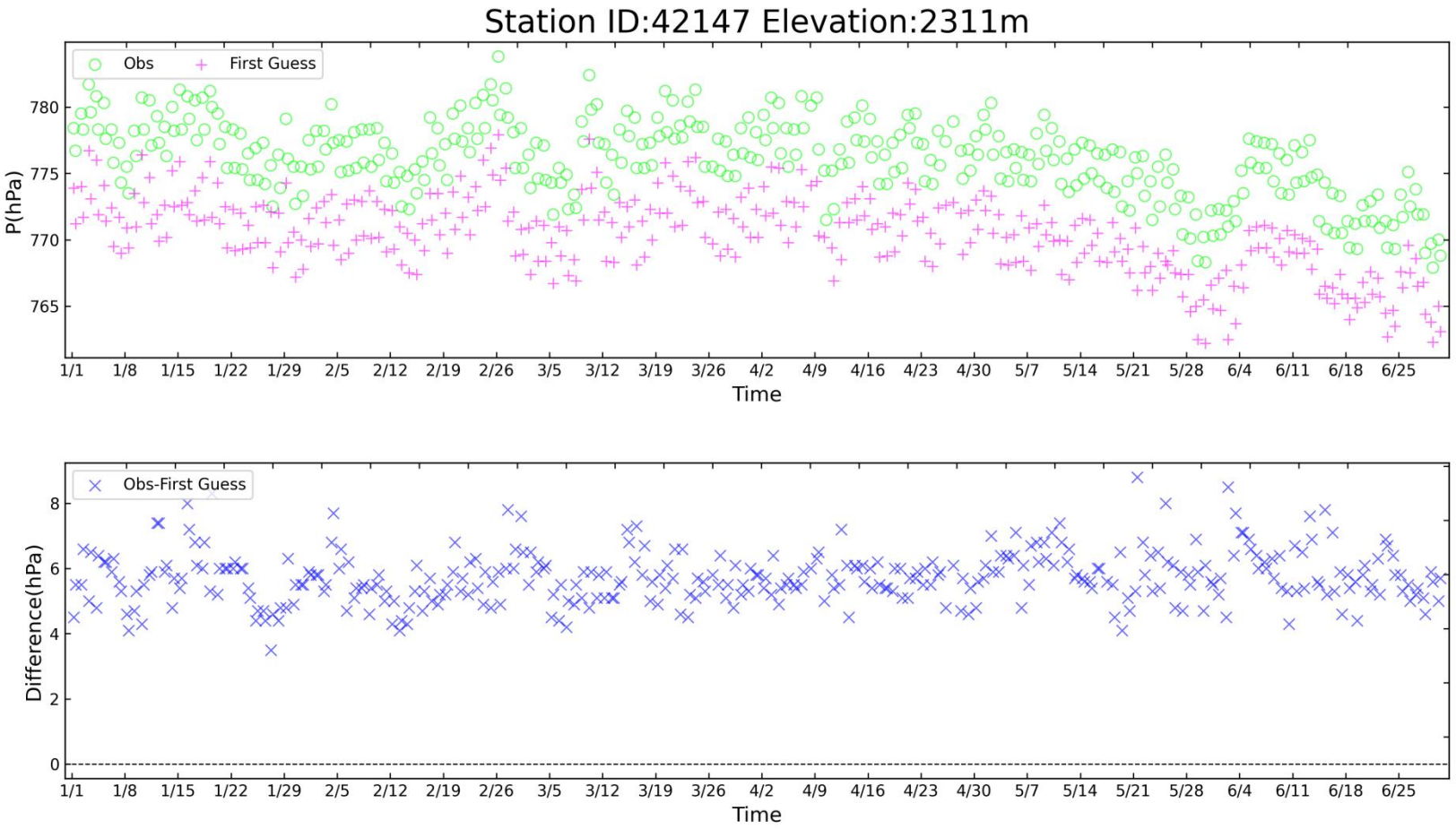

Figure 33 Time-series representation of SLP Obs minus FirstGuess for station 42147

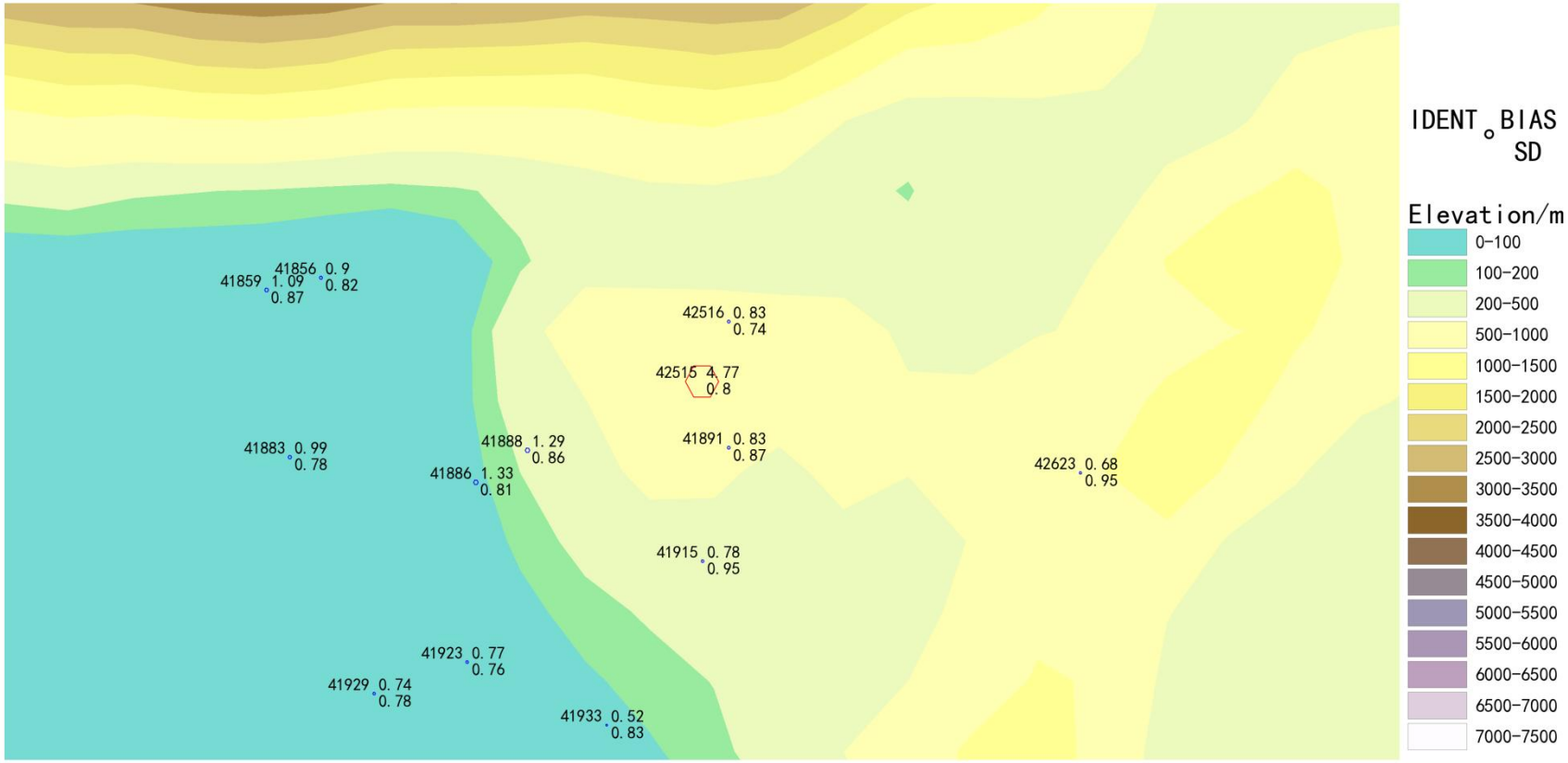

Figure 34 BIAS and SD of SLP for station 42515 (red) and surrounding stations (blue).

The number to the upper left of each symbol is the WMO IDENT, and those to the upper right are the values of BIAS and SD.

The size of each symbol is proportional to the value of BIAS, with hexagonal forms representing positive bias and triangular forms representing negative bias.

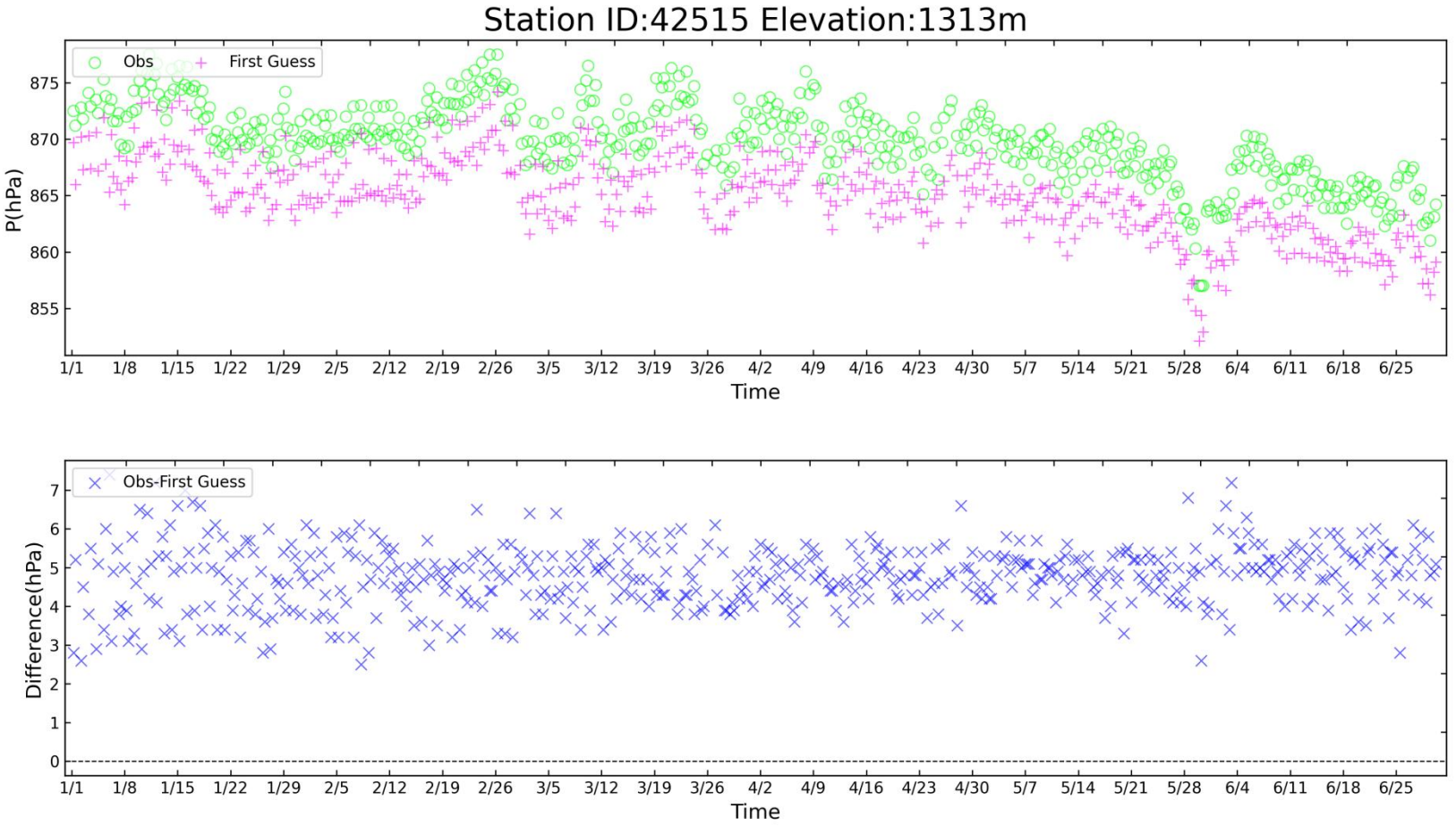

Figure 35 Time-series representation of SLP Obs minus FirstGuess for station 42515

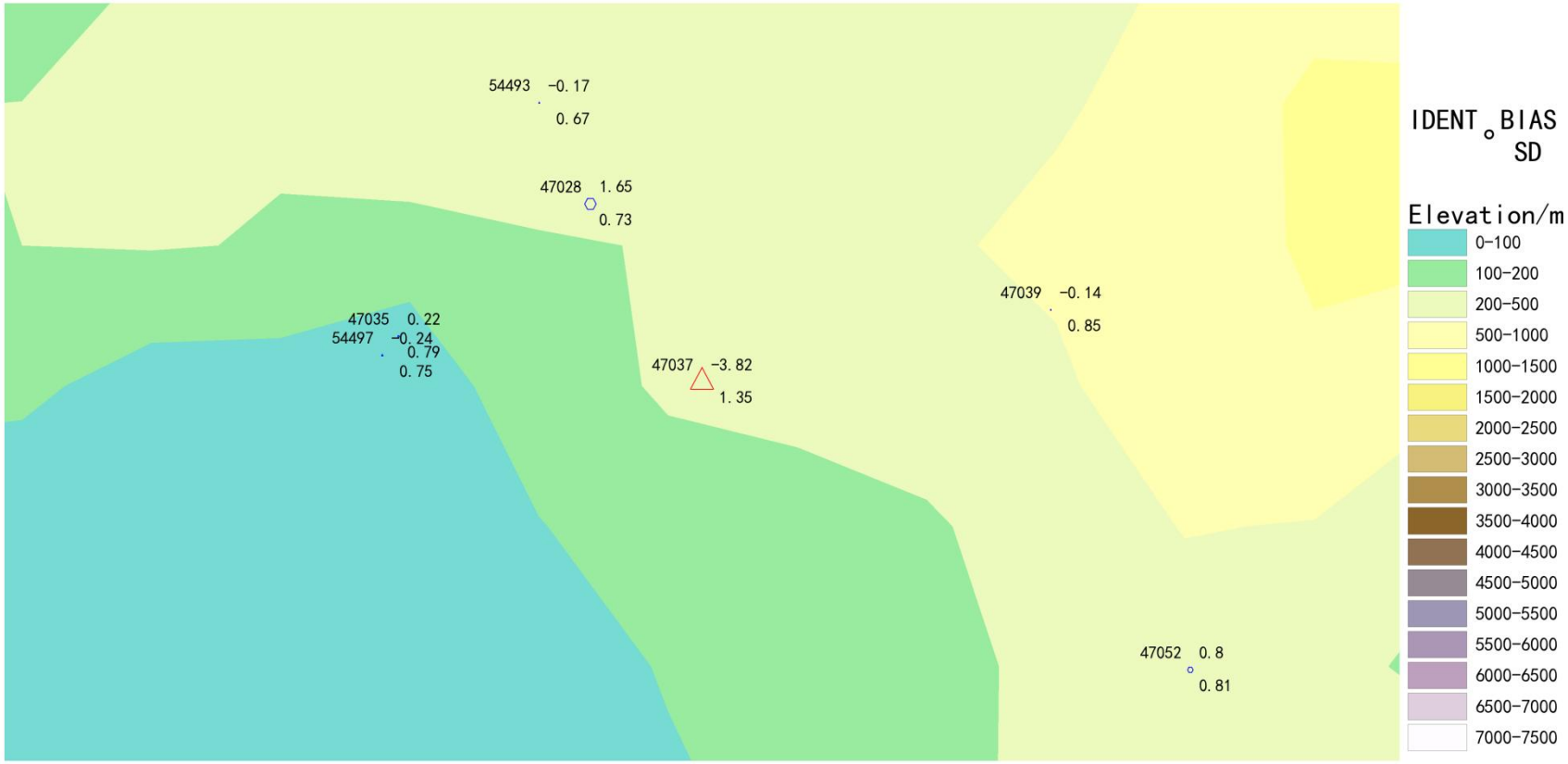

Figure 36 BIAS and SD of SLP for station 47037* (red) and surrounding stations (blue).

The number to the upper left of each symbol is the WMO IDENT, and those to the upper right are the values of BIAS and SD.

The size of each symbol is proportional to the value of BIAS, with hexagonal forms representing positive bias and triangular forms representing negative bias.

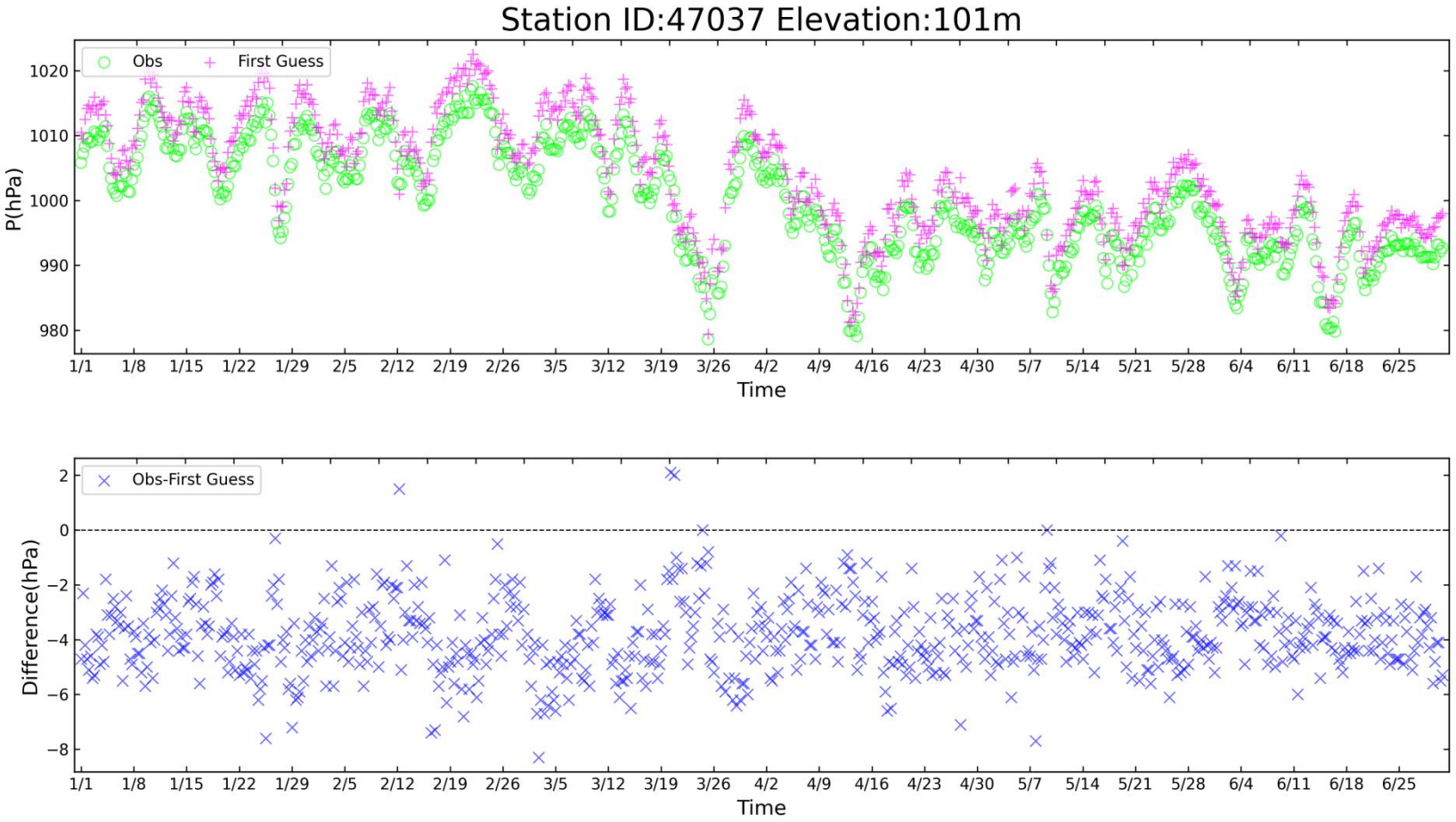

Figure 37 Time-series representation of SLP Obs minus FirstGuess for station 47037*

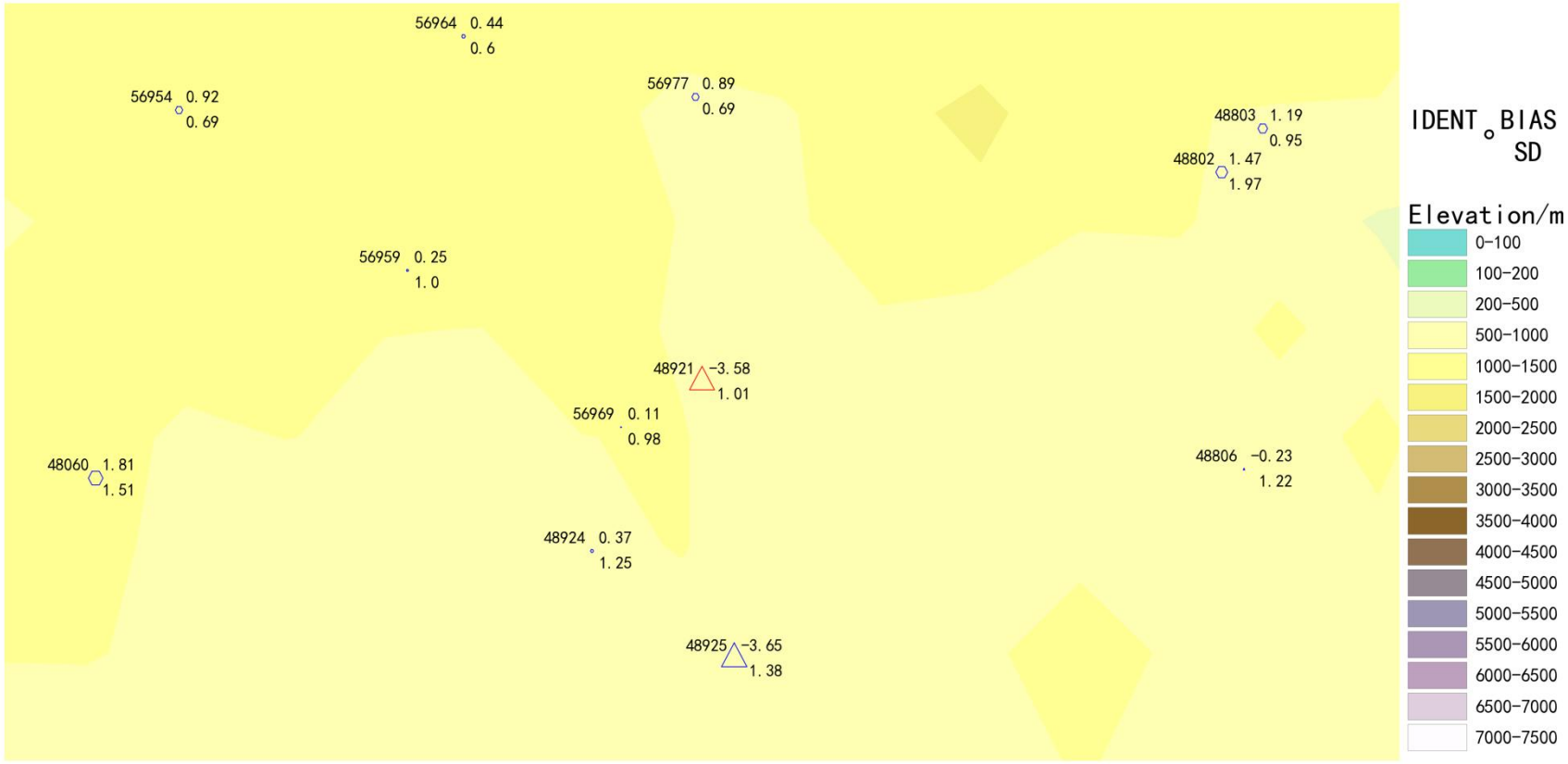

Figure 38 BIAS and SD of SLP for station 48921 (red) and surrounding stations (blue).

The number to the upper left of each symbol is the WMO IDENT, and those to the upper right are the values of BIAS and SD.

The size of each symbol is proportional to the value of BIAS, with hexagonal forms representing positive bias and triangular forms representing negative bias.

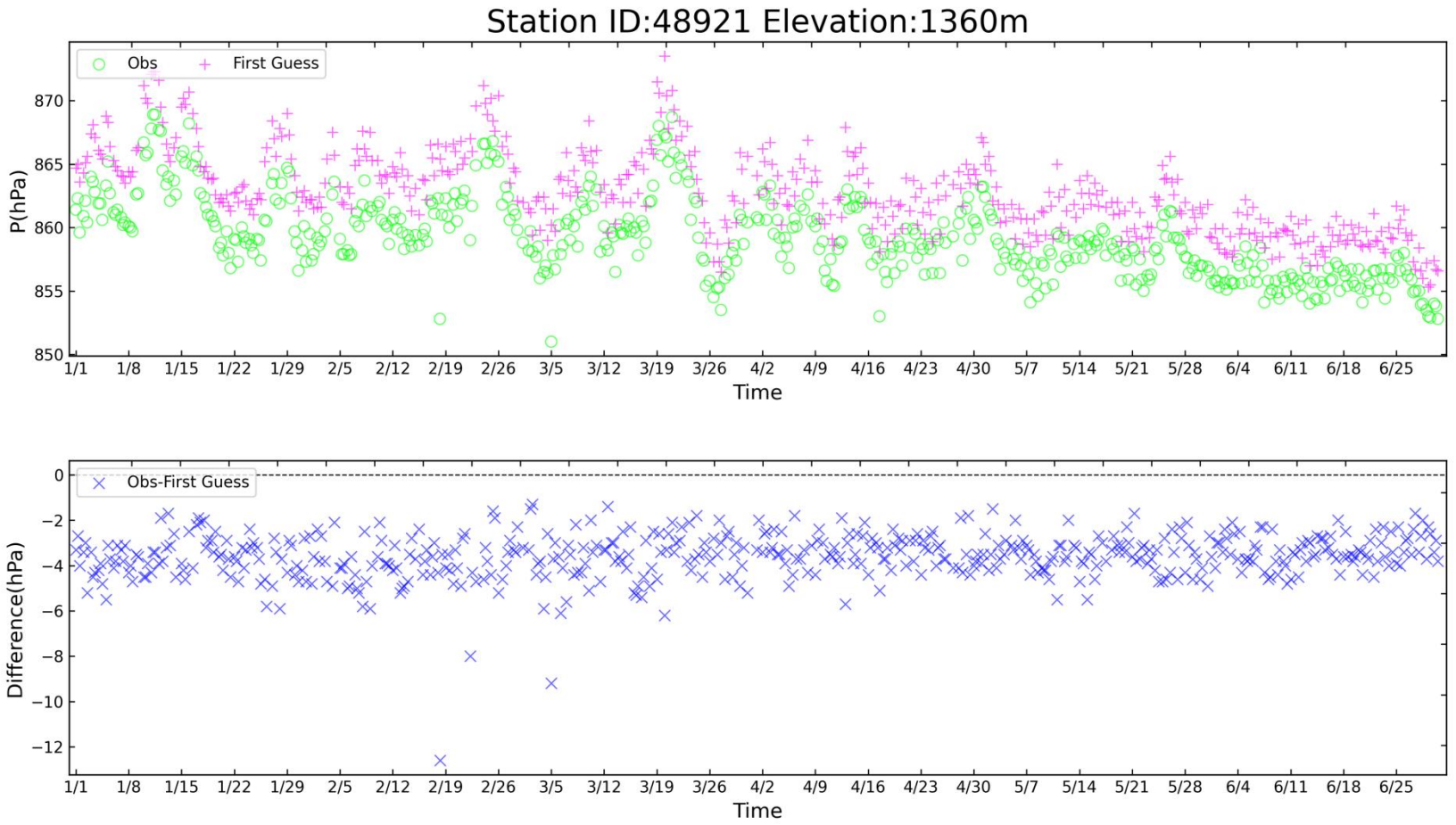

Figure 39 Time-series representation of SLP Obs minus FirstGuess for station 48921

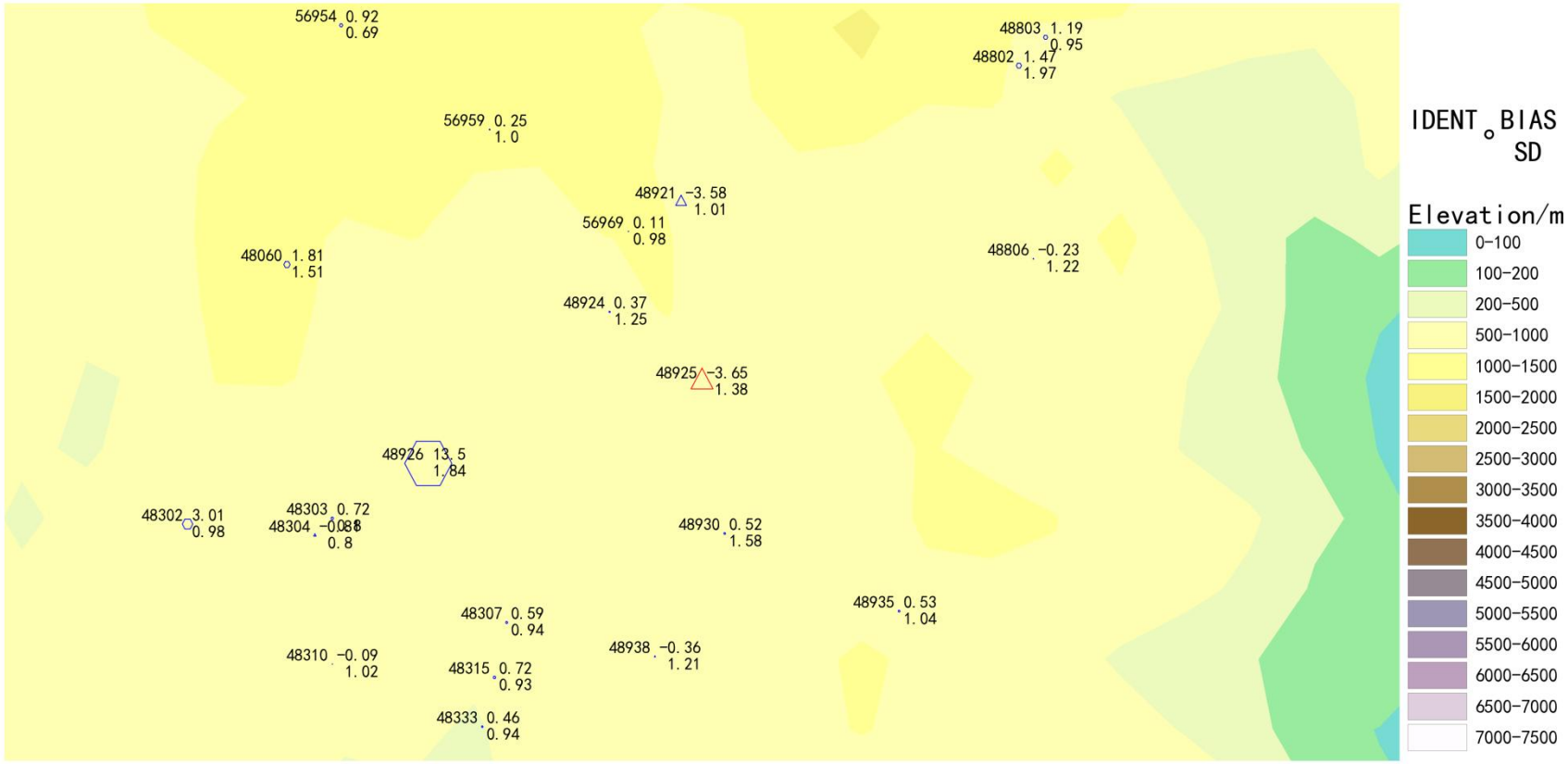

Figure 40 BIAS and SD of SLP for station 48925 (red) and surrounding stations (blue).

The number to the upper left of each symbol is the WMO IDENT, and those to the upper right are the values of BIAS and SD.

The size of each symbol is proportional to the value of BIAS, with hexagonal forms representing positive bias and triangular forms representing negative bias.

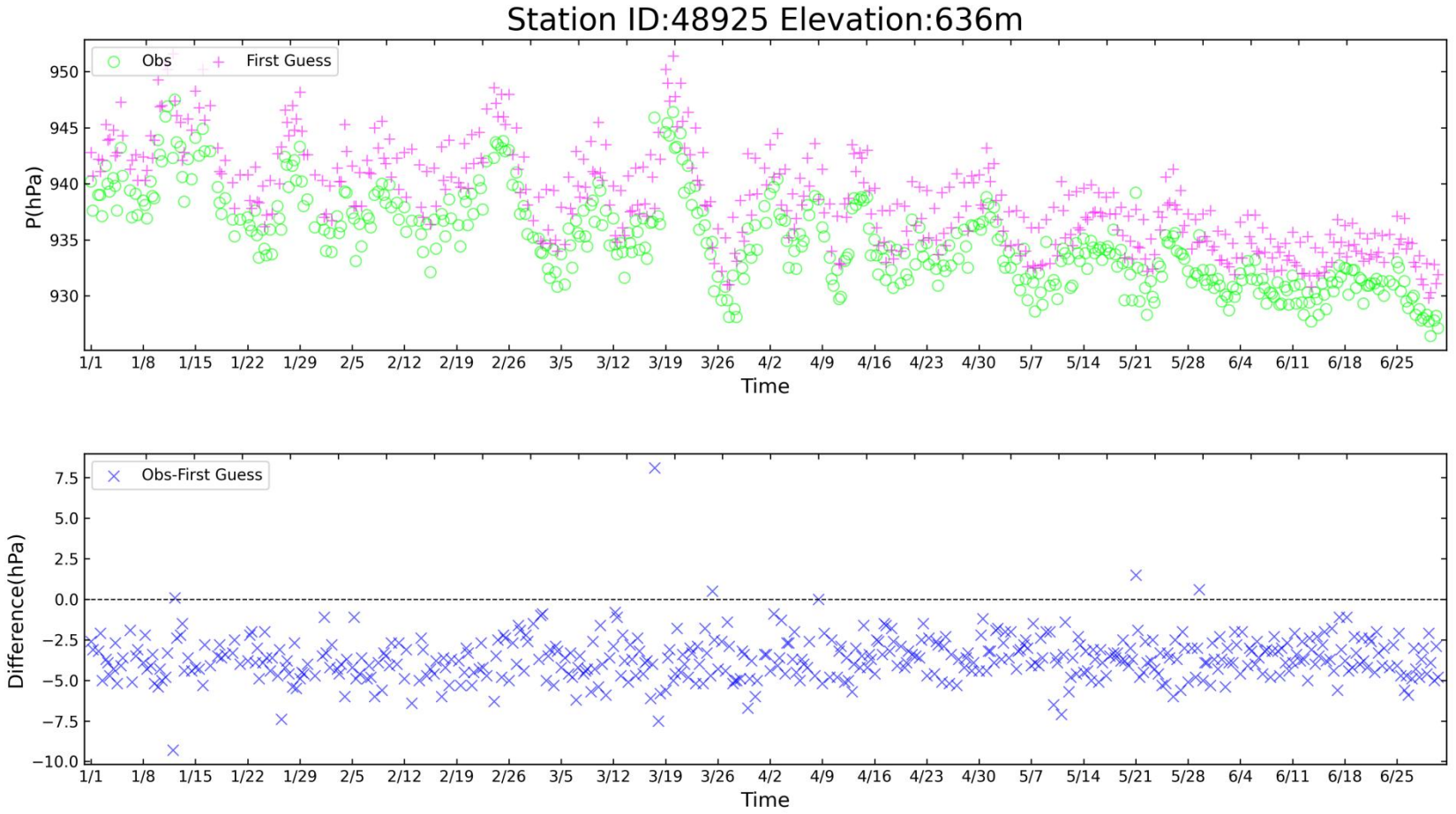

Figure 41 Time-series representation of SLP Obs minus FirstGuess for station 48925

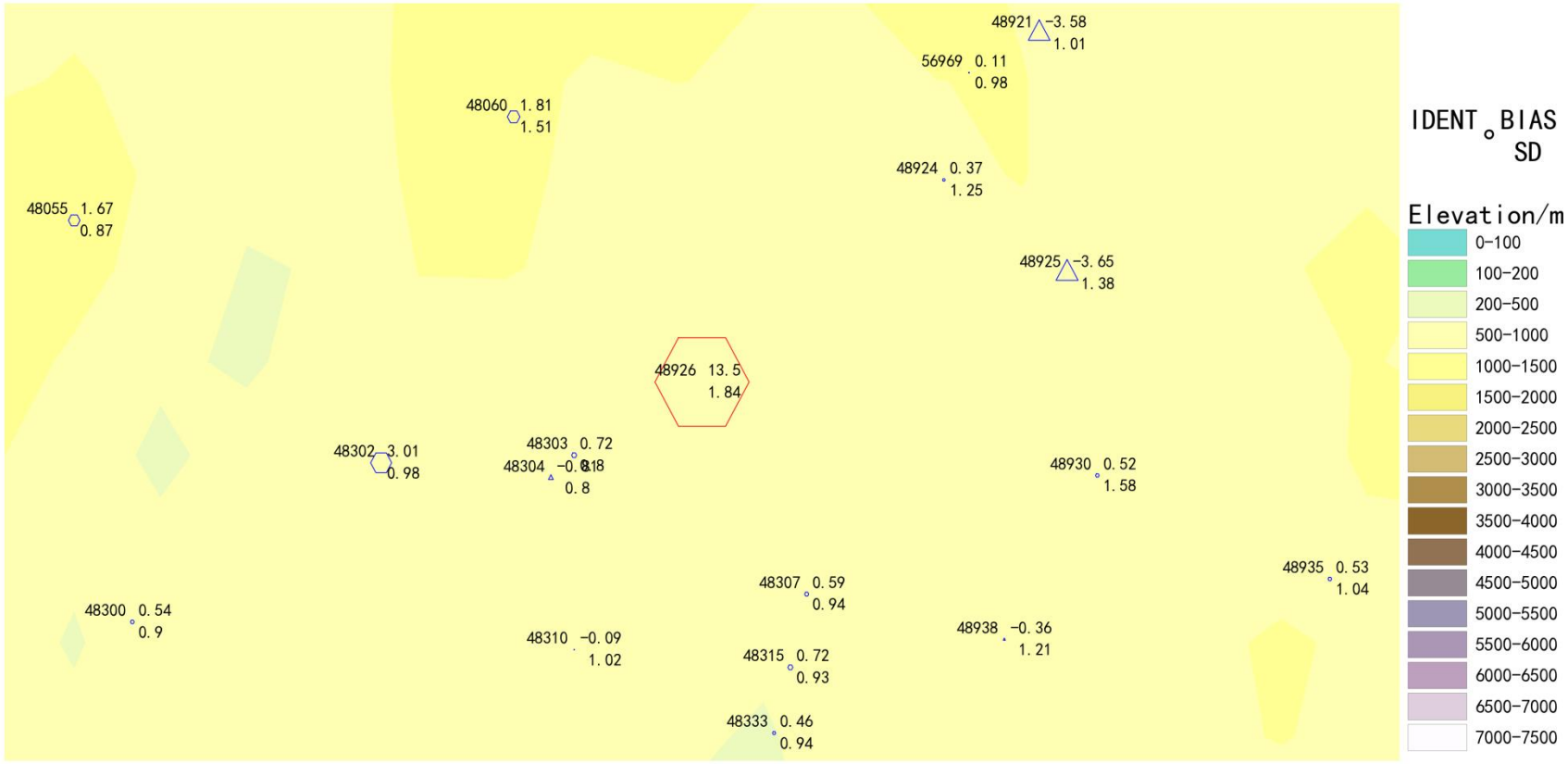

Figure 42 BIAS and SD of SLP for station 48926 (red) and surrounding stations (blue).

The number to the upper left of each symbol is the WMO IDENT, and those to the upper right are the values of BIAS and SD.

The size of each symbol is proportional to the value of BIAS, with hexagonal forms representing positive bias and triangular forms representing negative bias.

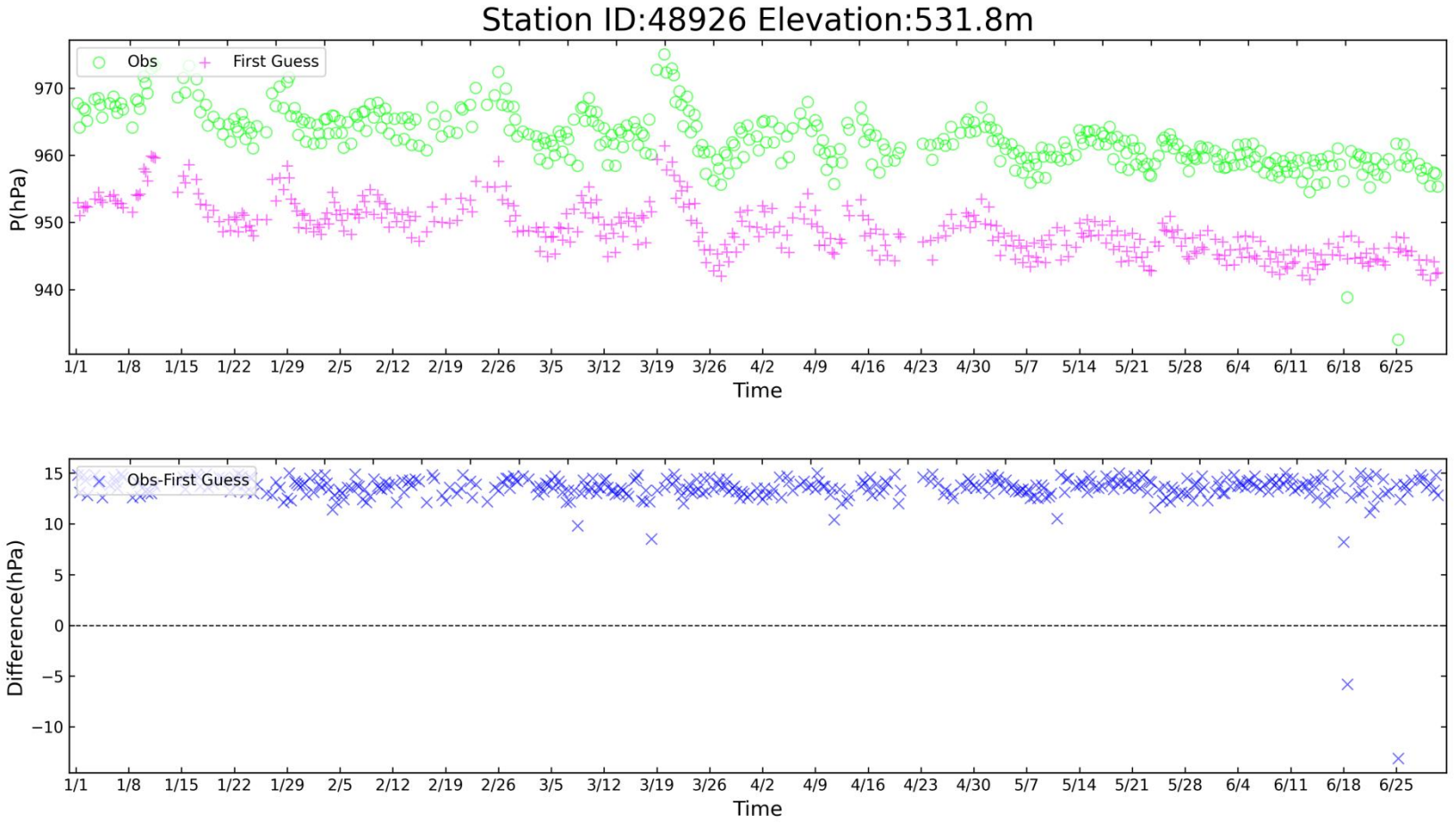

Figure 43 Time-series representation of SLP Obs minus FirstGuess for station 48926

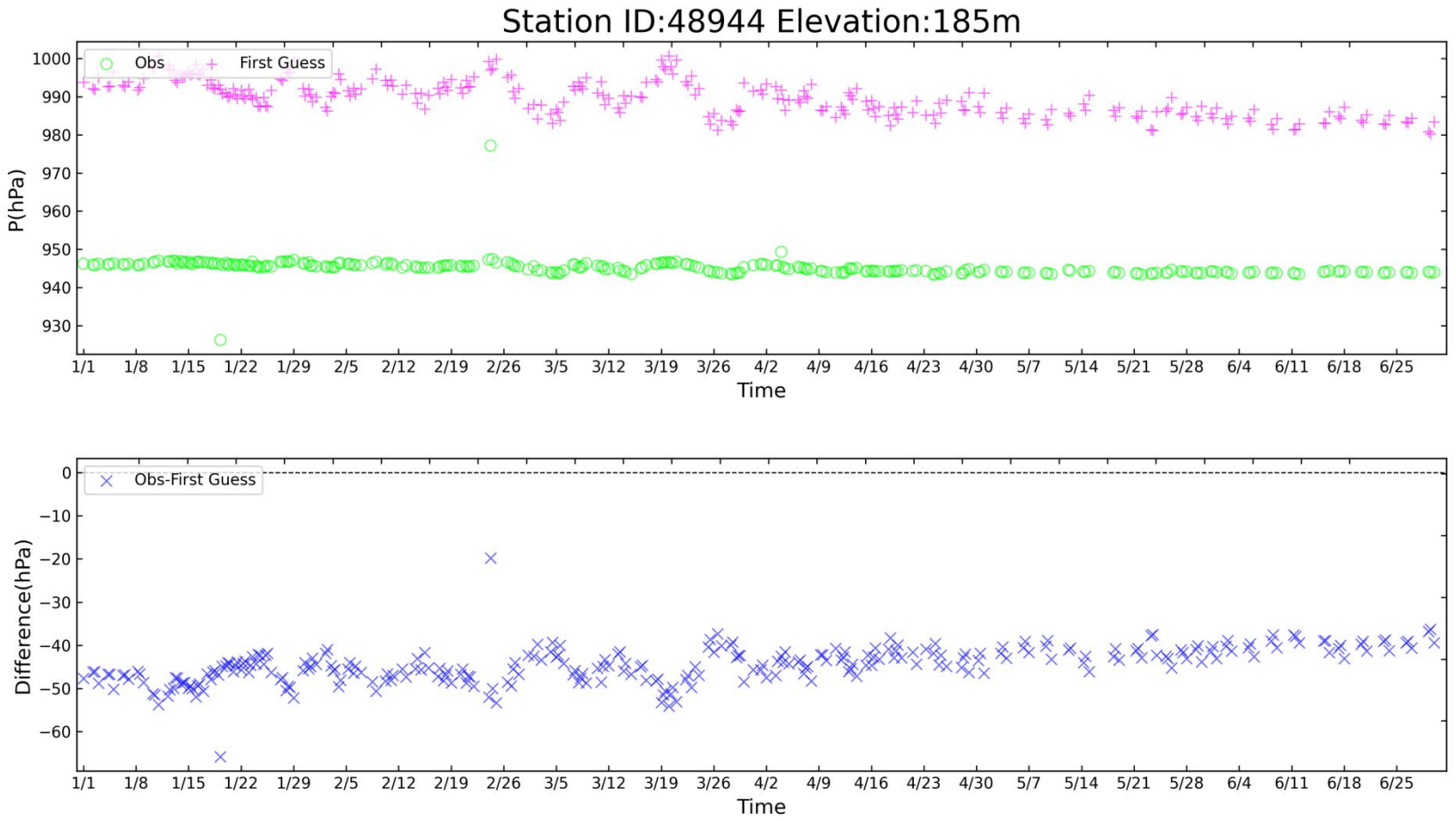

Figure 44 Time-series representation of SLP Obs minus FirstGuess for station 48944

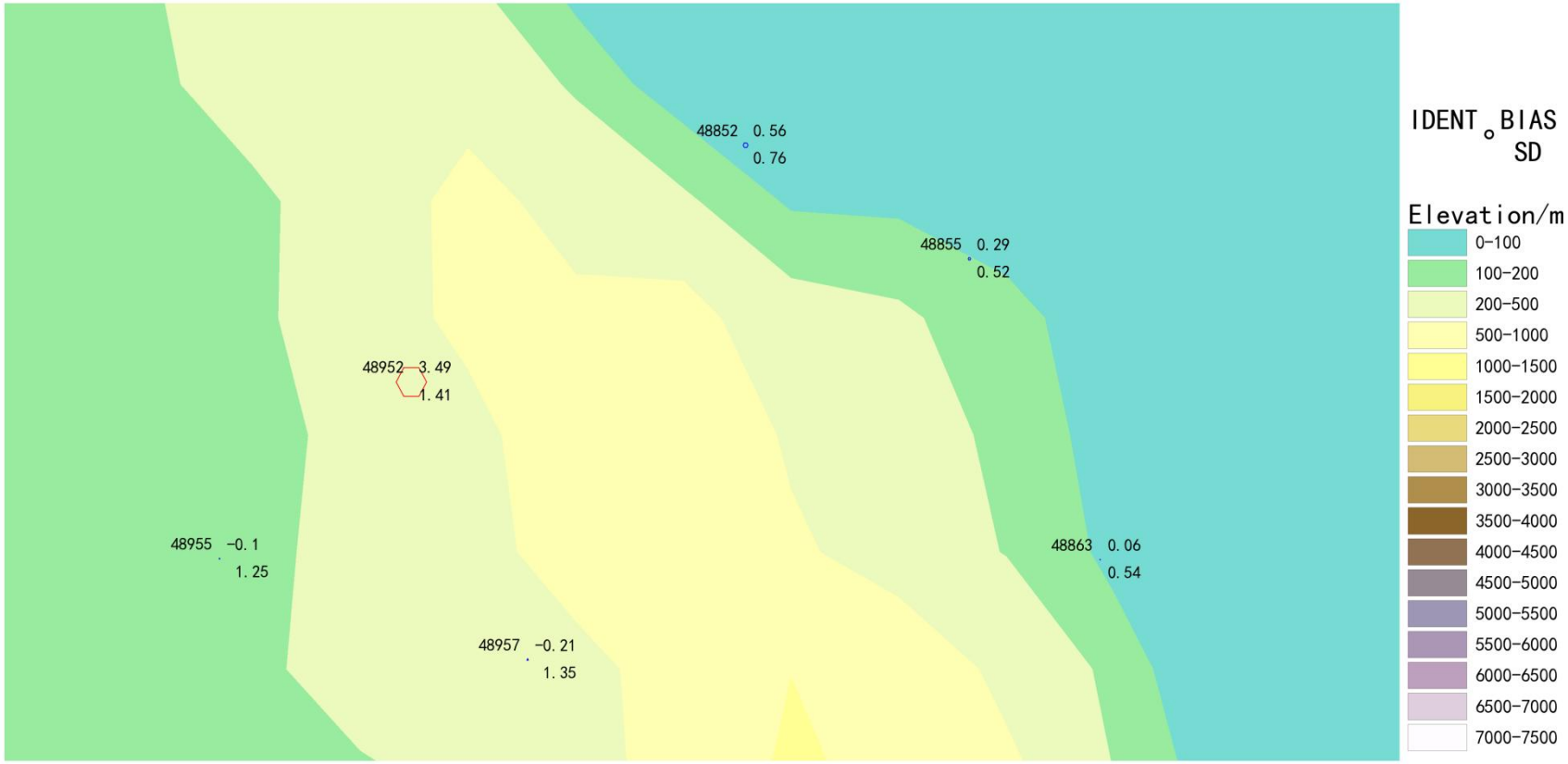

Figure 45 BIAS and SD of SLP for station 48952 (red) and surrounding stations (blue).
The number to the upper left of each symbol is the WMO IDENT, and those to the upper right are the values of BIAS and SD.
The size of each symbol is proportional to the value of BIAS, with hexagonal forms representing positive bias and triangular forms representing negative bias.

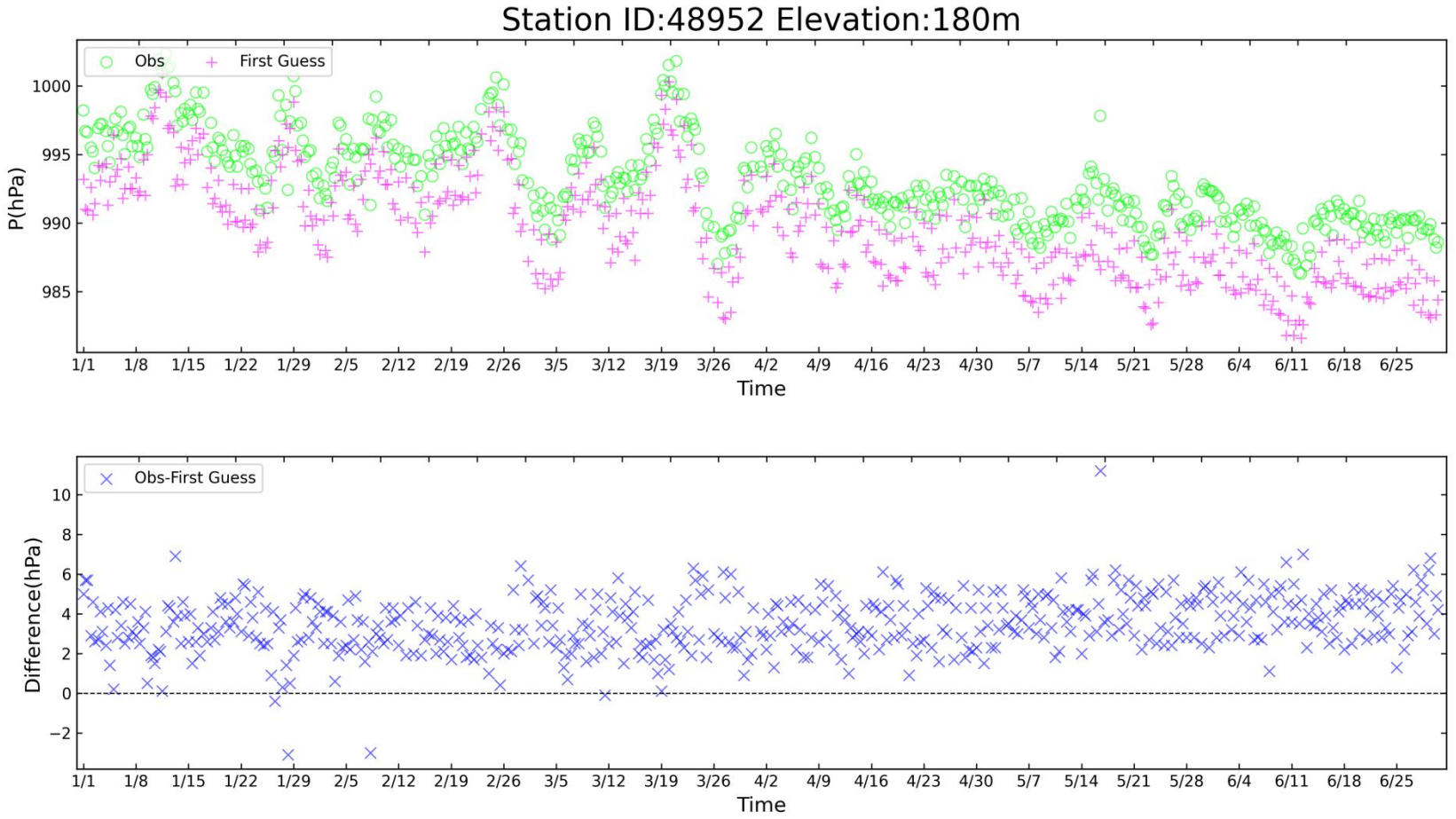

Figure 46 Time-series representation of SLP Obs minus FirstGuess for station 48952

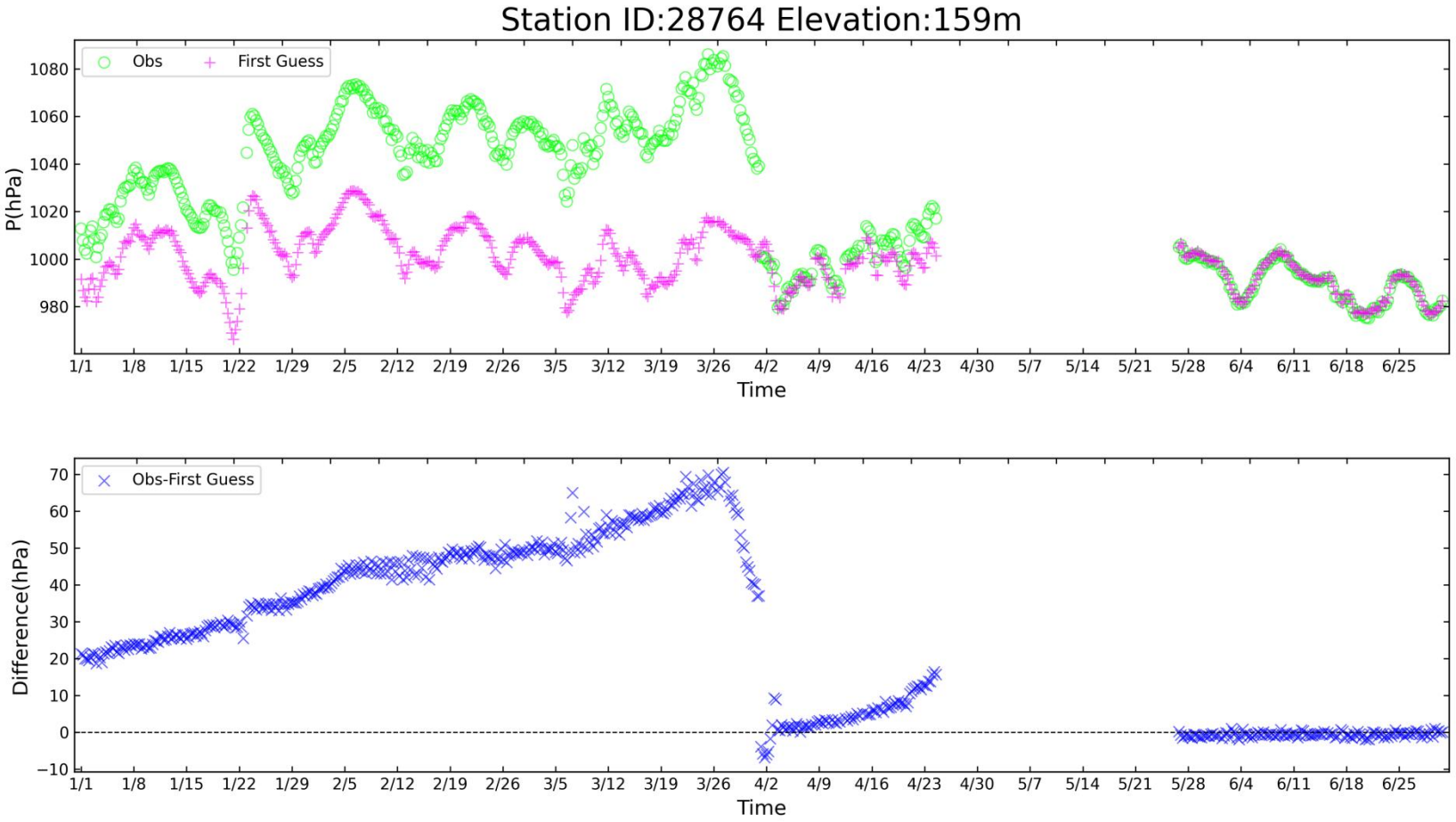

Figure 47 Time-series representation of SLP Obs minus FirstGuess for station 28764

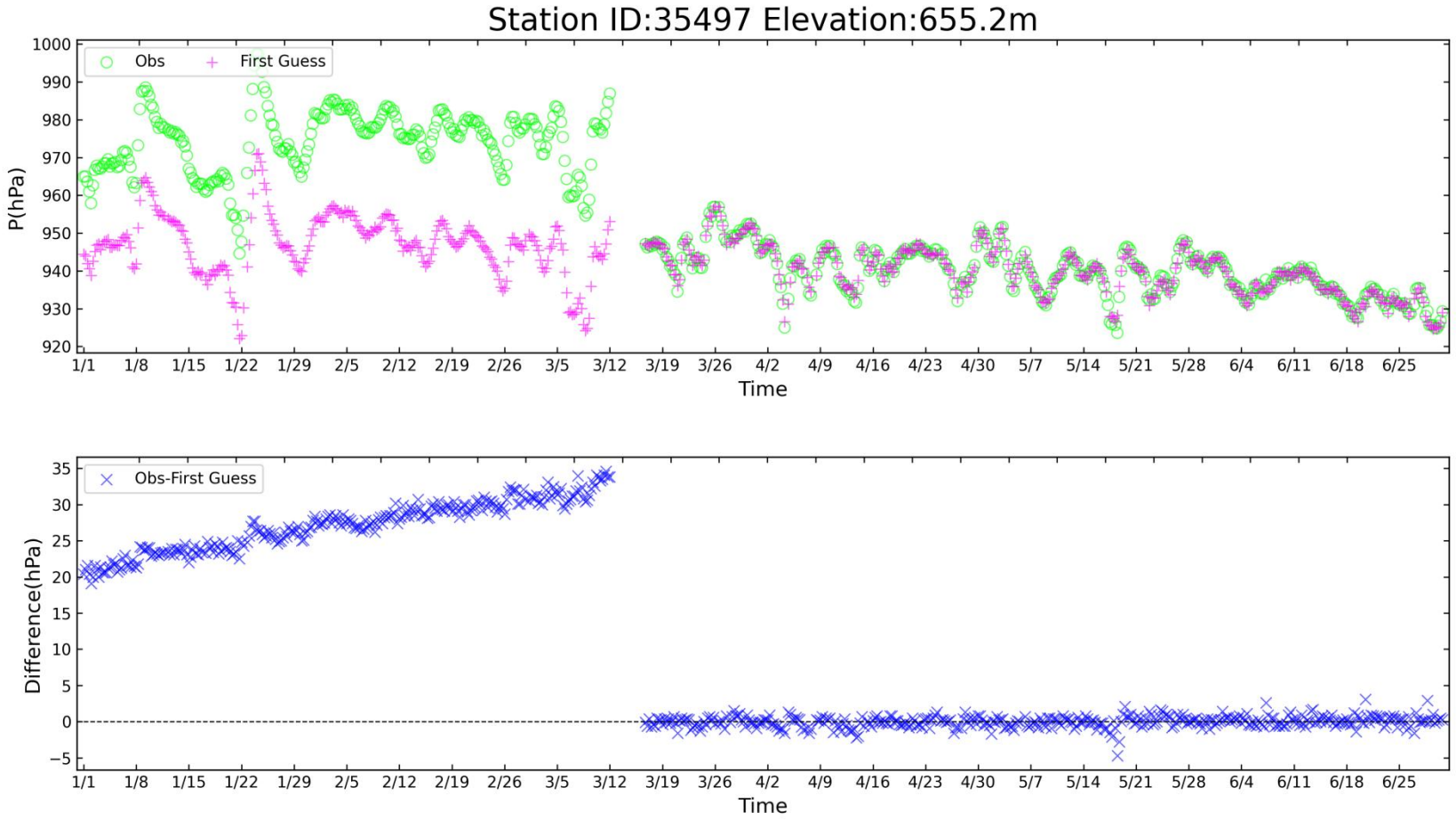

Figure 48 Time-series representation of SLP Obs minus FirstGuess for station 35497

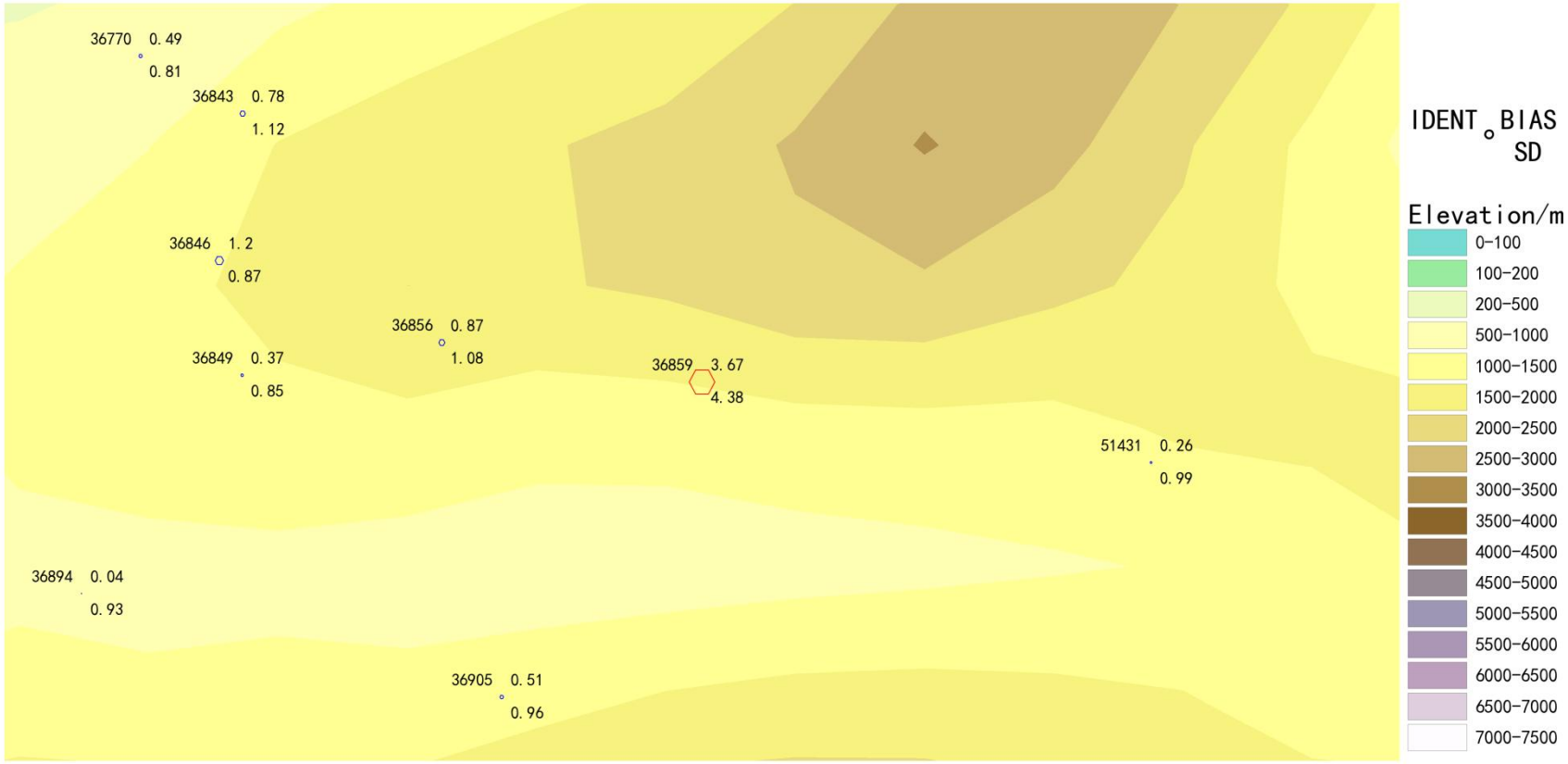

Figure 49 BIAS and SD of SLP for station 36859 (red) and surrounding stations (blue).

The number to the upper left of each symbol is the WMO IDENT, and those to the upper right are the values of BIAS and SD.

The size of each symbol is proportional to the value of BIAS, with hexagonal forms representing positive bias and triangular forms representing negative bias.

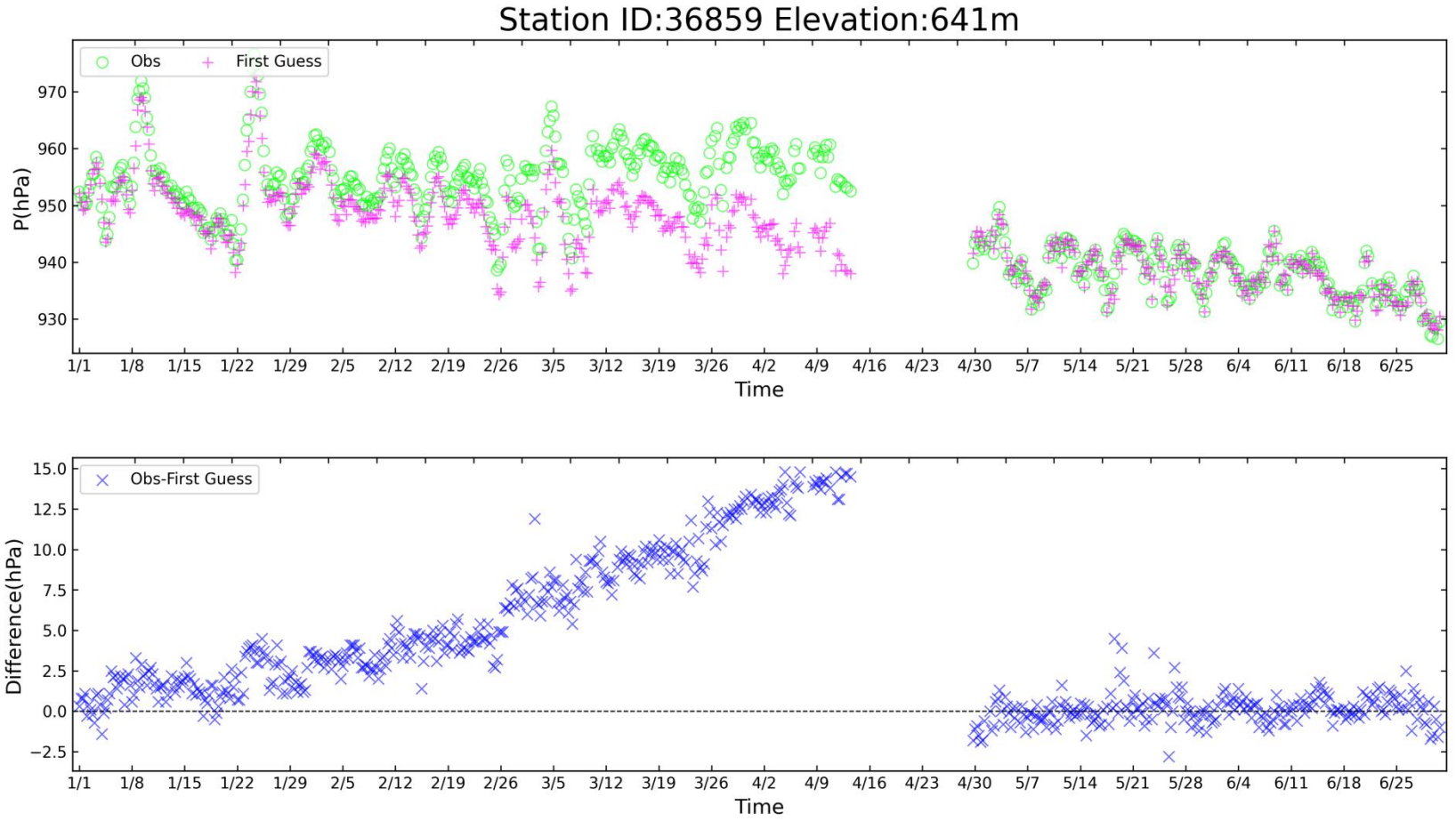

Figure 50 Time-series representation of SLP Obs minus FirstGuess for station 36859

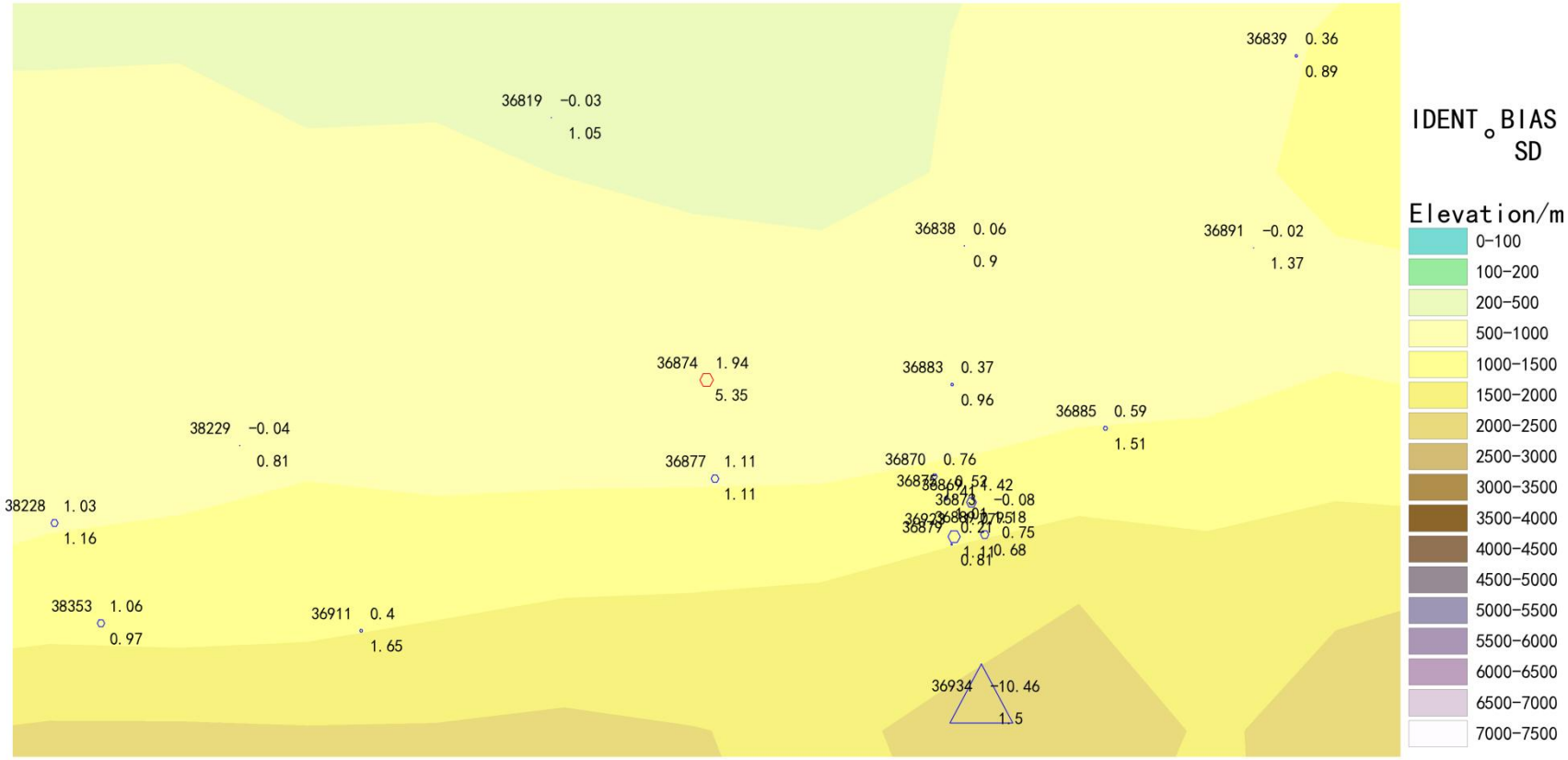

Figure 51 BIAS and SD of SLP for station 36874 (red) and surrounding stations (blue).

The number to the upper left of each symbol is the WMO IDENT, and those to the upper right are the values of BIAS and SD.

The size of each symbol is proportional to the value of BIAS, with hexagonal forms representing positive bias and triangular forms representing negative bias.

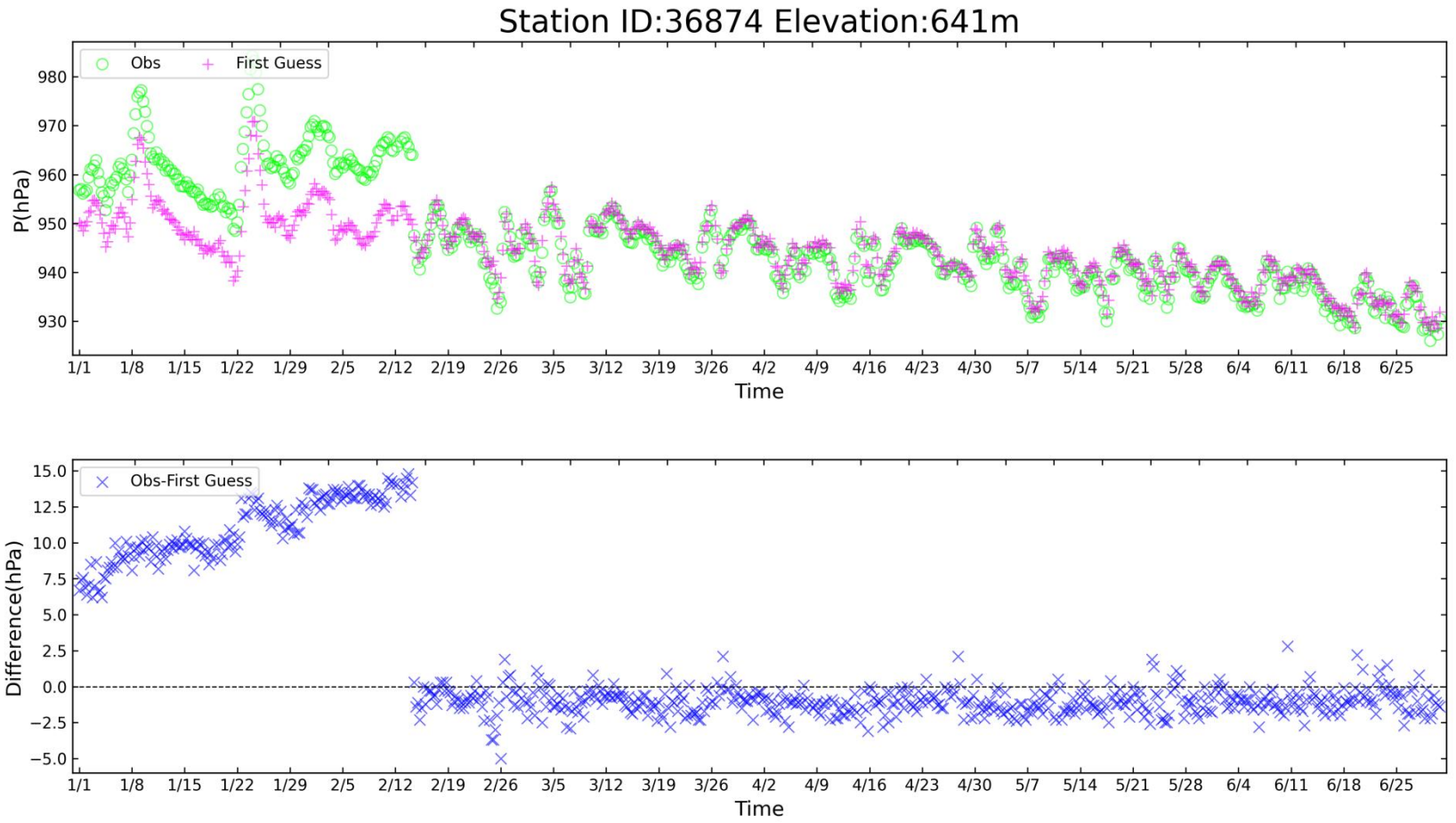

Figure 52 Time-series representation of SLP Obs minus FirstGuess for station 36874

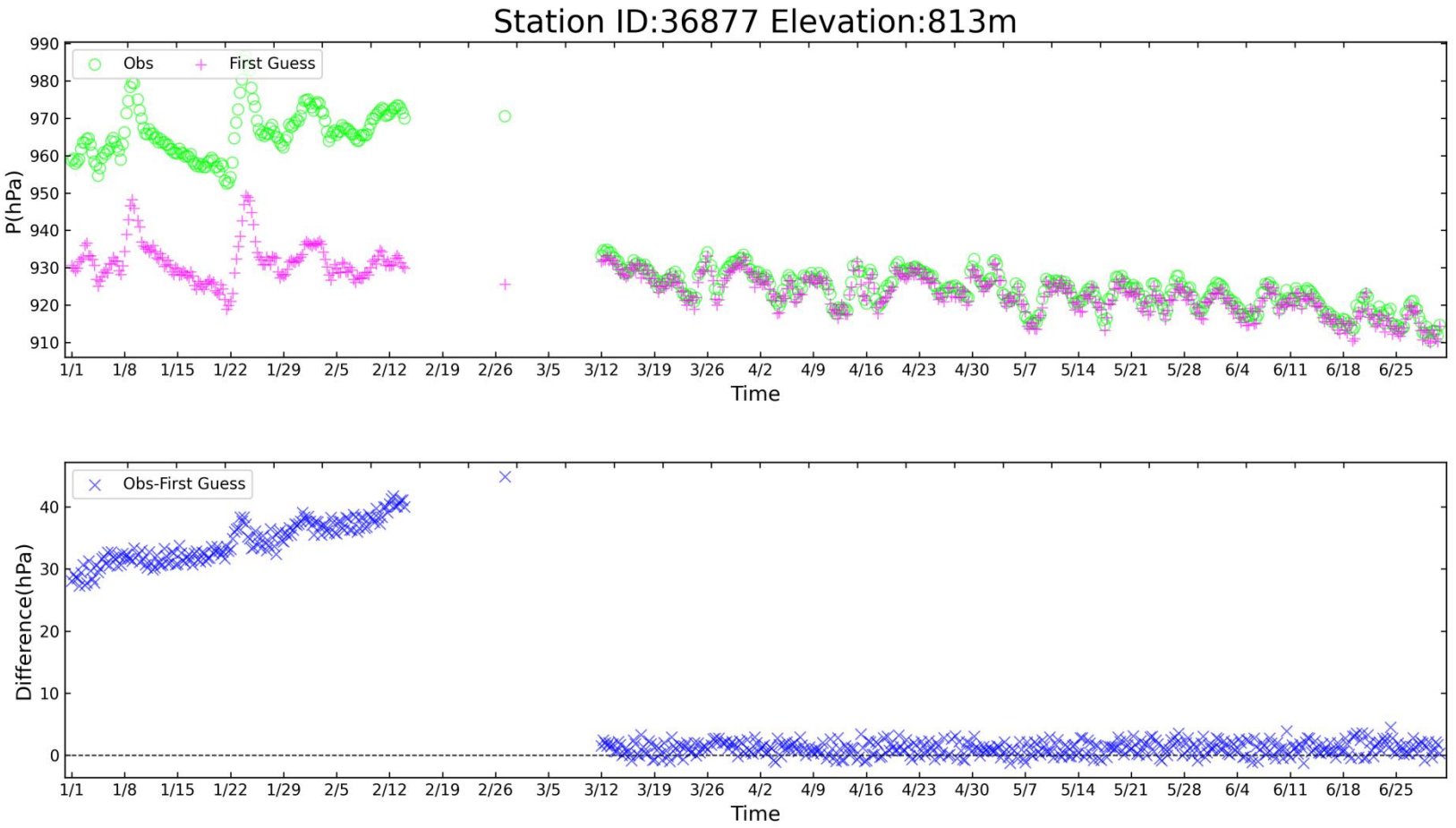

Figure 53 Time-series representation of SLP Obs minus FirstGuess for station 36877

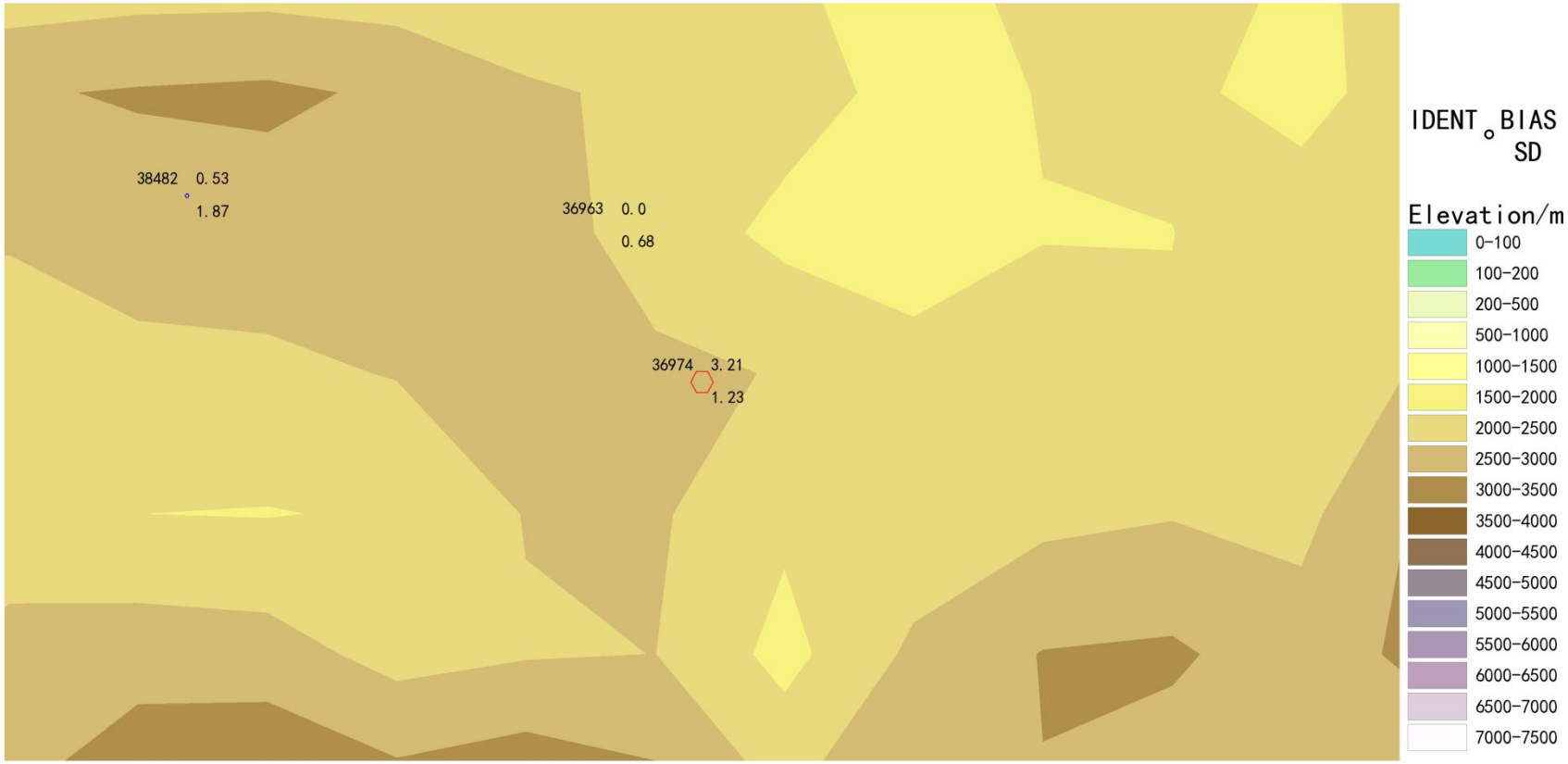

Figure 54 BIAS and SD of SLP for station 36974* (red) and surrounding stations (blue).
The number to the upper left of each symbol is the WMO IDENT, and those to the upper right are the values of BIAS and SD.
The size of each symbol is proportional to the value of BIAS, with hexagonal forms representing positive bias and triangular forms representing negative bias.

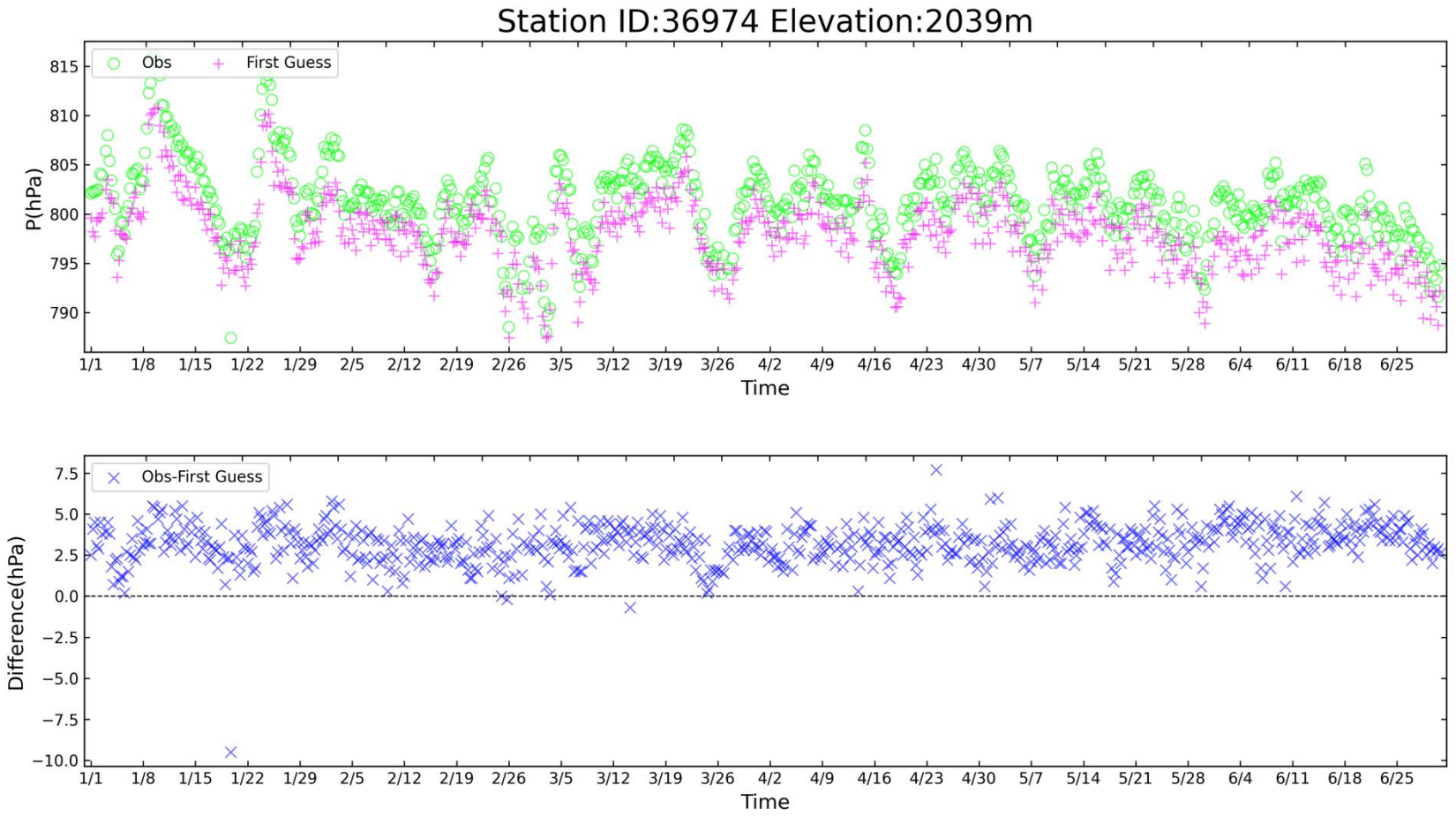

Figure 55 Time-series representation of SLP Obs minus FirstGuess for station 36974*

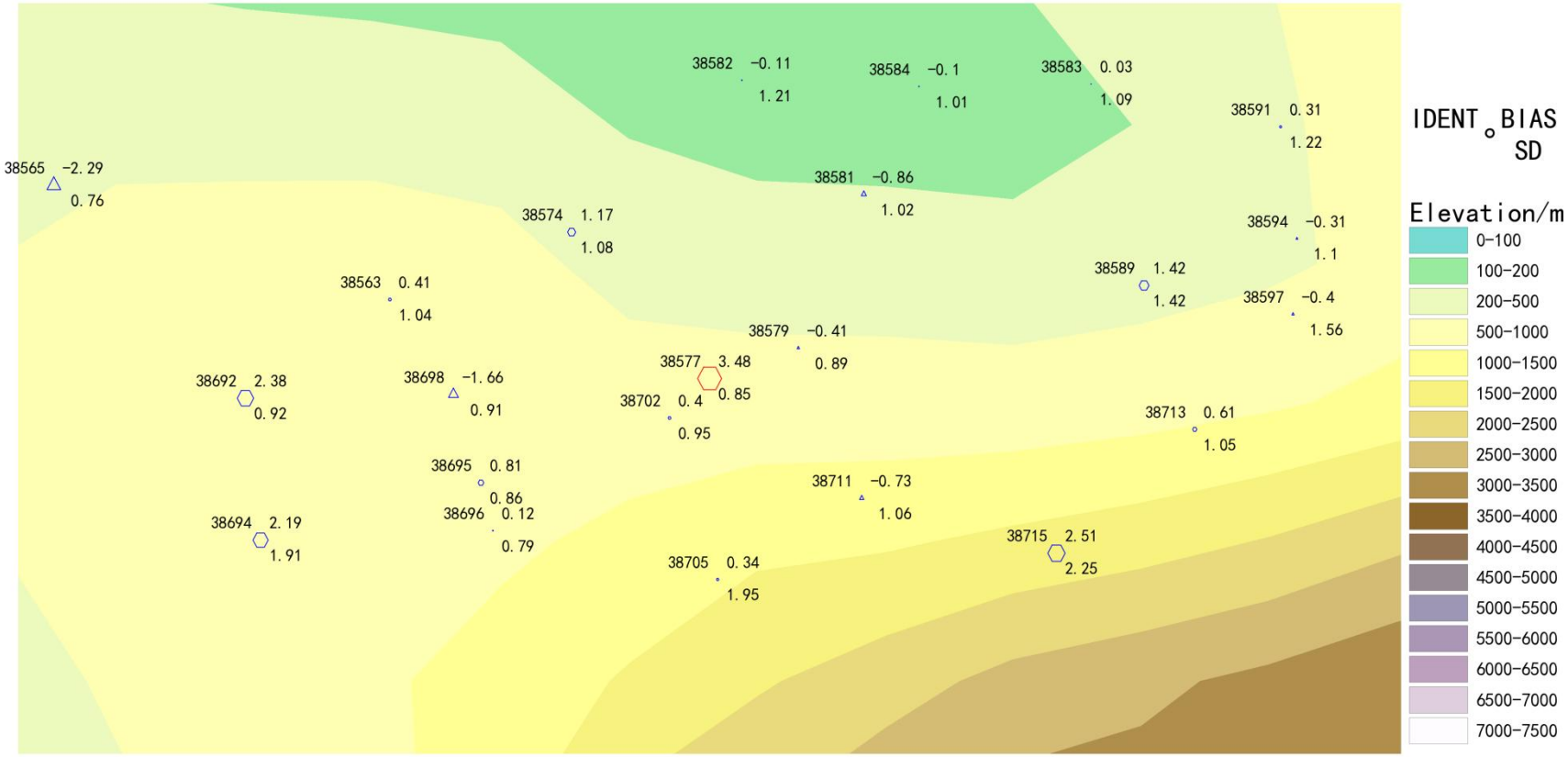

Figure 56 BIAS and SD of SLP for station 38577* (red) and surrounding stations (blue).

The number to the upper left of each symbol is the WMO IDENT, and those to the upper right are the values of BIAS and SD.

The size of each symbol is proportional to the value of BIAS, with hexagonal forms representing positive bias and triangular forms representing negative bias.

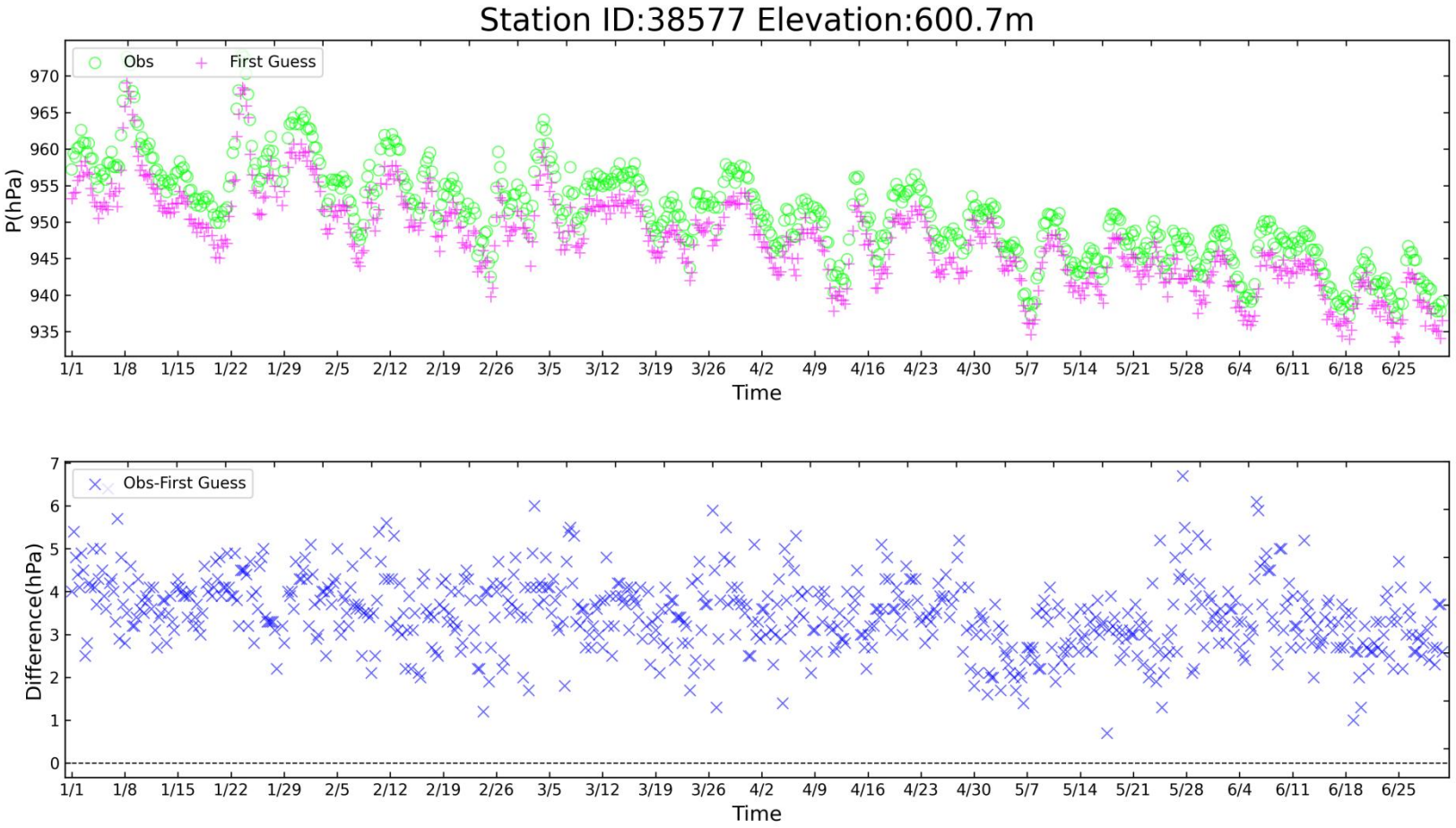

Figure 57 Time-series representation of SLP Obs minus FirstGuess for station 38577*

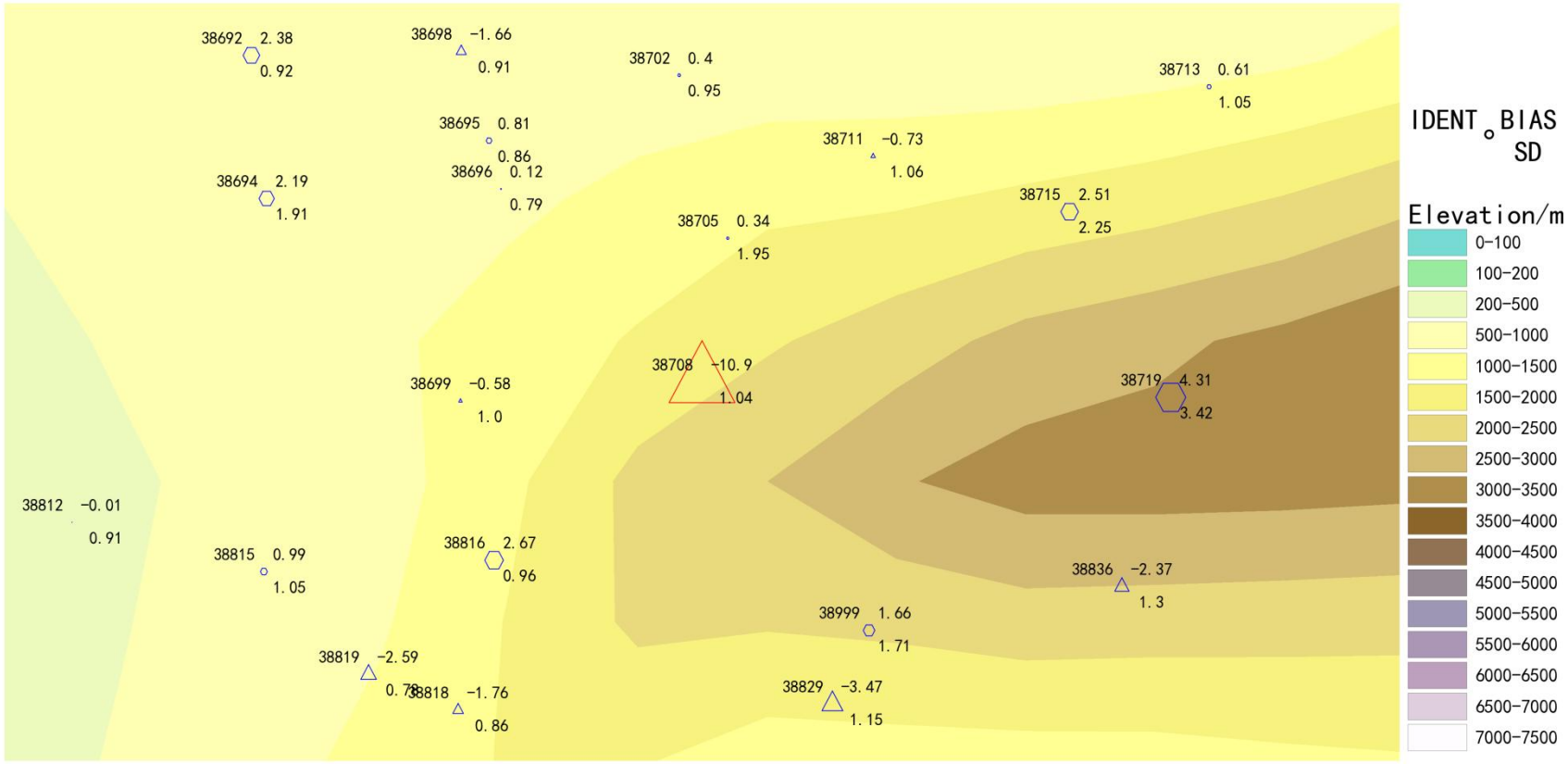

Figure 58 BIAS and SD of SLP for station 38708 (red) and surrounding stations (blue).

The number to the upper left of each symbol is the WMO IDENT, and those to the upper right are the values of BIAS and SD.

The size of each symbol is proportional to the value of BIAS, with hexagonal forms representing positive bias and triangular forms representing negative bias.

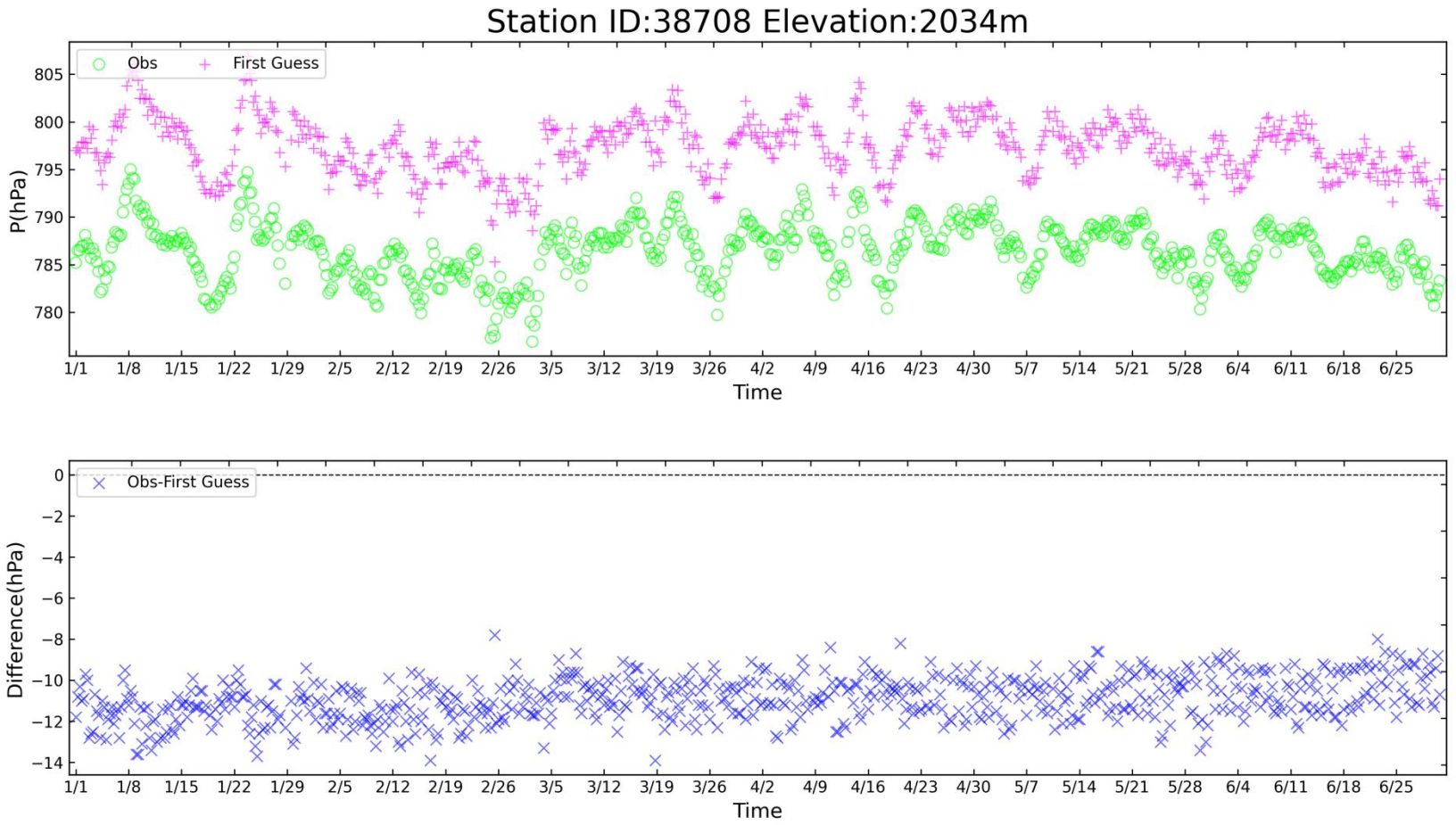

Figure 59 Time-series representation of SLP Obs minus FirstGuess for station 38708

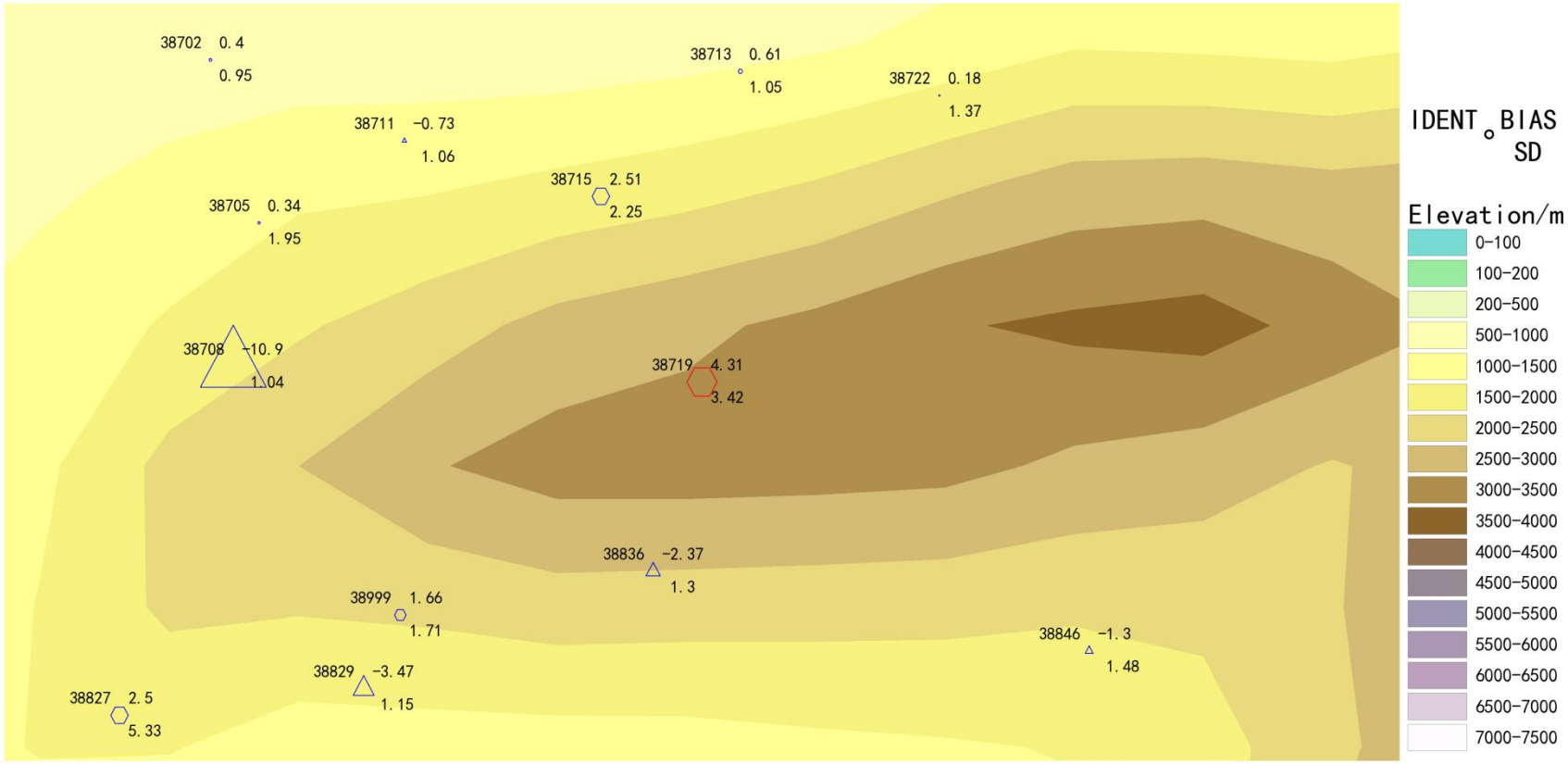

Figure 60 BIAS and SD of SLP for station 38719* (red) and surrounding stations (blue).
The number to the upper left of each symbol is the WMO IDENT, and those to the upper right are the values of BIAS and SD.
The size of each symbol is proportional to the value of BIAS, with hexagonal forms representing positive bias and triangular forms representing negative bias.

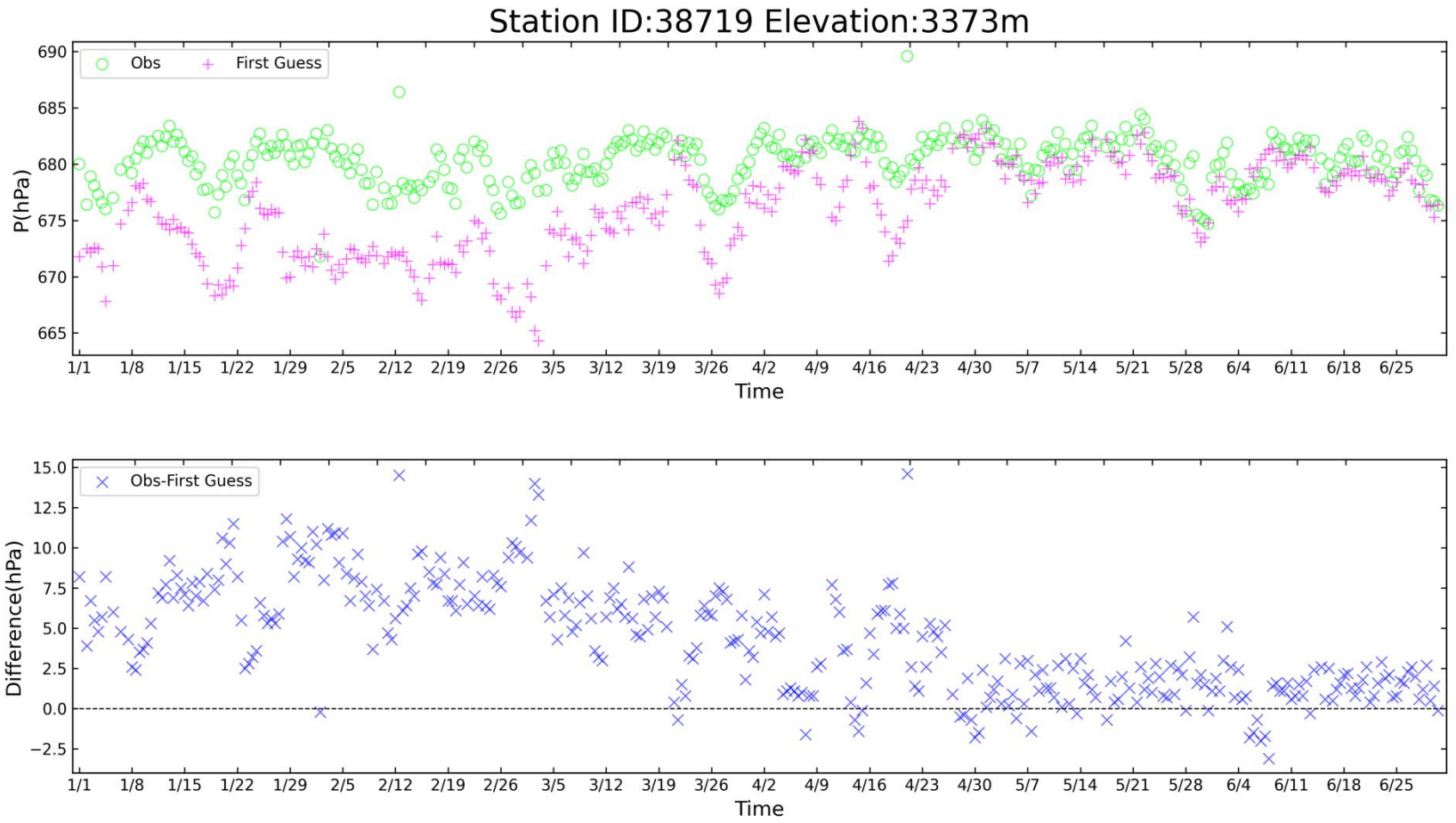

Figure 61 Time-series representation of SLP Obs minus FirstGuess for station 38719*

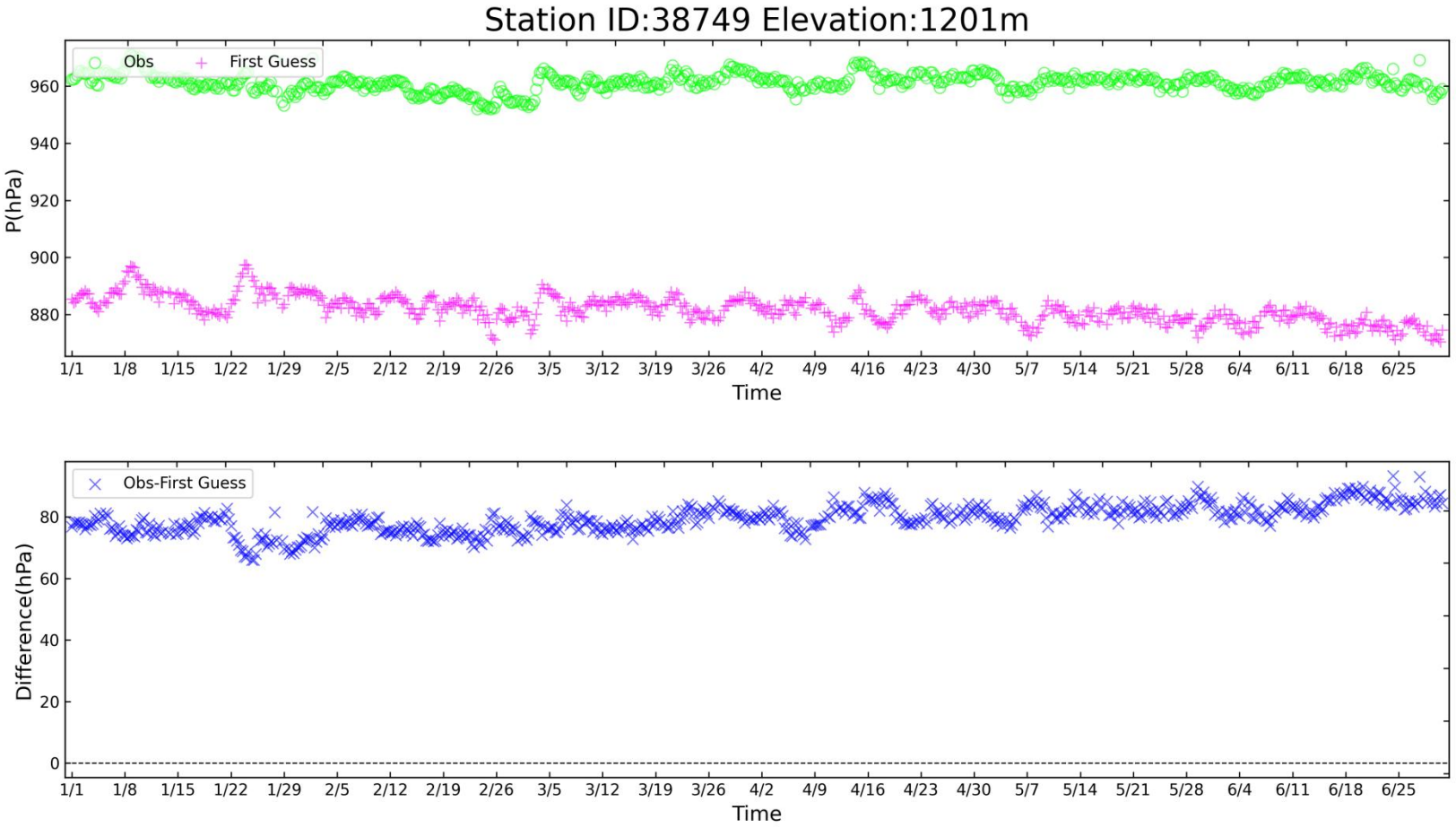

Figure 62 Time-series representation of SLP Obs minus FirstGuess for station 38749

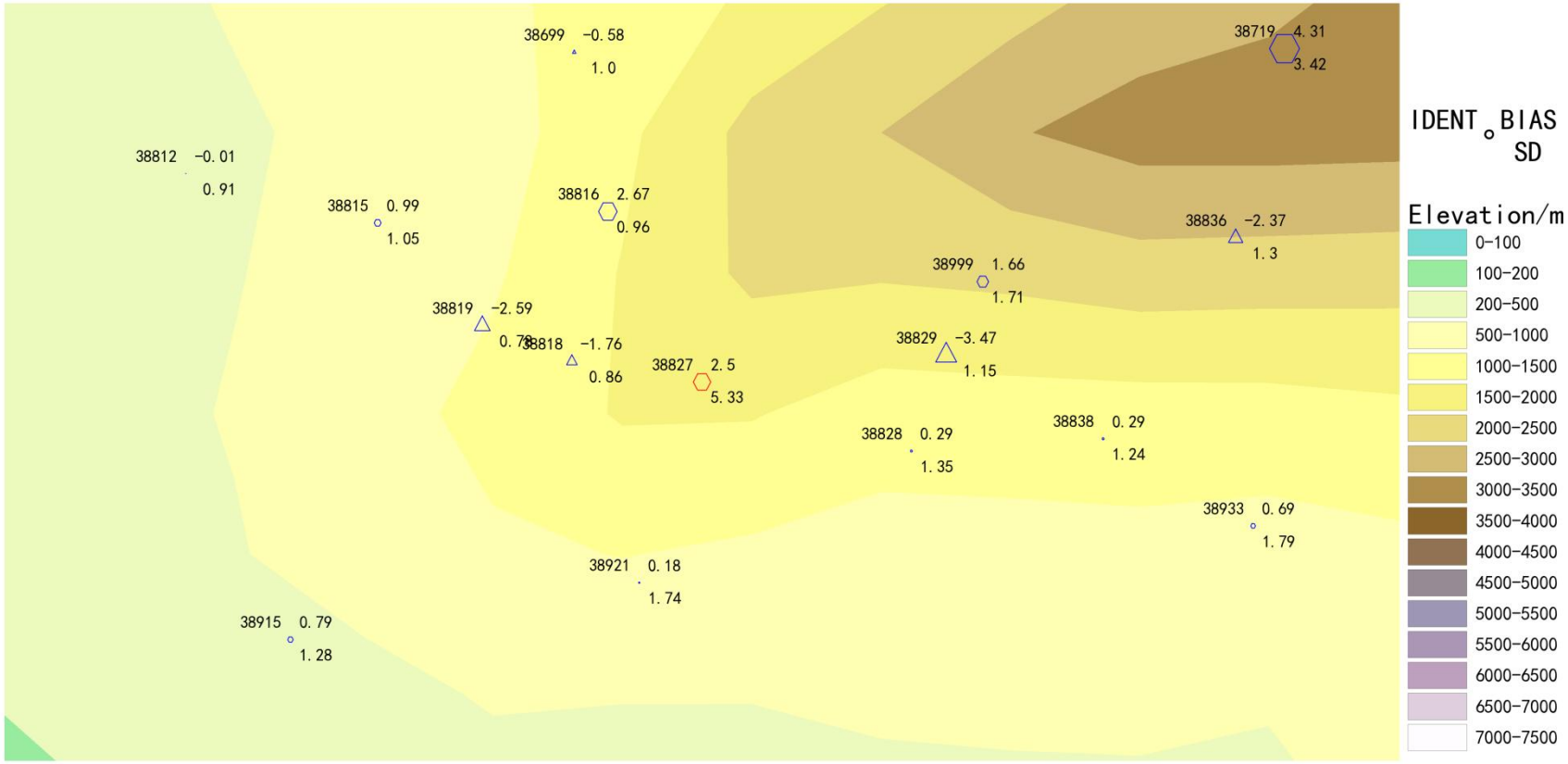

Figure 63 BIAS and SD of SLP for station 38827 (red) and surrounding stations (blue).

The number to the upper left of each symbol is the WMO IDENT, and those to the upper right are the values of BIAS and SD.

The size of each symbol is proportional to the value of BIAS, with hexagonal forms representing positive bias and triangular forms representing negative bias.

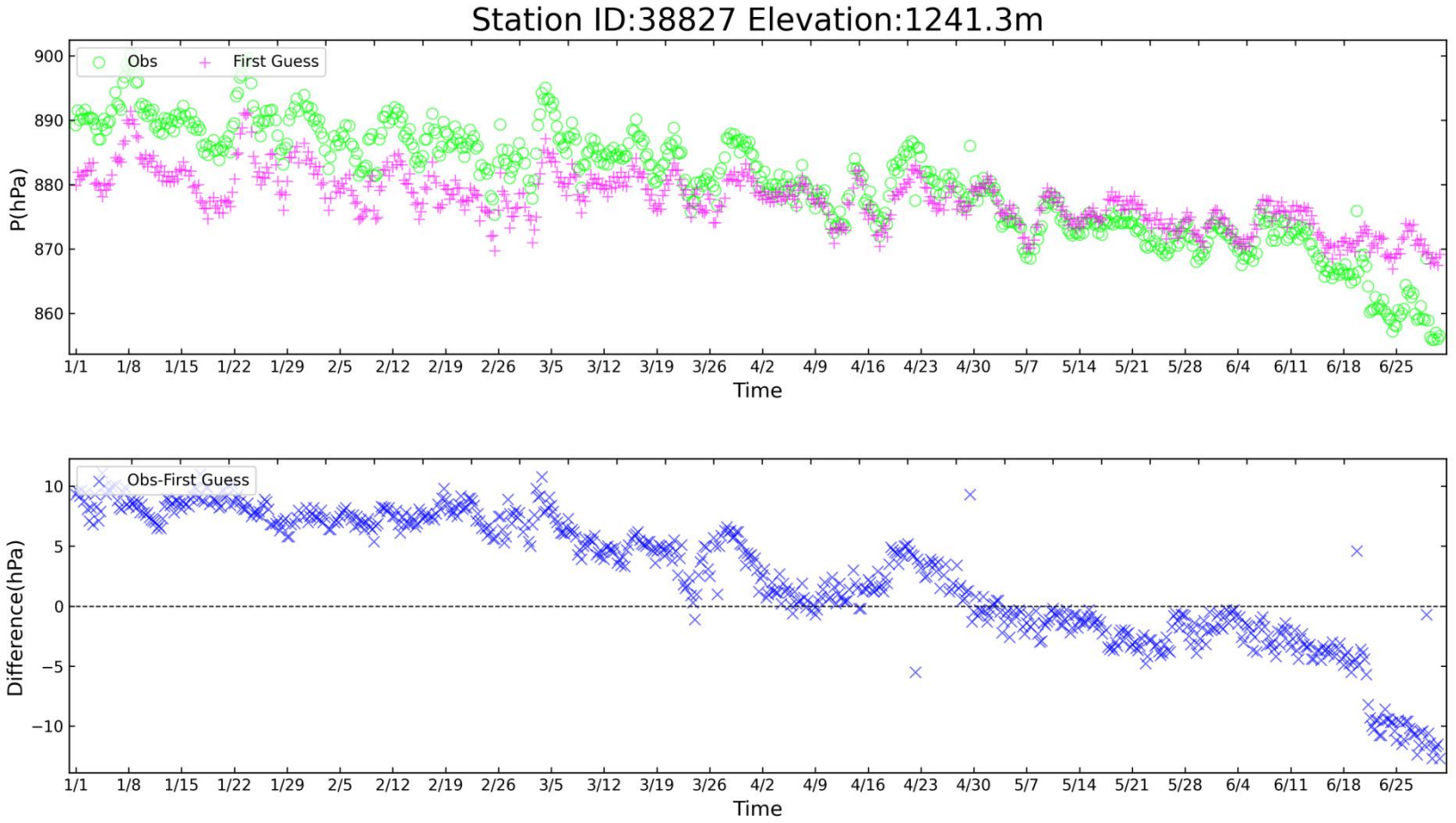

Figure 64 Time-series representation of SLP Obs minus FirstGuess for station 38827

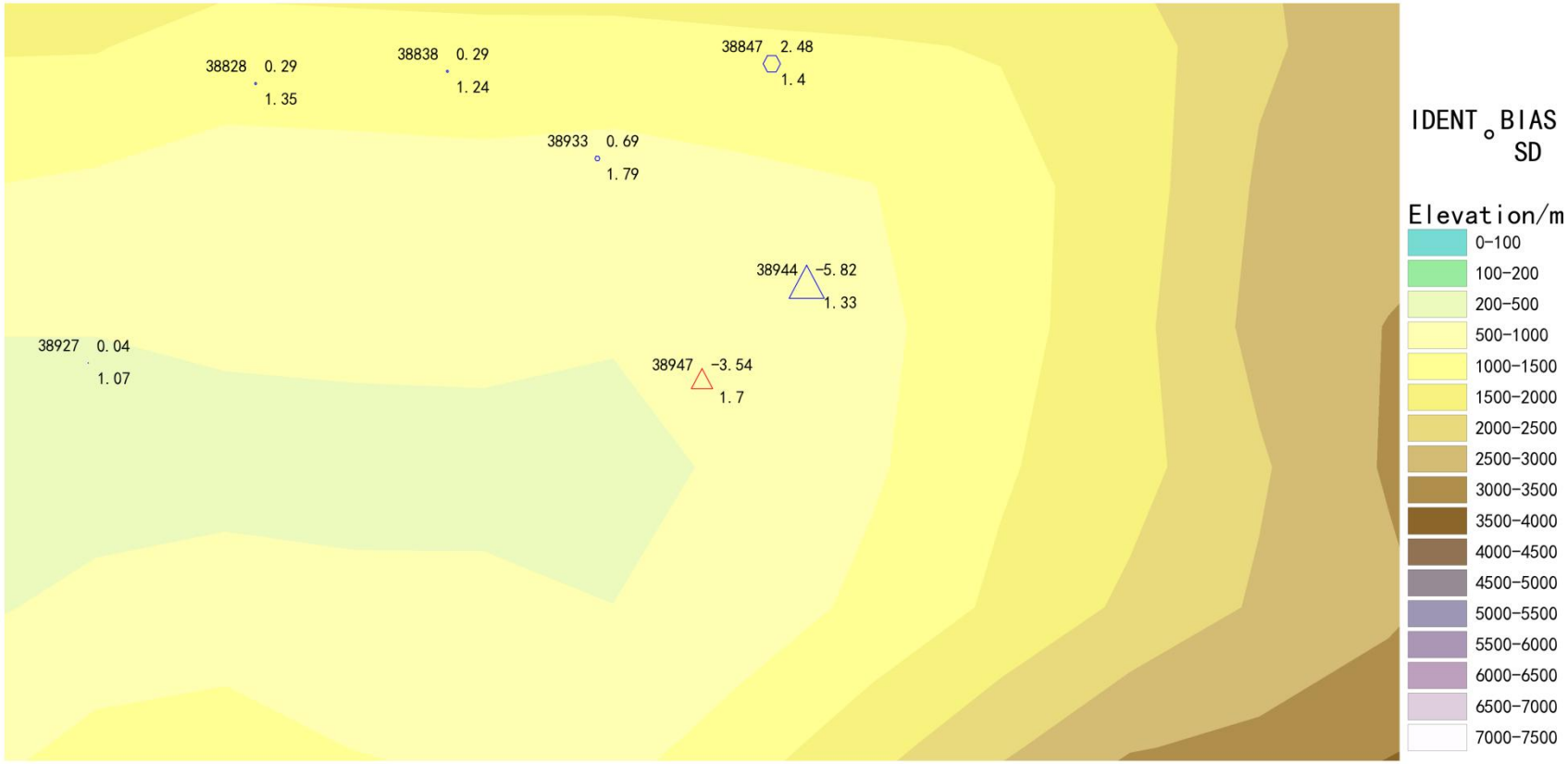

Figure 65 BIAS and SD of SLP for station 38947* (red) and surrounding stations (blue).

The number to the upper left of each symbol is the WMO IDENT, and those to the upper right are the values of BIAS and SD.

The size of each symbol is proportional to the value of BIAS, with hexagonal forms representing positive bias and triangular forms representing negative bias.

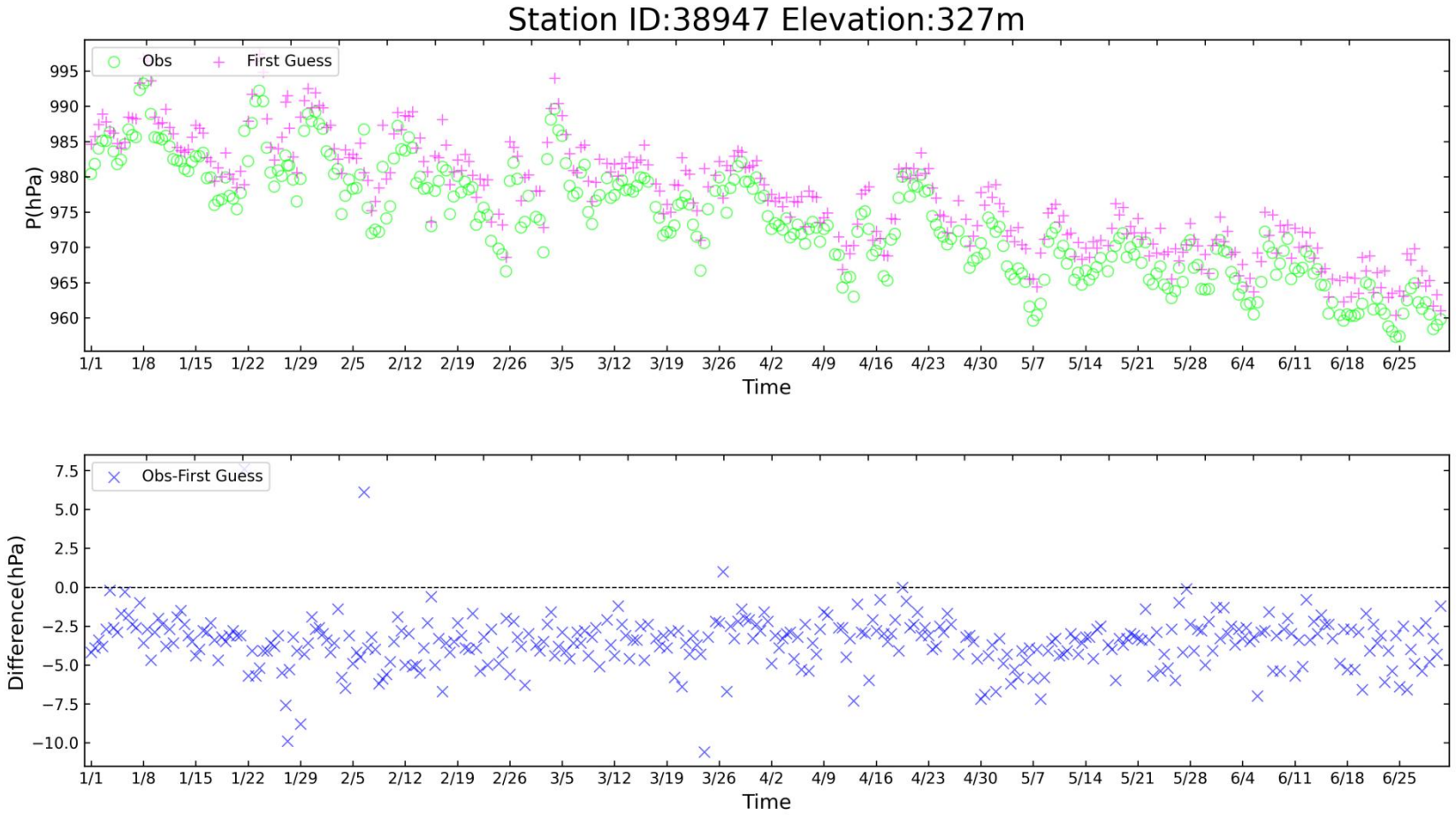

Figure 66 Time-series representation of SLP Obs minus FirstGuess for station 38947*

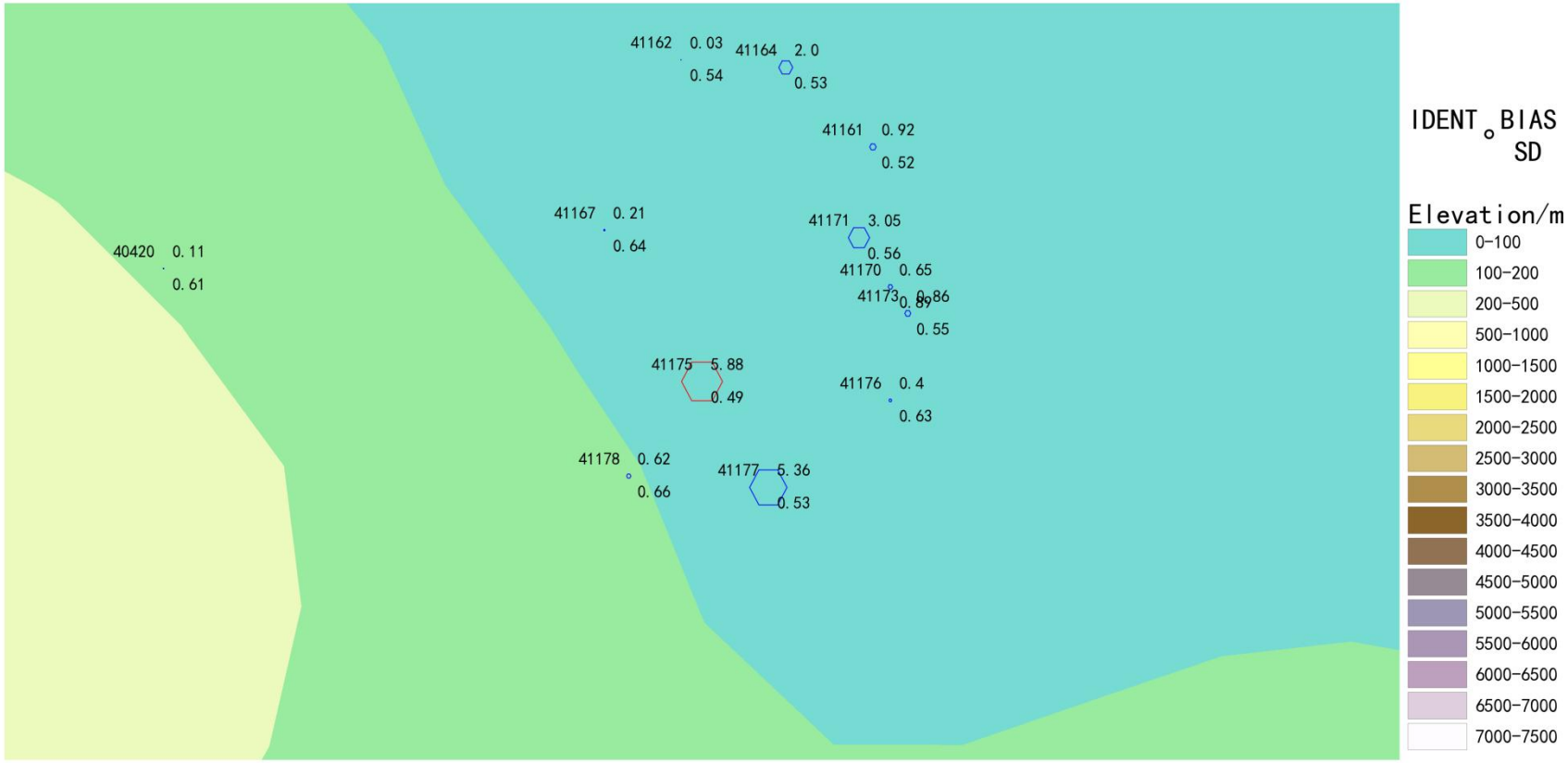

Figure 67 BIAS and SD of SLP for station 41175 (red) and surrounding stations (blue).

The number to the upper left of each symbol is the WMO IDENT, and those to the upper right are the values of BIAS and SD.

The size of each symbol is proportional to the value of BIAS, with hexagonal forms representing positive bias and triangular forms representing negative bias.

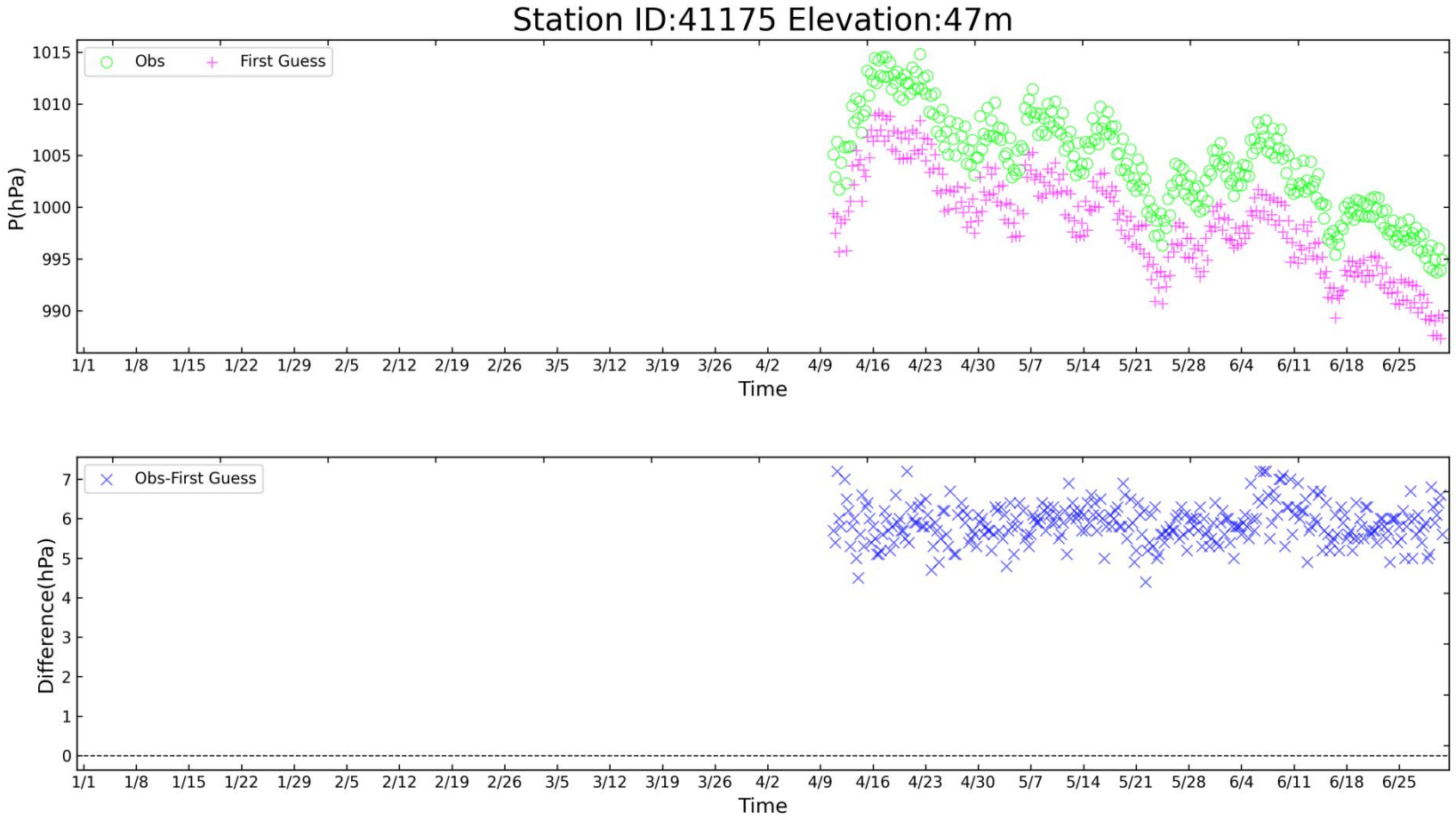

Figure 68 Time-series representation of SLP Obs minus FirstGuess for station 41175

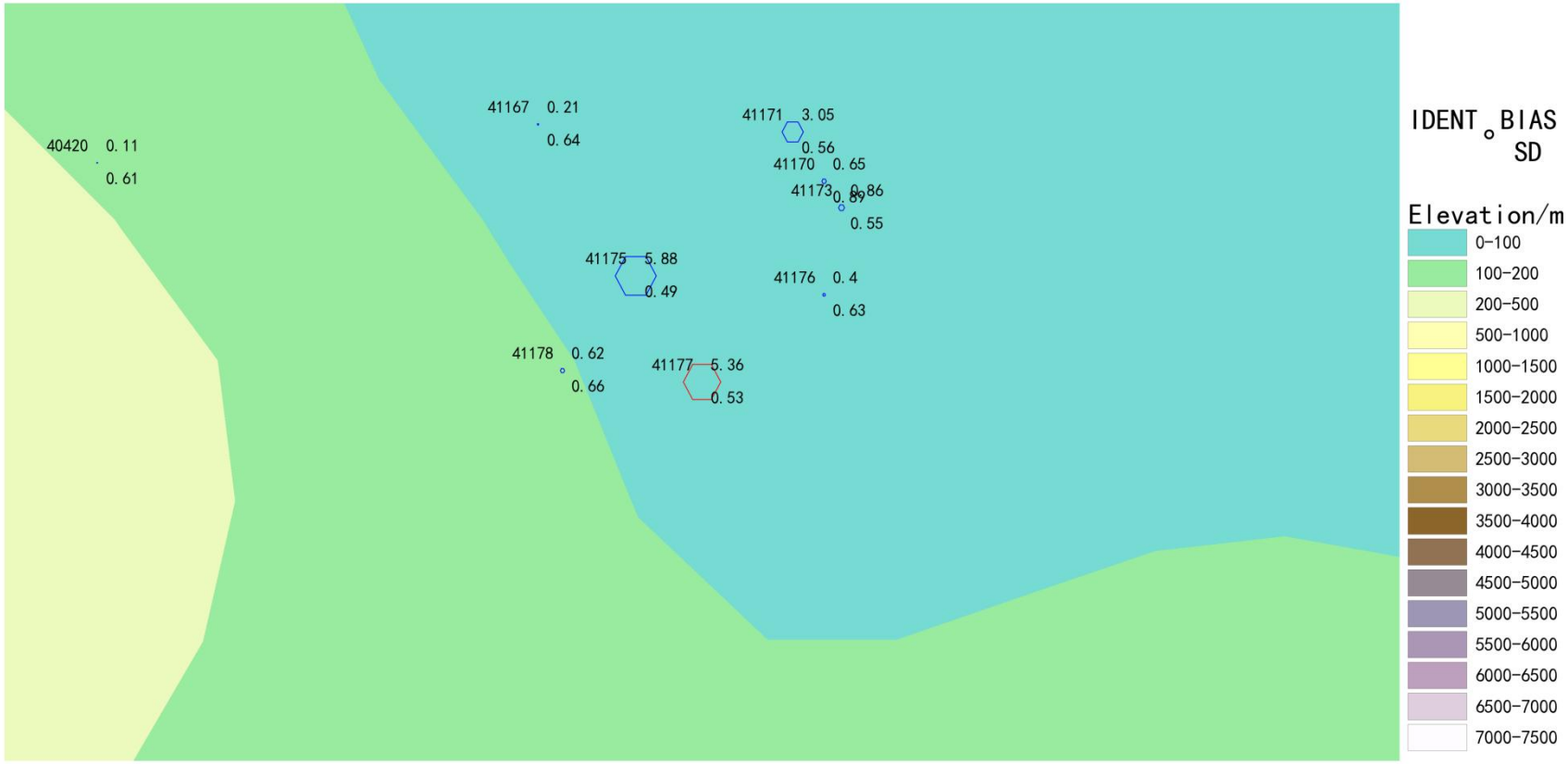

Figure 69 BIAS and SD of SLP for station 41177 (red) and surrounding stations (blue).

The number to the upper left of each symbol is the WMO IDENT, and those to the upper right are the values of BIAS and SD.

The size of each symbol is proportional to the value of BIAS, with hexagonal forms representing positive bias and triangular forms representing negative bias.

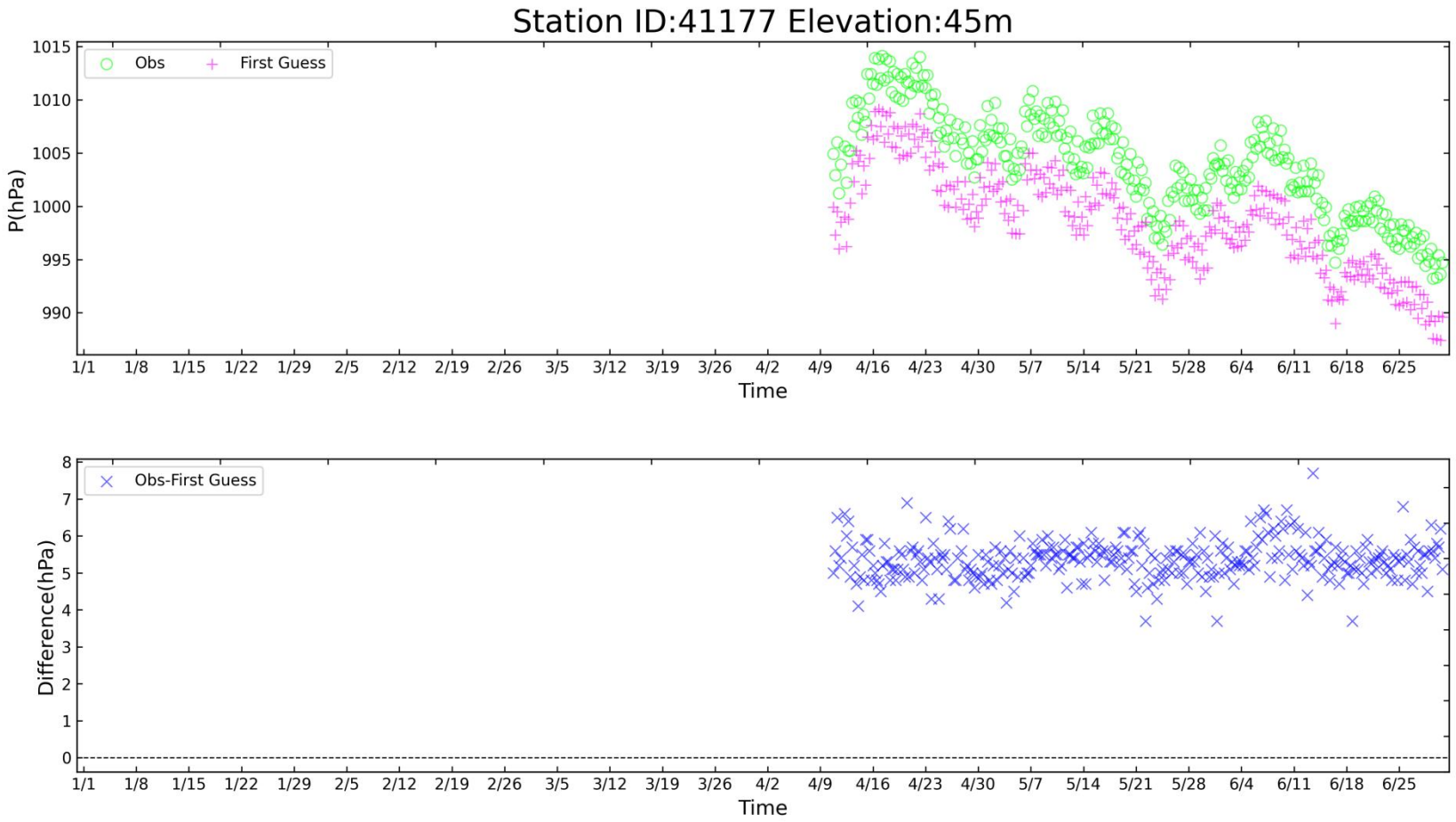

Figure 70 Time-series representation of SLP Obs minus FirstGuess for station 41177

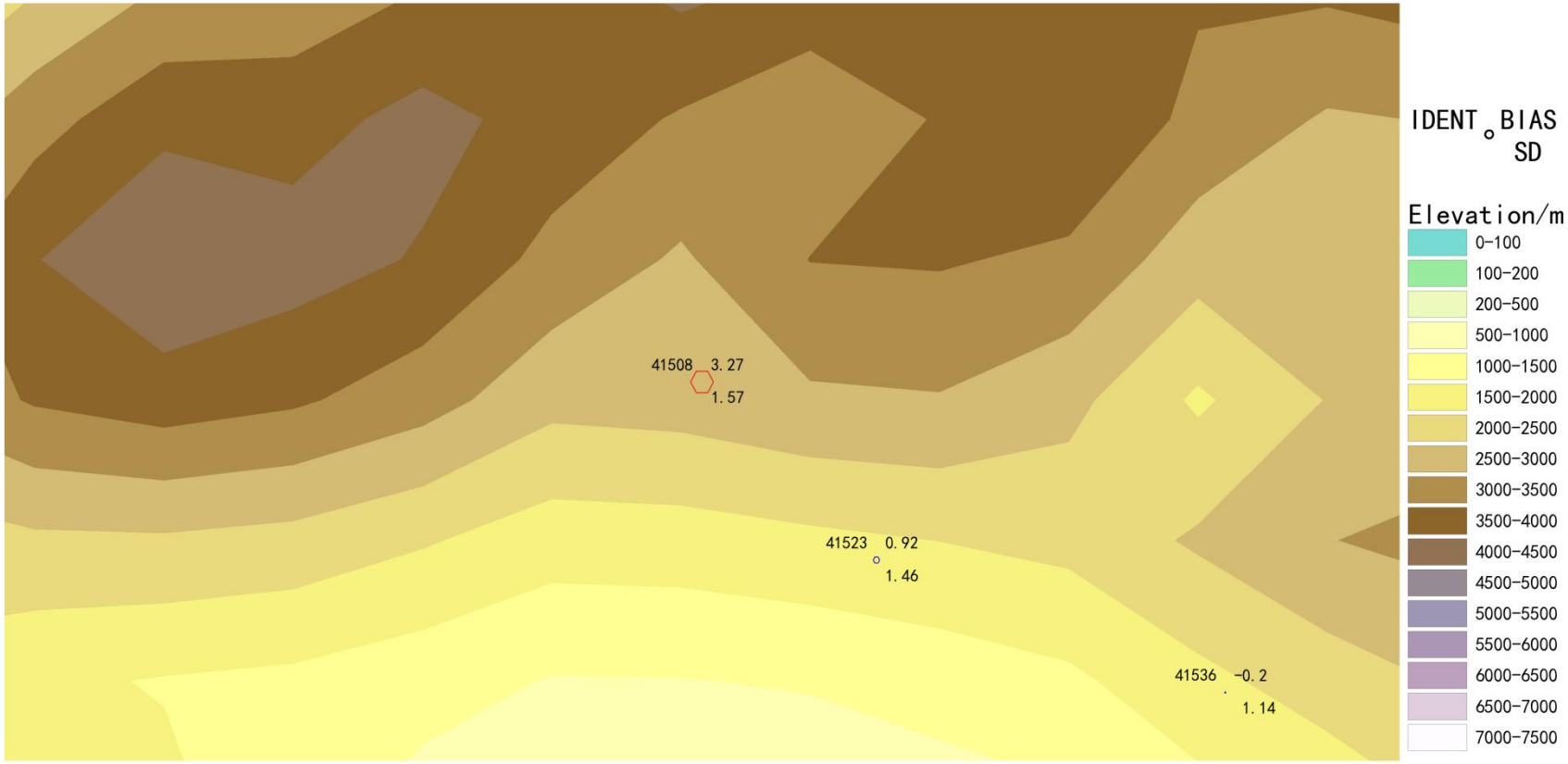

Figure 71 BIAS and SD of SLP for station 41508* (red) and surrounding stations (blue).
The number to the upper left of each symbol is the WMO IDENT, and those to the upper right are the values of BIAS and SD.
The size of each symbol is proportional to the value of BIAS, with hexagonal forms representing positive bias and triangular forms representing negative bias.

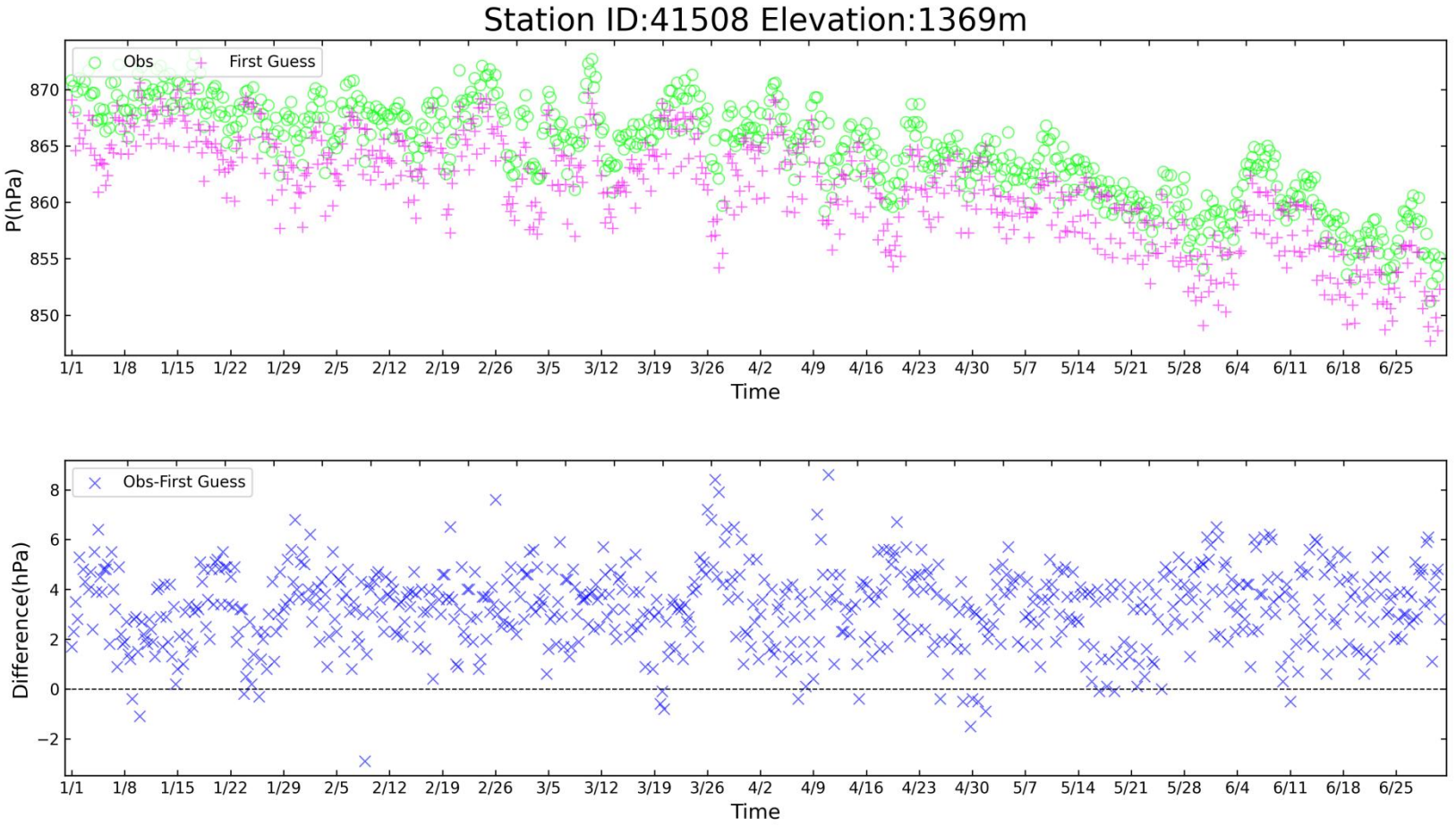

Figure 72 Time-series representation of SLP Obs minus FirstGuess for station 41508*

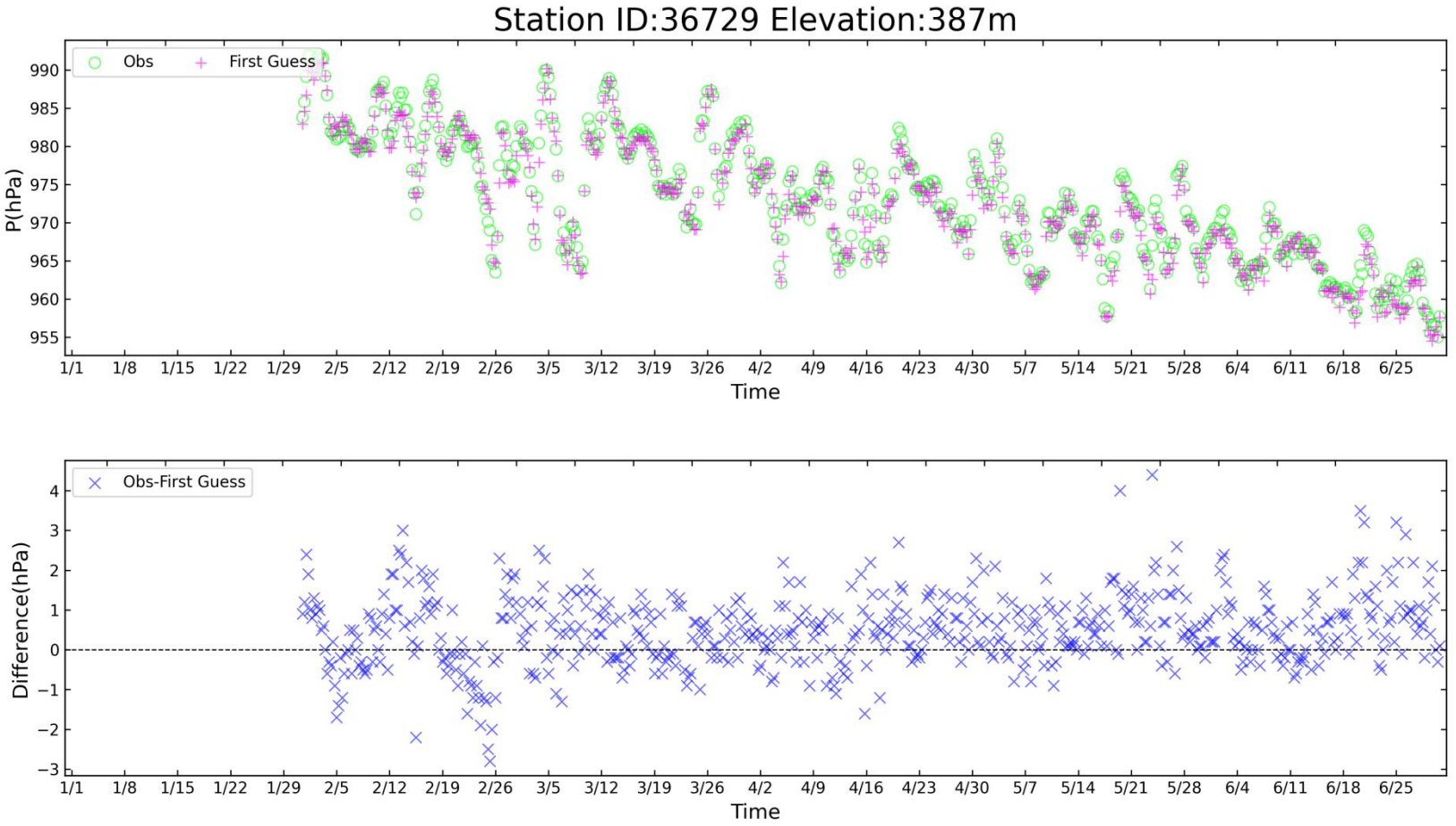

Figure 73 Time-series representation of SLP Obs minus FirstGuess for station 36729

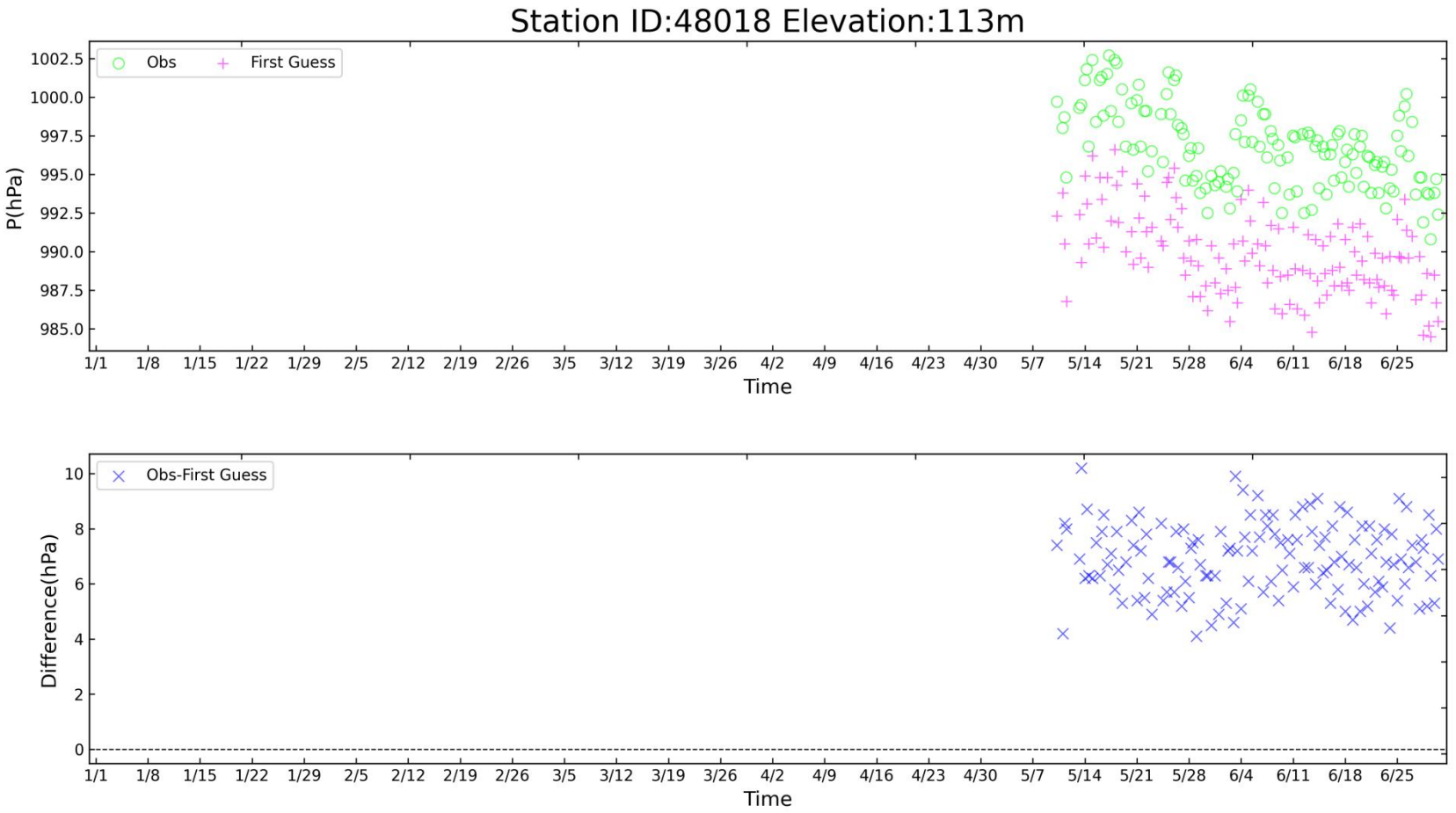

Figure 74 Time-series representation of SLP Obs minus FirstGuess for station 48018*

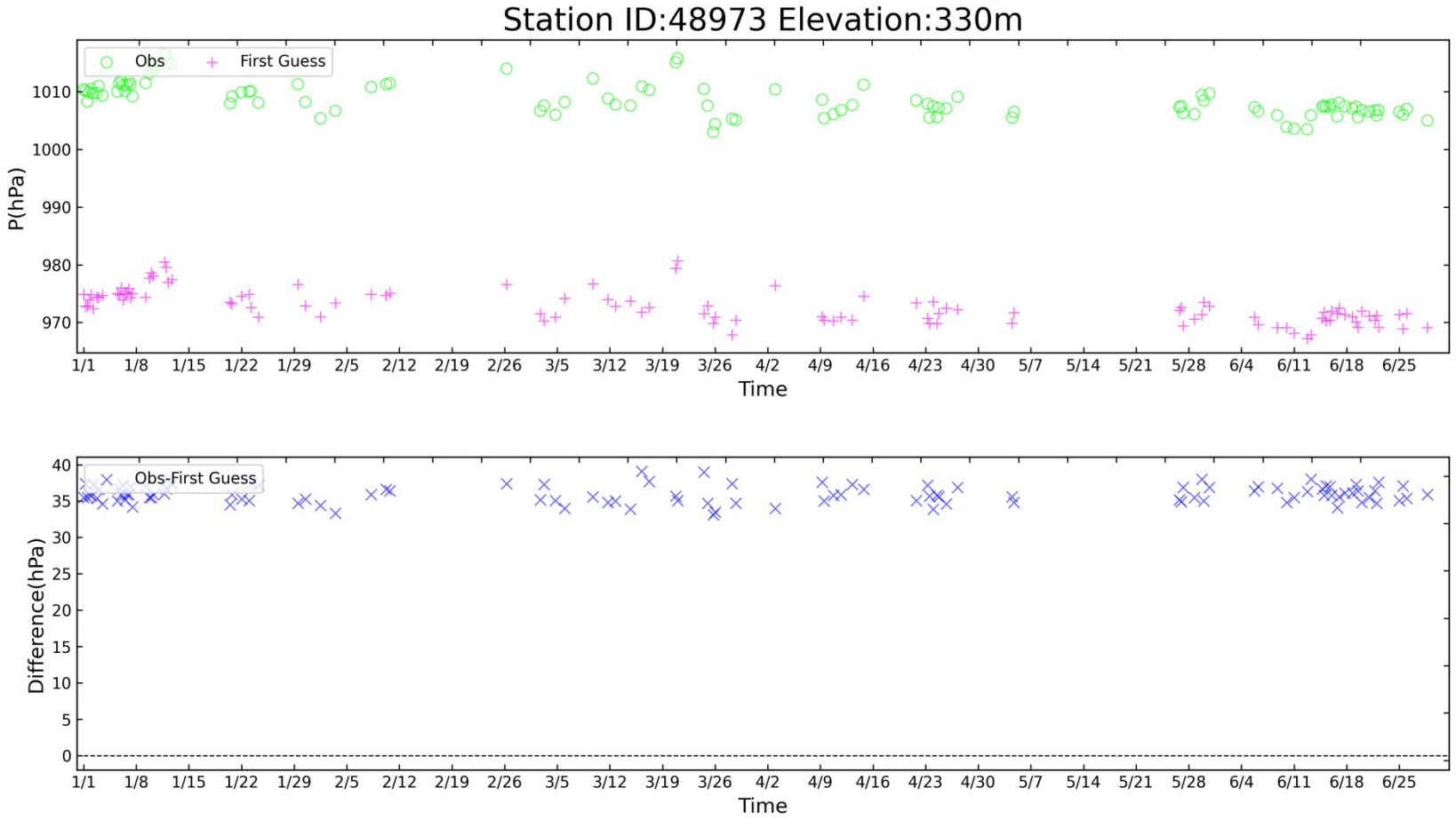

Figure 75 Time-series representation of SLP Obs minus FirstGuess for station 48973

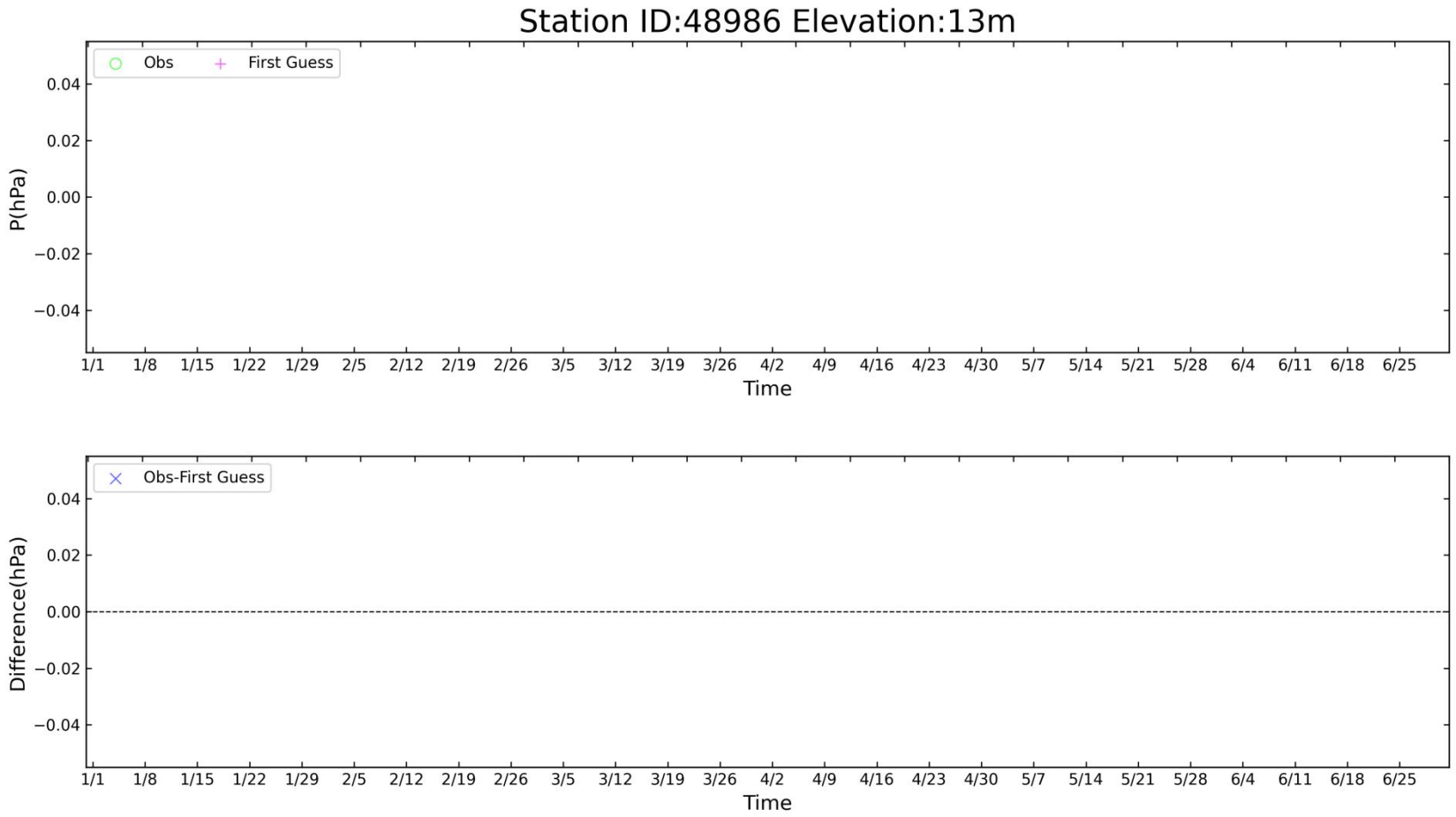

Figure 76 Time-series representation of SLP Obs minus FirstGuess for station 48986